IDENTIFICATION AND CHARACTERIZATION OF A STEM CELL-LIKE POPULATION IN OVARIAN CANCER

by
Allison Catherine Sharrow

A dissertation submitted to Johns Hopkins University in conformity with the requirements for the degree of Doctor of Philosophy

Baltimore, Maryland
January, 2014

ABSTRACT

Eighty percent of patients with advanced ovarian cancer show an initial clinical response to therapy, but seventy-five percent of these patients eventually relapse. This transient clinical response would be consistent with the cancer stem cell hypothesis. A substantial body of recent evidence supports the cancer stem cell hypothesis in ovarian cancer. However, controversy exists regarding the phenotype of ovarian cancer stem cells. Additionally, their clinical relevance remains unclear.

In order to test the hypothesis that ovarian cancer contains a population of stem-like cells, aldehyde dehydrogenase 1 high ($ALDH^{high}$) cells from two ovarian cancer cell lines with distinct subtypes were examined for cancer stem cell properties. Compared to $ALDH^{low}$ cells, $ALDH^{high}$ cells displayed nonadherent growth, an absence of contact inhibition, smaller size, quiescence, the ability to regenerate the phenotypic diversity of the cell line, *in vivo* tumorigenicity, multi-drug resistance, and gene expression differences consistent with a stem cell phenotype. Because $ALDH^{high}$ cells phenotypically resemble cancer stem cells, studying this population in two different subtypes may reveal biological properties of ovarian cancer stem cells. Differential gene expression suggested that the $ALDH^{high}$ population had increased tight junction signaling, downregulation of tumor suppressors, increased invasion, and decreased coagulation. No consistent differences were observed in previously reported ovarian cancer stem cell markers, hormone receptors, Her-2/neu, CA125 or developmental pathways. The only ABC transporter with consistent upregulation was

MDR1. The ultimate goal of studying ovarian cancer stem cells is to develop therapies to eradicate these cells. Gene expression patterns in $ALDH^{high}$ cells identified four potential therapeutic targets: mTOR, Her-2/neu, CD47 and FGF18.

This project provides further support for the existence of ovarian cancer stem cells as well as the use of high aldehyde dehydrogenase 1 activity for their isolation. Few studies have comprehensively examined ovarian cancer stem cells from multiple subtypes. This work demonstrated substantial variability between the two studied subtypes. However, those features that were consistent would likely represent universal features of ovarian cancer stem cells. Finally, the potential therapeutic targets identified in this study may allow patients with ovarian cancer to achieve durable remission.

Advisor: Richard J. Jones

Readers: Richard J. Jones

Edward Gabrielson

ACKNOWLEDGEMENTS

Throughout the course of my graduate career, I was blessed to have the support and guidance of my thesis committee members: Richard Jones, Edward Gabrielson, Deborah Armstrong, Richard Roden and David Berman. The project was fraught with technical difficulties and I never felt reproached by any of you. Instead, I could always count on your understanding and encouragement, for which I am greatly appreciative. I was also fortunate to have a thesis mentor, Richard Jones, who allowed me to develop as an independent researcher. You provided guidance when I needed it and independence when I was ready for it. I have learned a great deal about how to approach a project and the difficulties that come with it. I appreciate that you never chastised me for those difficulties or my mistakes but rather helped me to overcome them.

During my rotation in the Jones lab, I felt like I stepped into a family. I am glad to have been welcomed into that family. Each of you has helped me in different ways and has made my thesis work very enjoyable. Although faces have changed over time, I thank all of you for your help and camaraderie: Jamie Barber, Milada Vala, Brandy Perkins, Margaret Showel, Jon Gerber, Gabriel Ghiaur, Sarah Morse, Meng Su, Salvador Alonso, Bree Yanagisawa, Heather Johnson, Tina Bauer, Tenera Coates, and honorable member of the lab Qiuju Wang.

I am also grateful for the many collaborators that assisted me over the course of my graduate career. Michael Collector, thank you for putting up with my animals

and me for so many years. I could not have done it without you. Also, thank you for all of the cooking tips. I am indebted to Allan Hess and Chris Thoburn for providing me with the FNAR model and the knowledge I needed to handle the cells. I also need to thank Ie-Ming Shih, Tian-Li Wang and Alex Stoeck for providing me with the taxol-resistant SKOV3 subline. Dr. Shih, I also appreciate you input and guidance over the years. You helped me to overcome the difficulty of being the only person studying ovarian cancer in a hematological malignancies lab. Wayne Yu, thank you for all of your guidance on the microarray and PCR validation experiments. Brian Simons, thank you for helping with the animals and the tumor validation.

I am fortunate to have been a member of the Pathobiology program. My classmates made my first year as close to fun as classes would allow. Several of you have become dear friends over the years. I appreciate that the faculty and administration have always been available to lend support and guidance. I especially need to thank Noel Rose and our fabulous program coordinators: Wilhelmena Braswell, Nancy Nath and Tracie McElroy.

Several people helped shape the course of my early career and influenced my path to Johns Hopkins. James Pipas offered me my first research position, which led me to pursue a career in academic research. In the Pipas Lab, Paul Cantalupo and Sean Hasso introduced me to lab techniques and taught me how to design experiments. Thank you for laying the groundwork of my career. Harry Blair allowed me to expand my experience with a research associate position after graduation. The

time I spent in the Blair Lab confirmed that I had chosen the correct field. I was also fortunate to find a mentor, not just a boss. You encouraged me to continue with my education and believed in my ability to excel at an Ivy League institution. Thank you for continuing to mentor me long after I have left your lab. It gives me confidence to know that I always have you in my corner.

I must thank my friends and family for their continued support throughout my education. My friends in Baltimore and elsewhere helped to remind me to have fun in graduate school and accepted my absence when classes and lab work dominated my time. I am eternally grateful for your friendship. I will always feel blessed for my loving and supportive family. I do not know what I did in a past life to deserve all of you, but I am thankful that I have you. My parents, Paul and Janice Sharrow, have shaped me into the person I am today. Thank you for always believing in me and always being there for me. Thank you to my siblings, Ian and Molly Sharrow, for keeping me grounded and making sure that I never take myself too seriously. Thank you to my grandparents, Larry and Doris Foster and Harriet Sharrow, for your loving support. Finally, I need to thank my husband, Leo Ziegler. You have been my rock throughout graduate school. When I questioned myself, you reassured me. I could not imagine doing this without you. Thank you for putting up with me in graduate school. Hopefully, it gets easier now; but if not, I know we can handle anything together.

TABLE OF CONTENTS

TABLES

FIGURES

1 Introduction

Cancer Stem Cell Hypothesis

Current cancer treatments primarily employ three strategies: surgery, radiation and chemotherapy. Each of these approaches has a long history of clinical use. Surgical resection was first documented in 1500 B.C[1]. Radiation therapy for the treatment of cancers not able to be surgically removed was introduced in 1902[2]. Chemotherapy began in the middle of the 19th-century with the use of arsenic[3]. However, the basis for modern chemotherapy arose from nitrogen mustard after World War II[4]. Despite significant refinements to these strategies since their inception,

cancer persists as the second leading cause of death in the United States with 38% of cancer patients succumbing to their disease[5].

It is becoming increasingly apparent that simply refining current treatment approaches will not substantially impact patient outcomes, and novel approaches are necessary. Many patients show an initial clinical response to standard therapy, often achieving complete remission. However, a significant percentage of patients eventually relapse. The cancer stem cell hypothesis may explain this pattern of transient clinical response. This model proposes that cancer exhibits a similar hierarchy as normal tissues in that a small subset of primitive cells (cancer stem cells) produces the differentiated progeny that constitute the tumor bulk. The hypothesis further suggests that cancer stem cells persist after standard chemotherapy and initiate relapse. If this cell population could be specifically targeted for treatment, perhaps durable remission could be achieved.

Accepted properties of tissue stem cells provide theoretical support for the cancer stem cell hypothesis. Tissue stem cells typically survive longer than differentiated cells, providing sufficient time to accumulate the multiple genetic alterations necessary for malignancy[6]. Additionally, differentiated cells typically undergo only a limited number of cell divisions. In order to produce the large numbers of cells present in a tumor, significant cellular reprogramming of differentiated cells would be required to increase their proliferative potential. In

contrast, stem cells possess a substantially greater capacity for cell division, requiring fewer alterations to produce a malignant mass.

Although theoretically supported, insufficient evidence existed to confirm the cancer stem cell hypothesis. The stochastic model serves as an alternative explanation for treatment resistance. This model proposes that chemoresistance may develop in a random sampling of the initial population, and any cell remaining after treatment is potentially tumorigenic. The stochastic and cancer stem cell models present opposing explanations of cancer with profound implications for research. Research into the development of treatment strategies based on the stochastic model attempt to overcome first-order kinetic resistance with approaches such as increasing dose-intensity. In contrast, approaching cancer from the perspective of the cancer stem cell hypothesis requires identification of the tumorigenic population and the design of treatments to specifically eradicate this subset of cells. Until relatively recently, cancer researchers primarily accepted the assumptions of the stochastic model. Gradually, though, evidence accumulated in support of the cancer stem cell hypothesis, forcing some to reconsider their approach to cancer research.

Early Evidence of Cancer Stem Cells

The earliest evidence for the existence of cancer stem cells dates to the 1950's. Observations of chromosome numbers indicated that only a subset of cancer cells possessed the capacity for cell division[7]. Further analysis of chromosome patterns led to the proposal that this population was responsible for metastasis[8]. In the 1960's and

1970's, injections of tritiated thymidine permitted *in vivo* monitoring of cell division in leukemia cells. Initial results showed that cell division was restricted to the bone marrow, which houses hematopoietic stem cells[9]. Subsequent analysis revealed the existence of a quiescent leukemic population capable of reentering the cell cycle[10]. Thus, research spanning 25 years established heterogeneity in the capacity for proliferation within cancer. Additionally, these findings suggested that chemotherapies based on rapid proliferation would not eliminate the quiescent population[10].

Although results to this point were suggestive, the technology available at that time could not distinguish between the stochastic and cancer stem cell models. To support the cancer stem cell hypothesis, a tumorigenic population needed to demonstrate a stem cell-like phenotype distinct from the nontumorigenic cells. Additionally, it was essential that this tumorigenic population produce nontumorigenic cells. Conversely, the nontumorigenic population could not produce tumorigenic cells, consistent with the accepted unidirectional nature of differentiation. Recent advancements in technology permitted evaluation of these features. The introduction of cell sorters in the 1970's permitted isolation of individual cells from a heterogeneous sample. Initially though, cells could only be resolved based on size, DNA content or protein content. The ability to produce protein-specific antibodies in 1975 revolutionized cell sorting[11]. Cells could then be distinguished based on expression of particular proteins. The final necessary advancement was the ability to

reliably expand human cells *in vivo* using xenografts. With these technologies in place, cells could then be isolated based on protein expression, expanded in immunocompromised mice, and the resulting cells could be examined. Using this methodology, the specific cellular components of hematopoiesis were identified based on cell surface protein expression.

The first support to arise from these technological advancements was the identification of a subset of leukemia cells that shared cell surface markers with normal stem and progenitor cells[12]. These results indicated a differentiation hierarchy in cancer and implied a stem cell origin for cancer. What many considered to be definitive evidence was presented in 1994 when Lapidot et. al. demonstrated that tumorigenicity was restricted to the small subset of leukemia cells that shared cell surface expression patterns with normal hematopoietic stem cells[13]. With this data, a primary feature of the stochastic model was challenged. Every cell within the cancer did not possess the same tumorigenic capacity. Furthermore, the tumorigenic population displayed a stem cell phenotype.

Modern Evidence of Cancer Stem Cells in Hematological Malignancies

The first two cancers in which cancer stem cells were identified were acute myeloid leukemia (AML) and chronic myelogenous leukemia (CML). Initial reports indicated that the AML stem cell shared cell surface marker expression with normal hematopoietic stem cells ($CD34^+CD38^-$), although recent reports have challenged this phenotype[13-15]. This controversy may be due to reliance on engraftment into

immunocompromised mice as the primary assay of tumorigenicity. Recently, persistence of $CD34^+CD38^-$ AML stem cells has been shown to predict relapse in patients[16]. This provided the first evidence for the clinical relevance of cancer stem cells. This further showed that clinical correlations might more accurately identify tumorigenic populations than xenograft models. As in AML, the CML stem cell shares a phenotype with normal hematopoietic stem cells ($CD34^+CD71^-$)[17]. Additional characterization of the CML stem cell reported high aldehyde dehydrogenase activity[18].

Multiple myeloma has generally been considered to be a disease of plasma cells. Clonotypic plasma cells expand in the marrow, producing elevated levels of monoclonal antibodies in the blood. The multiple myeloma stem cell has been shown to phenotypically resemble a memory B cell, which differentiates into malignant plasma cells[19]. Subsequent analysis demonstrated that these clonotypic B cells are resistant to chemotherapy drugs used clinically to treat the disease[20]. Although multiple myeloma research lags behind that of leukemia, preclinical testing of a multiple myeloma stem cell-targeted therapy reported promising results. Multiple myeloma stem cells overexpress HLA class I, and an HLA class I-crosslinking antibody induced cytotoxicity[21]. Further testing should determine the clinical effectiveness of this treatment approach.

Similar to multiple myeloma, the prominent cells in Hodgkin lymphoma do not appear to drive the disease. In addition to the disease-defining Reed-Sternberg cells,

Hodgkin lymphoma contains a population of clonotypic memory B cells[22]. These cells generate Reed-Sternberg cells *in vitro* and likely represent the initiating cell in Hodgkin lymphoma[22]. Characterization of these cells also showed high aldehyde dehydrogenase activity[22].

Cancer Stem Cells in Solid Tumors

Knowledge of the normal differentiation hierarchy in hematopoiesis facilitated the identification of cancer stem cells in hematological malignancies. In addition to characterizing markers of each stage of hematopoiesis, this early work developed purification techniques as well as *in vivo* and *in vitro* functional assays. In contrast, identification of cancer stem cells in solid tumors is hampered by a lack of understanding of their normal counterparts. Markers of primitive cells must be empirically determined, which causes much controversy. Because of these difficulties, the first cancer stem cell in a solid tumor was not described until 2003 with the identification of tumorigenic breast cancer cells[23]. This work required evaluation of a variety of cell surface proteins in order to identify those with heterogeneous expression. Cells with high and low levels of expression were then compared for tumorigenicity in order to identify breast cancer stem cell markers. Since this early work, cancer stem cells have been reported in many types of solid tumors, including ovarian cancer.

Ovarian Cancer Stem Cells

Eighty percent of patients with advanced ovarian cancer show an initial clinical response to therapy, but seventy-five percent of these patients eventually relapse[24]. This transient clinical response would be consistent with the cancer stem cell hypothesis. The initial response could be attributed to the eradication of the bulk, differentiated cells. The persistence of drug resistant cancer stem cells could be responsible for the almost invariable relapse. Therefore, if the cancer stem cell hypothesis is accurate, ovarian cancer will likely contain a population of stem-like cells. A substantial body of recent evidence supports the cancer stem cell hypothesis in ovarian cancer. However, controversy exists regarding the phenotype of ovarian cancer stem cells. Additionally, their clinical relevance remains unclear.

In 2005, the first evidence for ovarian cancer stem cells described the enrichment of tumorigenic cells from patient samples using non-adherent culture[25]. This initial report initiated a body of research by describing the tumorigenic cells as $CD44^{+}$[25]. Several groups isolated $CD44^{+}$ ovarian cancer cells and reported the stem cell features of tumorigenicity, chemoresistance and expression of stem cell factors[25-31]. Clinical evaluation showed that a high percentage of $CD44^{+}$ cells correlates to shorter progression-free survival, but not overall survival[32, 33]. However, conflicting data challenges the use of CD44 as an ovarian cancer stem cell marker. Comparisons of tumorigenic and nontumorigenic ovarian cancer cells reported no difference in CD44 or reduced CD44 expression in the tumorigenic cells[34-37]. Furthermore, $CD44^{-}$

cells generated $CD44^+$ cells, which violates unidirectional differentiation if CD44 expression identifies ovarian cancer stem cells[30].

The second report of ovarian cancer stem cells employed side population for enrichment[34]. The side population phenotype is presumed to be the results of Hoechst 33342 dye extrusion due to increased expression of drug transporters, especially ABCG2[38, 39]. Ovarian cancer cells isolated based on the side population phenotype displayed the stem cell features of tumorigenicity, quiescence, chemoresistance and expression of stem cell genes[27, 34-36, 40-43]. Additionally, others reported increased expression of ABCG2 in their putative ovarian cancer stem cell population[29, 35, 44]. Clinically, relapsed patients demonstrated a higher percentage of side population cells compared to patients with primary, chemonaïve disease[41]. Although many reports support the use of side population as an ovarian cancer stem cell marker, conflicting reports also challenge this assertion. A survey of clinical samples only detected side population cells in one third of patients[45]. If side population enriches for ovarian cancer stem cells, all patients should possess this population. Although expression of ABCG2 is believed to cause the side population phenotype, expression of ABCG2 does not correlate with tumorigenicity[40, 46]. Finally, Hoechst 33342 dye induces cytotoxicity, causes DNA mutations and disrupts the cell cycle[47]. Because side population cells more efficiently remove the dye, their apparent increased tumorigenicity may in fact be due to the cytotoxic effects of the dye on non-side population cells.

The use of CD133 expression as an ovarian cancer stem cell marker began with the observation that $CD133^+$ primary tumor cells produce more cells than $CD133^-$ cells[48]. Subsequent work demonstrated multiple stem cell features in $CD133^+$ cells, including tumorigenicity, drug resistance, the ability to generate $CD133^-$ cells, and increased expression of stem cell genes[44, 49-53]. Evaluation of clinical specimens showed an increase in the percentage of $CD133^+$ cells in relapse tumors compared to primary tumors[54]. Furthermore, patients with $CD133^+$ cells showed a slightly poorer progression-free and overall survival than patients without $CD133^+$ cells[55]. However, for every stem cell feature reported in $CD133^+$ cells, conflicting data exists. Only 30-70% of patients possess any $CD133^+$ tumor cells[55, 56]. As with the side population phenotype, all patients should possess ovarian cancer stem cells. Furthermore, CD133 expression does not correlate with tumorigenicity[34, 46]. Both $CD133^+$ and $CD133^-$ cells produce tumors with heterogeneous CD133 expression, which would not occur if CD133 expression decreases with differentiation[50]. Finally, the percentage of $CD133^+$ cells in a patient's tumor provides no prognostic value[57, 58].

More recently, CD24 expression has been proposed to enrich for ovarian cancer stem cells. $CD24^+$ cells exhibited the stem cell features of tumorigenicity, chemoresistance, the ability to produce $CD24^-$ cells, and expression of stem cell genes[35, 59, 60]. However, a conflicting report showed stem cell features in $CD24^-$ cells instead[46]. While tumorigenic cells differentially express CD24, the direction of this difference varies[34].

Early reports of ovarian cancer stem cells indicated higher levels of KIT (CD117) expression, yet very few studies exclusively studied KIT. The one study that specifically compared KIT^+ to KIT^- cells demonstrated tumorigenicity in the KIT^+ population[61]. They additionally established a correlation between patients with detectable KIT^+ cells and chemoresistance[61]. The only other evidence for KIT as an ovarian cancer stem cell markers depends on measuring KIT expression in tumorigenic ovarian cancer cells isolated by other means. While some studies found increased KIT expression in tumorigenic cells, other studies detected the same or lower levels of KIT[25, 29, 34, 35, 44, 52]. Furthermore, only 40-45% of tumor samples contain any KIT^+ cells[56, 61].

The numerous reports of high aldehyde dehydrogenase 1 activity ($ALDH^{high}$) in normal and malignant stem cells have led some to propose that $ALDH^{high}$ ovarian cancer cells represent ovarian cancer stem cells[62-68]. $ALDH^{high}$ ovarian cancer cells display tumorigenicity, the ability to generate $ALDH^{low}$ cells, and chemoresistance[51, 56, 69-73]. Clinically, higher percentages of $ALDH^{high}$ cells correlate to poorer progression-free and overall survival[56, 69-71]. However, one study showed an improved prognosis with higher percentages of $ALDH^{high}$ cells[74]. In addition to this conflicting report, other inconsistencies exist. One study could not detect $ALDH^{high}$ cells in 23.1% of 65 ovarian cancer samples, however other studies detected $ALDH^{high}$ cells in all 18 and 25 samples tested[51, 56, 69]. Finally, some reports detected $ALDH^{high}$ cells in xenografts from $ALDH^{low}$ cells[51, 71].

The preponderance of evidence supports the existence of ovarian cancer stem cells. However, uncertainty remains surrounding the ideal marker for their isolation. For each proposed marker, reports exist both in support and opposition, and very few studies compare multiple markers. One study measured expression of CD44, CD133, CD24, KIT and ALDH1 in 13 primary tumors and five ascites samples. The only marker with limited expression in all samples was ALDH1[56]. Another study examined CD44 and ALDH1 expression in tumorigenic cells. Despite stable CD44 expression, the loss of ALDH1 activity correlated with reduced tumorigenicity[30]. These two studies support the use of ALDH1 expression as a marker of ovarian cancer stem cells over other proposed markers. Finally, expression of CD133 may enrich for endothelial progenitor cells to support the growth of the tumor, rather than ovarian cancer stem cells[75]. While this limited evidence begins to clarify the value of distinct ovarian cancer stem cell markers, further research is required.

Research Plan

I sought to test the hypothesis that ovarian cancer contains a population of stem-like cells. I selected two models of ovarian cancer for this study. The first is a rat model of ovarian cancer, termed FNAR-C1, that is described in detail in Chapter Two. Briefly, this spontaneously occurring ovarian tumor expands *in vivo* and forms tumors in immunocompetent rats. Histological evaluation determined that FNAR-C1 most closely resembles the endometrioid subtype. In order to control for potential subtype differences, the SKOV3 cell line was also utilized. The subtype of SKOV3

cells has been described as both clear cell and serous[76, 77]. In addition to the parental SKOV3 line, I also employed a taxol-resistant SKOV3 subline.

Next, I determined the methodology for isolation of putative ovarian cancer stem cells. At the initiation of this project, only two reports described stem-like cells in ovarian cancer. The isolation methods used nonadherent growth and side population. Tumorigenic cells expressed variable levels of cancer stem cell markers previously reported for other cancers (KIT, CD44, CD24 and CD133). Based on these results, I selected a marker not examined in these studies. High aldehyde dehydrogenase 1 (ALDH1) activity has been reported in many normal and malignant stem cells[62-68]. The ALDH superfamily of enzymes oxidizes intracellular aldehydes. Specifically, the ALDH1 family converts vitamin A into retinoic acid. On this basis, I chose high ALDH1 activity as a putative marker of ovarian cancer stem cells. In order to isolate viable cells on the basis of enzyme activity, I used the Aldefluor reagent developed in the laboratory of my advisor[78]. Aldefluor serves as a fluorescent substrate of ALDH1. BODIPY-acetaldehyde freely diffuses into cells, where ALDH1 converts it to BODIPY-retinoic acid. Once modified by ALDH1, Aldefluor can no longer exit the cell through passive diffusion. Fluorescence accumulates in cells with high ALDH1 activity, which can then be isolated with a cell sorter.

Once ovarian cancer cells were isolated based on ALDH1 activity, I tested the populations for cancer stem cell properties. On the basis of these tests, I confirmed that $ALDH^{high}$ cells represent a less differentiated population in ovarian cancer than

$ALDH^{low}$ cells. Next, I characterized expression differences between these populations to better understand the biology of ovarian cancer stem cells. Finally, expression patterns revealed potential therapeutic targets to more effectively treat ovarian cancer.

This project contributes to the understanding of ovarian cancer in several ways. First, FNAR-C1 cells provide a novel model for the study of ovarian cancer with advantages over current animal models. This model circumvents current controversy surrounding assessment of *in vivo* tumorigenicity in immunocompromised animals with its transplantability into immunocompetent rats. The cell line expands *in vitro*, allowing for more detailed analysis. Because the tumor arose spontaneously, it lacks artificial genetic manipulations that may not occur in the human disease. Overall, this model may serve as a valuable experimental model to improve understanding of the biology of ovarian cancer.

This project further supports the existence of ovarian cancer stem cells and the use of high aldehyde dehydrogenase activity as an ovarian cancer stem cell marker. Comparison of expression differences between stem and differentiated cells provides insight into the biological differences between these cell populations. Additionally, the use of models from two discrete ovarian cancer subtypes controls for potential subtype-specific differences. Since few studies compare the various proposed ovarian cancer stem cell markers, analyses included all previously reported markers. Finally, this project proposes potential therapeutic targets based on examination of expression

patterns, which has not yet been explored in detail. Thus, this project expands understanding of ovarian cancer stem cells with the purpose of designing targeted therapeutics.

Hypothesis

Ovarian cancer contains a population of cells with stem-like characteristics that is responsible for relapse.

Research Objectives:

1. Isolate and validate cancer stem cells in ovarian cancer
2. Characterize cancer stem cells in ovarian cancer
3. Identify potential therapeutic targets

2 Identification and characterization of a spontaneous ovarian carcinoma in Lewis rats.

Sharrow AC, Ronnett BM, Thoburn CJ, Barber JP, Giuntoli RL, Armstrong DK, Jones RJ, Hess AD. J Ovarian Res. 2010 Mar 31; 3:9.

Background

Ovarian cancer is the fifth most commonly diagnosed cancer in women and the fourth most common cause of death from cancer [79]. The high mortality can be attributed to the high percentage of affected women presenting at an advanced stage, with spread within the peritoneal cavity [80, 81]. With current therapies, including surgical debulking and platinum-based chemotherapy, patients in stage III or stage IV only have a 20% chance of long-term survival [80, 81]. Better understanding ovarian carcinoma biology, as well as the development of new therapies for the disease, has been hampered by the lack of suitable animal models.

Current ovarian cancer models fall into three broad categories: rare spontaneous carcinomas, induced tumors, and human xenografts [82]. Although these models have allowed researchers to gain valuable insights into the biology of ovarian cancer, each model exhibits important limitations [82, 83]. Spontaneous ovarian cancer has been observed in mice, rats, and hens [84-86]. The drawback to these models is that the cancers tend to occur at an advanced age and at similar low frequencies as in humans. The low incidence and the length of time required for the development of these tumors render them of limited use for studying the biology and treatment of ovarian carcinoma. Induced tumor models circumvent these problems but create their own artificial systems, which may not accurately reflect the human disease. In one model of *in vitro* transformation, ovarian surface epithelium cells are subcloned until they exhibit the loss of contact inhibition, the capacity for substrate-independent growth, cytogenetic abnormalities, and the ability to form tumors when injected subcutaneously and/or intraperitoneally into athymic mice [87]. This model, though, fails to account for critical interactions between the cancer cells and the host. Also, it is uncertain if these cells or their malignant transformation are representative of normal human cells or clinical disease.

Animal models have been generated by expressing simian virus 40 large T antigen [88], by inactivating p53 and Rb1 [89], by inactivating p53 and activating an oncogene [90], and through hormone treatment [91-93]. The high rate of cancer development in these animals makes these models attractive, but they may not reliably

represent human cancer because a majority of these genetic changes usually do not occur in patients. Xenografts of human cancers have undergone continuous improvement over the past twenty years [94-97]. These models allow for direct examination of the human cancer but do not allow the study of the early stages of the cancer. These models also rely on an immune-deficient host, which eliminates the interaction between the cancer and the immune system.

We present a new model of ovarian carcinoma, designated FNAR, that spontaneously developed in an untreated, previously normal Lewis rat. The tumor could be serially passaged both *in vivo* as malignant ascites in rats and *in vitro*. Importantly, the biologic characteristics of the tumor closely paralleled one type of human ovarian carcinoma.

Methods

Animals. Female Lewis strain rats aged 4-6 weeks (purchased from Charles River Breeding Laboratories, Inc., Wilmington, MA) were kept in sterile micro-isolator cages and fed food and water *ad libitum*. The institutional guidelines of Johns Hopkins University concerning the care and use of research animals were followed. The animals were challenged intraperitoneally with graded numbers of FNAR cells and monitored daily for abdominal swelling. At various intervals after tumor challenge or when animals appeared moribund (pallor, lethargy, and marked abdominal distension), the animals were sacrificed by CO_2 asphyxiation and the cells within the peritoneal cavity harvested by flushing the abdomen with 35 milliliters of

sterile phosphate buffered saline (PBS, Grand Island Biological Co., Gibco BRL, Grand Island, NY). At sacrifice, the animals were examined for tumor growth and tissues taken for histological examination.

In vitro propagation and growth curve. A cell line (FNAR) that grows *in vitro* as an adherent monolayer was established by culture in RPMI 1640 (Gibco) supplemented with 10% fetal calf serum in 30 ml tissue culture flasks (Corning Flask 3056, Corning Inc., Corning NY). Cells used for experiments were low passage and maintained in culture for one to three months. The doubling time of the cell line was measured by plating 10^4 cells into macrotiter wells then harvesting and counting at 19.5, 43.5, and 115.5 hours.

Flow Cytometric Analysis. Flow cytometry was utilized to assess *in vitro* FNAR cells for expression of known phenotypic markers. Briefly, 5 x 10^5 tumor cells were incubated in polystyrene tubes. Analysis of the intracellular antigens estrogen receptor α, progesterone receptor, and androgen receptor first required fixation in 2% formaldehyde (Polysciences, Warrington, PA) in phosphate buffered saline (PBS, Gibco Invitrogen, Carlsbad, CA) for 15 minutes at 4°C followed by permeabilization with 0.1% Triton-X-100 (Sigma-Aldrich, St. Louis, MO) in PBS for 15 minutes at 4°C. The cells were then incubated for 30 minutes at 4°C with commercially purchased murine monoclonal antibodies. The concentrations of antibodies used are as follows: estrogen receptor (ER) α at 8 $\mu g/10^6$ cells (Abcam, Cambridge, MA), progesterone receptor (PR) at 16 $\mu g/10^6$ cells (Affinity Bioreagents, Golden, CO), or

androgen receptor (AR) at 2 μg/10^6 cells (Pharmingen, San Diego, CA). The cells were washed and counterstained with phycoerythrin (PE) rat anti-mouse IgG_1 (Becton Dickinson, San Jose, CA) at 125 ng/10^6 cells for 30 minutes at 4°C. Commercially purchased murine monoclonal antibody to the rat c-neu oncogene product (Calbiochem, San Diego, CA) was used at 1 μg/10^6 cells and was counterstained with PE rat anti-mouse IgG_{2a+b} (Becton Dickinson, San Jose, CA) at 30 ng/10^6 cells for 30 minutes at 4°C. Tumor cells incubated with secondary antibody alone served as a negative control. Epithelial cell adhesion molecule (EPCAM) expression was analyzed using a PE-conjugated antibody (Santa Cruz, Santa Cruz, CA) at 1 μg/10^6 cells with mouse IgG_1-PE as a negative control (Becton Dickinson, San Jose, CA). A commercially available rabbit polyclonal antibody to CA125 (Abbiotec, San Diego, CA) was used at 2 μg/10^6 cells and counterstained with 1 μg/10^6 cells APC goat anti-rabbit IgG (Invitrogen Molecular Probes, Carlsbad, CA). The cells were analyzed on a Becton-Dickinson FACSCalibur flow cytometer and data was analyzed using FlowJo (Tree Star, Inc, Ashland, OR).

Immunocytochemistry. FNAR cells were plated onto four-well CultureSlides (BD Falcon, San Jose, CA). Cells were fixed in 2% formaldehyde in PBS for 20 minutes followed by permeabilization in 0.5% Triton X-100 in PBS for 10 minutes. Cells were then incubated with a mouse monoclonal antibody to beta-catenin conjugated to Cy3 (Abcam, Cambridge, MA) at 6 μg/ml for one hour and counterstained with 500 ng/ml DAPI for five minutes (Invitrogen Molecular Probes,

Carlsbad, CA). Images were captured using the Nikon Eclipse E800 (Tokyo, Japan) at 200x magnification with standard filters for DAPI and Cy3, the DS-QiMc digital camera (Nikon, Tokyo, Japan), and the Advanced Research Elements AR 3.0 software (Nikon, Tokyo, Japan).

Gene Expression Analysis by cDNA Microarrays. RNA was extracted and purified from cell lysates of 1-5 x 10^5 *in vitro* FNAR tumor cells and the REH cell line of normal rat endothelial cells, as a control, with 500 µl Trizol reagent (Invitrogen, Carlsbad, CA). Tissue samples were frozen in liquid nitrogen and pulverized with a mortar and pestle. The powder was dissolved in Trizol and centrifuged. Purified RNA was dissolved in 20µl diethyl-pyrocarbonate-treated distilled water. The resulting RNA was analyzed at the Johns Hopkins microarray core. RNA from control and experimental samples was processed using the RNA amplification protocol described by Affymetrix (Affymetrix Expression Manual). Briefly, 5 µg of total RNA was used to synthesize first strand cDNA using the SuperScript Choice System (Invitrogen, Carlsbad, California) and oligonucleotide primers with 24 oligo-dT plus the T7 promoter (Proligo LLC, Boulder, Colorado). Following the double stranded cDNA synthesis, the product was purified by phenol-chloroform extraction and biotinilated anti-sense cRNA was generated through *in vitro* transcription using the BioArray RNA High Yield Transcript Labeling Kit (ENZO Life Sciences Inc., Farmingdale, New York). Fifteen µg of the biotinilated cRNA was fragmented at 94°C for 35 minutes in buffer (100mM Tris-acetate, pH 8.2, 500mM potassium

acetate, and 150mM magnesium acetate), and 10μg of total fragmented cRNA was hybridized to the Affymetrix GeneChip rat 230 2.0 array (Santa Clara, CA) for 16 hours at 45ºC with constant rotation (60 rpm). Affymetrix Fluidics Station 450 was then used to wash and stain the chips with a streptavidin-phycoerythrin conjugate. The staining was then amplified as follows: blocking was performed using goat IgG, then a biotinilated anti-streptavidin antibody (goat) was bound to the initial staining, and amplification was completed by the addition of a streptavidin-phycoerythrin conjugate. Fluorescence was detected using the Affymetrix 3000 7G GeneArray Scanner and image analysis of each GeneChip was done through the GeneChip Operating System 1.4.0 (GCOS) software from Affymetrix using the standard default settings. For comparison between different chips, global scaling was used to scale all probesets to a user defined target intensity (TGT) of 150.

Quantitative RT-PCR for Cytokine Expression. Quantitative RT-PCR (Taqman, Applied Biosystems, ABI, Foster City, CA) was utilized to assess levels of cytokine mRNA transcripts of *in vitro* FNAR cells as previously described [98]. The oligonucleotide primers and fluoresceinated probes for the cytokine genes (IL-6, IL-12, and IL-18), ER, PR, and stathmin were purchased from ABI. Data were analyzed in real-time with Sequencer Detection version 1.6 software, with the results normalized against mRNA transcripts for the housekeeping gene glyceraldehyde-3-phosphate dehydrogenase (GADPH).

Results

Description of proband. Examination of a normal female Lewis rat sacrificed for harvesting normal splenic T cells showed a spontaneously occurring tumor (approximately 0.5 cm^3) derived from the left ovary and attached to and invading the abdominal wall (Figure 2.1A). In addition, tumor studding was observed at several sites on the wall of the peritoneum, and ascites was present. Histologic evaluation revealed an epithelial neoplasm with features most consistent with an adenocarcinoma (Figure 2.1B). The tumor was composed of nests displaying admixed cribriform and solid architecture. The tumor cells had modest amounts of amphophilic/eosinophilic cytoplasm and relatively uniform, moderately atypical oval nuclei that were predominantly vesicular to modestly hyperchromatic with small nucleoli. Occasional mitotic figures and apoptotic bodies were noted, as was focal necrosis. Based on analogy to human ovarian epithelial tumors, this tumor most closely resembled a moderately differentiated endometrioid carcinoma (a cribriform variant of that subtype, with cells being less columnar than the classical human endometrioid carcinoma), with disease distribution paralleling a typical high-stage (human FIGO stage IIIB) ovarian carcinoma. Lymphocyte infiltration into the tumor mass was minimal at best, although numerous lymphocytes were present in the peritoneal fluid. The tumor was excised and pushed through a 100 micron wire mesh screen to obtain a single cell suspension.

Figure 2.1: Gross and Histologic Examination of Proband

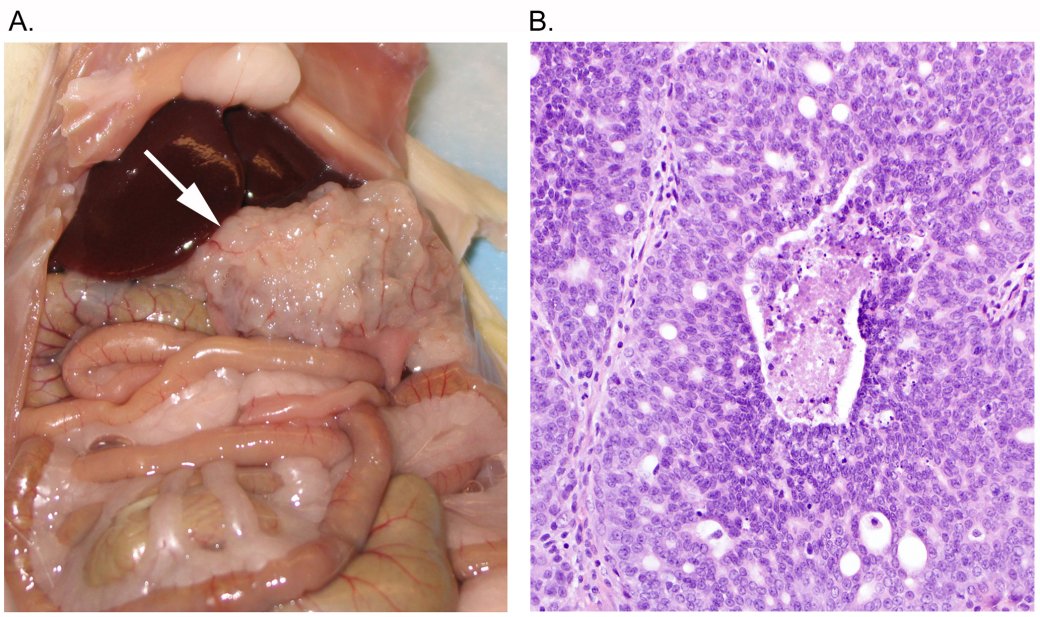

Intraperitoneal tumor arising spontaneously in a Lewis rat has pathologic appearance of an ovarian adenocarcinoma. (A) Proband shows tumor of the left ovary and intraperitoneal tumor studding. (B) Histology reveals an adenocarcinoma.

In vivo and in vitro growth characteristics. Normal Lewis rats were given either intraperitoneal (IP) or subcutaneous injection of graded numbers (5×10^4, 1×10^5, 5×10^5, or 1×10^6) of tumor cells. The animals were monitored daily for overall general health as well as degree of abdominal extension. The tumor repeatedly failed to grow subcutaneously, even with the administration of systemic immunosuppression (Cyclosporine, 10 mg/kg/d) or passage into thymectomized animals. However, all rats became moribund at 150-160 days after IP injection with 5×10^5 or 1×10^6 cells (Table 2.1). Rats injected with 1×10^5 cells became moribund around 175 days. Rats receiving IP injections of 5×10^4 cells generally did not appear ill by 6 months, but

tumor cells were detected in the peritoneal cavity when sacrificed on day 175. Tumor growth recapitulated that seen in the initial rat with IP tumoral masses adhering to all of the visceral organs and the abdominal wall. Histologically, the tumors appeared to be of epithelial origin. Affected rats also showed enlargement of the ovaries and fallopian tubes, with a marked increase in vascularization. Successful serial passage was conducted by IP challenge with 1 X 10^5 tumor cells harvested by flushing of the peritoneal cavity.

Table 2.1: Survival After Intraperitoneal Injection of FNAR Cells

Survival Following Tumor Challenge		
No. of Cells Injected	**No. of Animals**	**Survival – Days (No. of Animals)**
5 X 10^4	N = 6	175 (6)
1 X 10^5	N = 8	150 (4) 155 (3), 160 (1)
5 X 10^5	N = 6	155 (2), 160 (4)
1 X10^6	N = 6	150 (5), 152 (1)

The survival time of rats corresponds to the number of FNAR cells injected intraperitoneally. Animals were observed daily for general health and abdominal extension. The animals were sacrificed upon becoming moribund, which was characterized by extreme lethargy, paleness, and abdominal extension. The abdominal cavity was examined histologically for the presence of tumor cells in the peritoneal fluid and for tumor masses attached to the visceral organs and the abdominal wall.

The doubling time of the FNAR cell line was measured by plating 10^4 cells into macrotiter wells then harvesting and counting at 19.5, 43.5, and 115.5 hours (Figure 2.2). The slope of the line of log number of tumor cells versus hours estimates a doubling time of 22.9 hours.

Figure 2.2: *In Vitro* Growth Characteristics

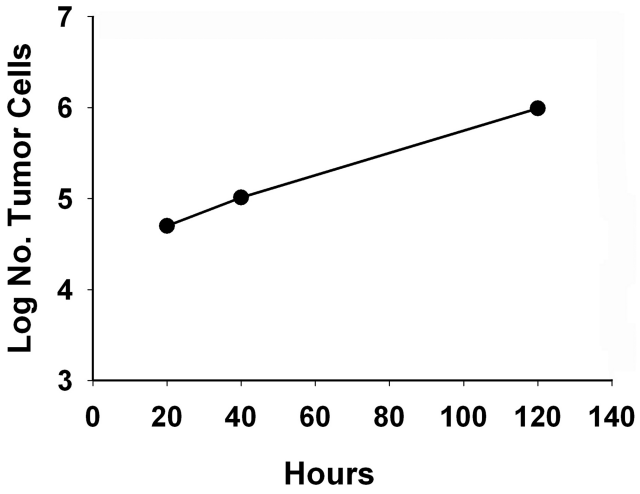

In vitro doubling time was measured by plating 10^4 cells into large flat bottom macrotiter wells. At the designated intervals, cells were harvested and counted. Data is presented as log number of tumor cells versus growth time. The slope of the line represents an estimate of the doubling time.

Biological characterization of FNAR. ER is detected in 60-90% of ovarian carcinomas [99-103], 25-50% express PR [99, 101-104], and 45% expressed both [101, 103]. AR is expressed in 50-70% of ovarian carcinomas [102, 104]. Accordingly, in the appropriate clinical and pathologic setting, sex hormone receptor expression is characteristic of ovarian carcinoma [103, 105]. The tumor expressed ER, PR, and AR by flow cytometry (Figure 2.3A-C), with ER and PR confirmed by PCR (data not shown). The tumor also expressed her-2/neu (Figure 2.3D), which is expressed in 25-35% of ovarian carcinomas [106, 107]. The epithelial origin of this carcinoma was confirmed by its expression of EPCAM (Figure 2.3E). Consistent with previous reports of endometrioid carcinoma, FNAR cells display cell-surface expression of CA125 (MUC16, data not shown) [108]. FNAR cells also show nuclear staining of ß-catenin (Figure 2.4), which is strongly associated with the endometrioid subtype [109].

Figure 2.3: FNAR Expression of ER, PR, AR, Her-2/neu, and EPCAM

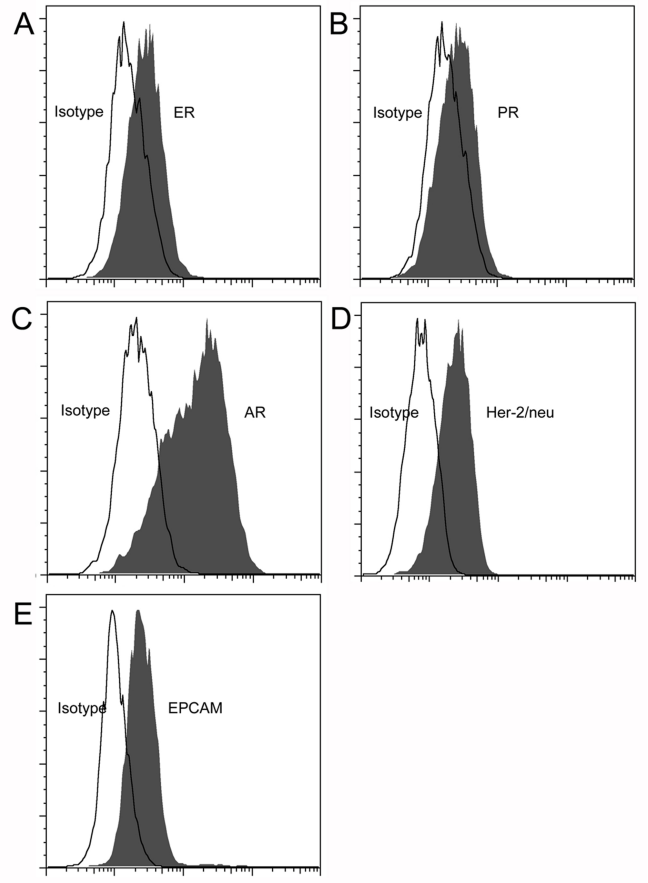

Flow cytometric evaluation of FNAR cells for expression of (A) ER, (B) PR, (C) AR, (D) Her-2/neu, and (E) EPCAM. In all five graphs, isotypic control is shown with a solid line and the antibody of interest is shown with a shaded area.

Figure 2.4. FNAR Expression of ß-catenin

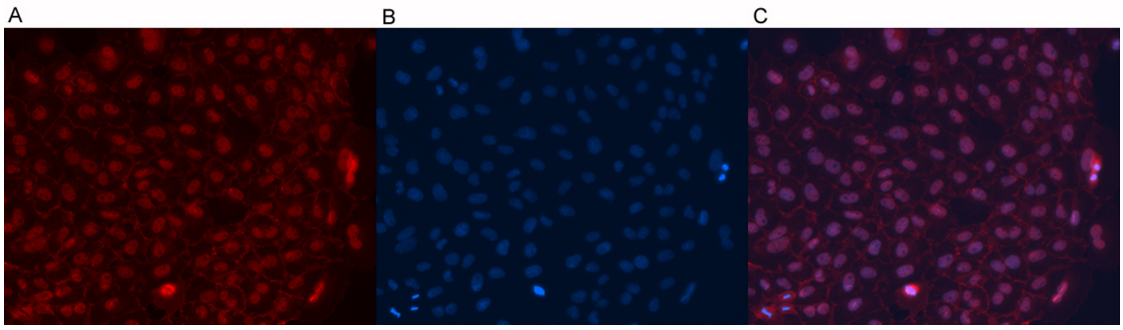

FNAR cells were stained with (A) ß-catenin and (B) DAPI. The third panel (C) shows an overlay of the two images.

Gene expression profiling demonstrated that FNAR gene expression was similar to that reported for human ovarian carcinoma (Table 2.2). Metallothioneins are generally not found at immunohistochemically detectable levels in normal cells, but their expression increases in ovarian carcinoma with increasing grade [110-112]. Metallothionein I was overexpressed 11.38-fold in FNAR cells when compared to endothelial cells, and metallothionein II showed 3.56-fold increased expression.

Table 2.2: Gene Chip Analysis of FNAR

Gene Expression Profiling of FNAR Cells

Gene Description	EST Accession #	Relative Expression
Metallothionein I	AW141679	11.38
Metallothionein II	AW916991	3.56
Thioredoxin	AW140607	3.07
Stathmin	BF281472	3.23
b-myb	RGIAC37	3.33

Gene chip analysis of FNAR shows similarities to human ovarian carcinoma. RNA was harvested from FNAR and REH endothelial cell lines and analyzed by GeneChip at a Johns Hopkins core facility. Data are presented as the relative expression of the gene in FNAR compared to expression in endothelial cells.

Thioredoxin expression correlates with cis-diaminedichloroplatinum resistance [113] and is expressed in FNAR cells 3.07-fold higher than in endothelial cells. Stathmin regulates microtubules during the formation of the mitotic spindle and is not expressed at detectable levels in normal cells; however, high-level expression is generally seen in ovarian carcinoma [114-116]. Accordingly, stathmin expression was 3.23-fold higher in FNAR cells than in endothelial cells. This data was confirmed by PCR (data not

shown). A nuclear factor that it is involved in cell cycle progression, b-myb, is also highly expressed in both FNAR cells (3.33-fold) and human ovarian carcinoma [117].

High levels of interleukin-6 (IL-6), a proinflammatory cytokine and hematopoietic growth factor, are found in both normal ovarian epithelium and human ovarian carcinoma [118, 119]. Interleukin-18 (IL-18) is a proinflammatory cytokine that stimulates interferon-γ production. Ovarian carcinoma expresses IL-18, but it is predominantly the pro-IL-18 form [120]. Interleukin-12 (IL-12) is a cytokine that encourages a T_h1 immune response. IL-12 has been detected in ascites fluid and serum of ovarian cancer patients [121], although no reports have examined the expression of IL-12 by the ovarian carcinoma cells themselves. Expression of all three cytokines by FNAR cells was detected by real time RT-PCR (Figure 2.5).

Figure 2.5: FNAR Expression of IL-6, IL-12, and IL-18

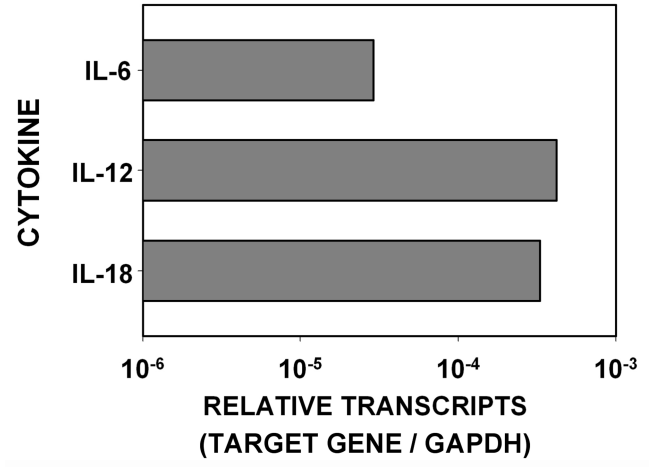

FNAR tumor cells express IL-6, IL-12, and IL-18. Expression was assessed by qPCR. Data are standardized against GAPDH.

Discussion

We present here a model of ovarian carcinoma, designated FNAR, that arose spontaneously in a normal Lewis rat. Importantly, FNAR's biology closely parallels the human disease. IP transplantation into rats produces malignant ascites and peritoneal carcinomatosis, leading to death at 5-6 months. The tumor only develops in the peritoneal cavity, suggesting the tumor microenvironment is intact during formation. Cells from the tumor can be easily passaged *in vitro,* and the cell line shows similar growth characteristics when returned to rats. Its morphology and expression of EPCAM are consistent with an epithelial carcinoma, and like human ovarian carcinoma, it expresses her-2/neu, sex hormone receptors, and characteristic cytokines. FNAR also displays a similar gene expression pattern to the human disease. Consistent with the endometrioid subtype, FNAR cells show cell-surface expression of CA125 and nuclear expression of ß-catenin.

The FNAR model may address many of the limitation of current model systems for ovarian carcinoma. Rats transplanted with FNAR consistently become moribund by 5-6 months, avoiding the low frequency and long latency of spontaneous animal models. Xenografts of primary human tumors in immunodeficient mice are perhaps the most attractive current model [94-97]. Although spontaneous human cancers can be studied and used to test treatments in these mice, the study of immunotherapeutic approaches is problematic. Conversely, FNAR develops in immunocompetent rats, allowing the study of immunotherapeutic approaches. The

expression of all three sex hormone receptors and her-2/neu also allows for manipulations of these pathways using this model. However, the application of this model to the treatment of human disease remains to be established.

3 Materials and Methods

Cell Lines and Culture

FNAR-C1 rat ovarian cancer cells were obtained as previously described[122]. The human ovarian cancer cell line SKOV3 and taxol-resistant SKOV3 cells were the kind gifts of Drs. Alexander Stoeck, Tian-Li Wang and Ie-Ming Shih. Cells were maintained in two different media. The first was KnockOut medium, which is a proprietary serum-free medium designed for culturing embryonic stem cells in an undifferentiated state and consists of KnockOut DMEM (Life Technologies, Grand Island, NY) with 10% KnockOut Serum Replacement (Life Technologies, Grand Island, NY), 2 mM L-glutamine (Life Technologies, Grand Island, NY), 100 U/mL

penicillin (Life Technologies, Grand Island, NY) and 100 μg/mL streptomycin (Life Technologies, Grand Island, NY). Cells were also cultured in standard medium: RPMI (Life Technologies, Grand Island, NY) with 10% FBS (Sigma, St. Louis, MO), 2 mM L-glutamine, 100 U/mL penicillin and 100 μg/mL streptomycin. For reasons described in Chapter 4, standard medium will hereafter be referred to as differentiation medium. Taxol-resistant SKOV3 cells were continuously incubated with 33.3 nM paclitaxel (taxol; Sigma-Aldrich, St. Louis, MO). Cells were expanded in vented T175 tissue culture flasks.

Cell Sorting

For cell sorting, adherent cells were released from flasks with 0.05% trypsin-EDTA (Life Technologies, Grand Island, NY) and pipetting. Cells were stained with Aldefluor reagent (STEMCELL Technologies Inc., Vancouver, BC, Canada) using the manufacturer's protocol then stained with 0.5-1 μg/mL propidium iodide (Sigma-Aldrich, St. Louis, MO) for 5 minutes. FNAR-C1 cells grown in KnockOut medium were sorted using a MoFlo cell sorter (Beckman Coulter, Miami, FL). Because of substantial death after sorting, these cells were allowed to recover before use in the following experiments: doubling time, cell cycle analysis and drug resistance. No greater than $3x10^6$ cells were plated in KnockOut medium in vented T175 tissue culture flasks for three to four days. After this time, cells were released from the flasks using trypsin and pipetting as described above. All other cells were sorted using

a FACSAria II cell sorter (BD Biosciences, San Jose, CA). Representative images were generated using FlowJo 8 (Tree Star, Inc, Ashland, OR).

Photomicrographs

Sorted cells were plated into 6-well tissue culture plates. When cells were at the desired level of confluency, photomicrographs were generated using a Nikon Eclipse TE2000E with 4x, 10x and 20x phase contrast objectives; Nikon DS-Qi1Mc CCD camera; and Nikon NIS Elements 3 software (Nikon Instruments Inc., Melville, NY).

Cell Size Analysis

Unsorted cells were trypsinized then stained with Aldefluor and propidium iodide as described above. Cells were analyzed on a FACSCalibur flow cytometer (BD Biosciences, San Jose, CA) and plots were generated using FlowJo 8.

Doubling Time

Sorted cells were plated into vented T25 tissue culture flasks with the medium they were cultured in prior to sorting. At 24-hour intervals ranging from 24 to 120 hours, cells were released from flasks with trypsin and pipetting as described above. FNAR-C1 cells grown in KnockOut medium and sorted for Aldefluor high tended to form aggregates, which were disrupted after trypsinization using Accumax and pipetting (EMD Millipore, Billerica, MA). Viable cells were counted by mixing cells

with an equal volume of trypan blue (Life Technologies, Grand Island, NY) and pipetting onto a hemacytometer (Hausser Scientific, Horsham, PA). Ten 1 mm^2 squares were counted and averaged to obtain the final cell count. Time points that appeared to be in lag phase or plateau phase were excluded from the doubling time calculations. Doubling times were calculated using an online doubling time calculator (Roth V. 2006 http://www.doubling-time.com/compute.php). Graphs were generated using Excel 2008 for Mac (Microsoft, Redmond, WA).

Cell Cycle Analysis

Sorted cells were allowed to recover overnight after sorting. No more than $5x10^5$ Aldefluor low FNAR-C1 or SKOV3 cells were plated into vented T75 tissue culture flasks with differentiation medium. $1.75x10^5$ Aldefluor high taxol-resistant SKOV3 cells were plated in a vented T25 tissue culture flask with KnockOut medium. Cells were released from flasks using trypsin and pipetting as described above. Aldefluor high FNAR-C1 cells were harvested from recovery flasks as described in Cell Sorting. No greater than $2.5x10^5$ cells were resuspended in 2 ml ice-cold PBS (Life Technologies, Grand Island, NY). Cells were fixed with the dropwise addition of 1 ml ice-cold methanol (Fisher, Waltham, MA) then incubated overnight at 4°C. Cells were rehydrated in PBS then stained with 50 μg/ml propidium iodide and 10 μg/ml RNase (Roche, Indianapolis, IN) in PBS for 30 minutes at room temperature. Data was collected on a FACSCalibur flow cytometer and analyzed using FlowJo 8.

Microarray and Pathway Analysis

Cells were sorted into RNAprotect Cell Reagent (Qiagen, Valencia, CA) to preserve RNA. Total RNA was isolated from sorted cells using the RNeasy Mini Kit with QIAshredder columns (Qiagen, Valencia, CA). Quality assessment and microarray analysis was performed at The Sidney Kimmel Cancer Center Microarray Core Facility at Johns Hopkins University, supported by NIH grant P30 CA006973 entitled Regional Oncology Research Center. RNA quality was determined with a NanoDrop ND-1000 spectrometer (Thermo Scientific, Waltham, MA) for OD260/280 and OD260/230 ratio and a 2100 Bioanalyzer (Agilent Technologies, Santa Clara, CA).

The following rat samples were analyzed: FNAR-C1 grown in differentiation medium and sorted for Aldefluor low, and FNAR-C1 grown in KnockOut medium and sorted for Aldefluor high. Rat samples were analyzed using the Rat Gene Expression Microarray 4x44K v3 (Agilent Technologies, Santa Clara, CA). Sample amplification and labeling procedures were carried out using the Low RNA Input Fluorescent Linear Amplification Kit (Agilent Technologies, Santa Clara, CA) with minor modifications. Briefly, 0.4 μg total RNA was reverse-transcribed into cDNA by MMLV-RT using an oligo(dT) primer that incorporates a T7 promoter sequence (System Biosciences, Mountain View, CA). The cDNA was then used as a template for *in vitro* transcription in the presence of T7 RNA polymerase and Cyanine-3 (Cy3) labeled CTP (Perkin Elmer, Waltham, MA). Labeled cRNA was purified using the

RNeasy Mini Kit. RNA spike-in controls (Agilent Technologies, Santa Clara, CA) were added to RNA samples before amplification and labeling according to manufacturer's protocol. 0.825 μg of each Cy3-labeled sample was used for hybridization at 65ºC for 17 hours in a hybridization oven with rotation. After hybridization, microarrays were washed and dried according to the Agilent microarray processing protocol using Stabilization and Drying Solution (Agilent Technologies, Santa Clara, CA). Microarrays were scanned using an Agilent G2565AA Scanner controlled by Agilent Scan Control 7.0 software (Agilent Technologies, Santa Clara, CA). Data were extracted with Agilent Feature Extraction 9.5.3.1 software (Agilent Technologies, Santa Clara, CA).

The following human samples were analyzed: SKOV3 grown in differentiation medium and sorted for Aldefluor low, and taxol-resistant SKOV3 grown in KnockOut medium and sorted for Aldefluor high. Human samples were analyzed using the Human HT-12 v4 bead chip (Illumina, San Diego, CA). 500 ng of total RNA from each sample was amplified and labeled using the Illumina Total Prep RNA Amplification Kit (Ambion, Austin, TX) as described in the instruction manual. For array assay, 750 ng biotin-labeled cRNA was combined with hybridization buffer and hybridized to the array at 58°C for 16-20 hours. After hybridization, the hybridization cartridge was disassembled and the array was washed with buffer at 55°C and blocked at room temperature. Bound biotinylated cRNA was stained with streptavidin-Cy3 and then washed. Dried arrays were stored in a dark box until scanned with the iScan

System (Illumina, San Diego, CA). Data were extracted with the Gene Expression Module in GenomeStudio Software (Illumina, San Diego, CA).

Microarray data were further analyzed, especially for differentially regulated pathways, using iReport (Ingenuity® Systems, www.ingenuity.com, Redwood City, CA). Data from iReport only shows genes above the fold-change cutoff used for pathway analysis, which was 2.5 for FNAR-C1 cells and 1.5 for SKOV3 cells. For genes below the 1.5-fold SKOV3 cutoff and between 1.5- and 2.5-fold change in FNAR-C1 cells, data was analyzed using GeneSpring GX software version 11 (Agilent Technologies, Inc, Santa Clara, CA). Normalization was done with all intensities higher than 5, log2 transformation and cross-array quartile normalization. For FNAR-C1 genes below the 1.5-fold cutoff, fold-change was calculated manually from the Agilent Feature Extraction output.

PCR Validation of Microarray

PCR validation of microarray data used custom 96-well TaqMan array plates (Life Technologies, Grand Island, NY). For FNAR-C1 samples, RNA came from the same isolation as the microarray experiment. For SKOV3 samples, cells were sorted as described for the microarray. The rest of the procedure was performed at The Sidney Kimmel Cancer Center Microarray Core Facility at Johns Hopkins University, supported by NIH grant P30 CA006973 entitled Regional Oncology Research Center. RNA was isolated using TRIzol isolation followed by the RNeasy Mini Kit. cDNA synthesis was performed using the High Capacity RNA-to-cDNA Kit (Life

Technologies, Grand Island, NY). 20 ng of cDNA was added to each well of the custom TaqMan array plates along with TaqMan Universal PCR Master Mix (Life Technologies, Grand Island, NY) in a final volume of 20 µl. Each sample was assayed in triplicate using three identical plates. Data was collected using the ABI 7500 Real-Time PCR System (Life Technologies, Grand Island, NY). Data was analyzed using 7500 Fast System SDS software version 1.4 (Life Technologies, Grand Island, NY). For FNAR-C1 samples, CXCL1 was used as the endogenous control. For SKOV3 samples, EEF1A1 was used as the endogenous control.

Regeneration of Phenotypic Diversity Assay

Sorted cells were plated into vented T25 tissue culture flasks with either KnockOut or differentiation medium. After four days of culture, cells were released from the plastic as described above and stained with Aldefluor and propidium iodide as described above. Cells were analyzed on a FACSCalibur flow cytometer. Plots were generated using FlowJo 8.

***In vivo* Tumorigenicity**

Cells were stained with Aldefluor and PI then sorted as described above. However, FNAR-C1 cells from KnockOut medium were sorted using a FACSAria 1 or 2 and were not recovered in culture after sorting. Sorted cells were counted and resuspended in RPMI such that injection of 1 ml provided the desired cell dose. Female Lewis rats received intraperitoneal injections with graded numbers of cells.

Rats were monitored weekly and euthanized when becoming moribund or when tumors were detected by palpating the abdomen. Two years after the injection date, any remaining rats were euthanized and necropsy was performed to evaluate the presence of undetected cancer. All animals were handled in accordance with the Johns Hopkins University Animal Care and Use guidelines. All tumors underwent histological evaluation in a blinded manner to exclude any spontaneously occurring tumors. Statistical significance was calculated using the Fisher's Exact Test in EpiStat.

In Vitro Drug Resistance

Sorted cells were plated at a density of 100 cells per well into 24-well tissue culture plates with six wells per condition. FNAR-C1 cells were plated in differentiation medium with the following concentrations of paclitaxel (taxol): 10 nM, 20 nM, 40 nM, and 60 nM ($ALDH^{high}$: n=4; $ALDH^{low}$: n=5). Taxol-resistant SKOV3 cells were plated in differentiation medium with the following concentrations of taxol: 100 nM (n=6), 200 nM (n=7), 400 nM (n=8), 600 nM (n=7), and 800 nM (n=3); the following concentrations of carboplatin (Sigma-Aldrich, St. Louis, MO): 250 ng/ml (n=1), 500 ng/ml (n=5), 750 ng/ml (n=5), 1 μg/ml (n=5), and 1.25 μg/ml (n=4); and the following concentrations of gemcitabine (Gemzar; Eli Lilly and Company, Indianapolis, IN): 2 nM (n=3), 3 nM (n=3), 4 nM (n=5), 5 nM (n=5), 6 nM (n=2), and 7 nM (n=2). Cells were continuously exposed to taxol and gemcitabine. Cells were

incubated with carboplatin for 72 hours, which was then washed off and replaced with fresh medium. Cells were examined weekly with a Nikon Eclipse T1-S with 4x, 10x and 20x objectives (Nikon Instruments Inc., Melville, NY). Growth was defined as at least one colony of greater than ten cells in a well and data is presented as the percentage of wells that grew relative to no drug control. Data for FNAR-C1 cells is from two to four weeks of growth. Data for taxol-resistant SKOV3 cells is from two to three weeks of growth. Graphs were generated using Excel 2008 for Mac. Statistical significance was determined using Excel 2008 for Mac to calculate the unpaired, 2-tailed Student's t-test. For drug concentrations with only two data points per population, the unpaired, 2-tailed Student's t-test was calculated using GraphPad QuickCalcs (http://www.graphpad.com/quickcalcs/ttest1/).

Resistance to taxol was additionally evaluated by determining the percentage of $ALDH^{high}$ cells remaining after treatment. Unsorted FNAR-C1 and SKOV3 cells were plated in differentiation medium with or without taxol. For FNAR-C1, n = 3 for no drug and n = 4 for taxol. Taxol doses ranged from 10 nM to 1 μM for 72 hours. For SKOV3, five individual assays were performed comparing SKOV3 cells to taxol-resistant SKOV3 cells continuously cultured in the presence of 33.3 nM taxol. Cells were released from plastic then stained with Aldefluor and propidium iodide as described above. Data was collected on a FACSCalibur flow cytometer and analyzed using FlowJo 8. Plots were generated using Excel 2008 for Mac and p-values were calculated using the unpaired, 2-tailed Student's t-test.

4 Results

Aldefluor Defines Distinctive Populations

Initial observations of the FNAR-C1 rat model of ovarian cancer showed a small aldehyde dehydrogenase 1 high ($ALDH^{high}$) population, as measured with the Aldefluor reagent. However, continued culture in standard medium containing serum resulted in the loss of $ALDH^{high}$ cells. Serum has been reported to promote the differentiation of stem cell populations; and for this reason, standard medium with serum will be referred to as differentiation medium[123-126]. Despite numerous attempts, it was not possible to identify a culture condition that maintained both $ALDH^{high}$ and $ALDH^{low}$ populations. However, culturing FNAR-C1 cells in Knockout medium,

which is a proprietary, serum-free medium designed for the maintenance of embryonic stem cells in an undifferentiated state, maintained a large ALDH^{high} population.

Figure 4.1: Aldefluor Sorting

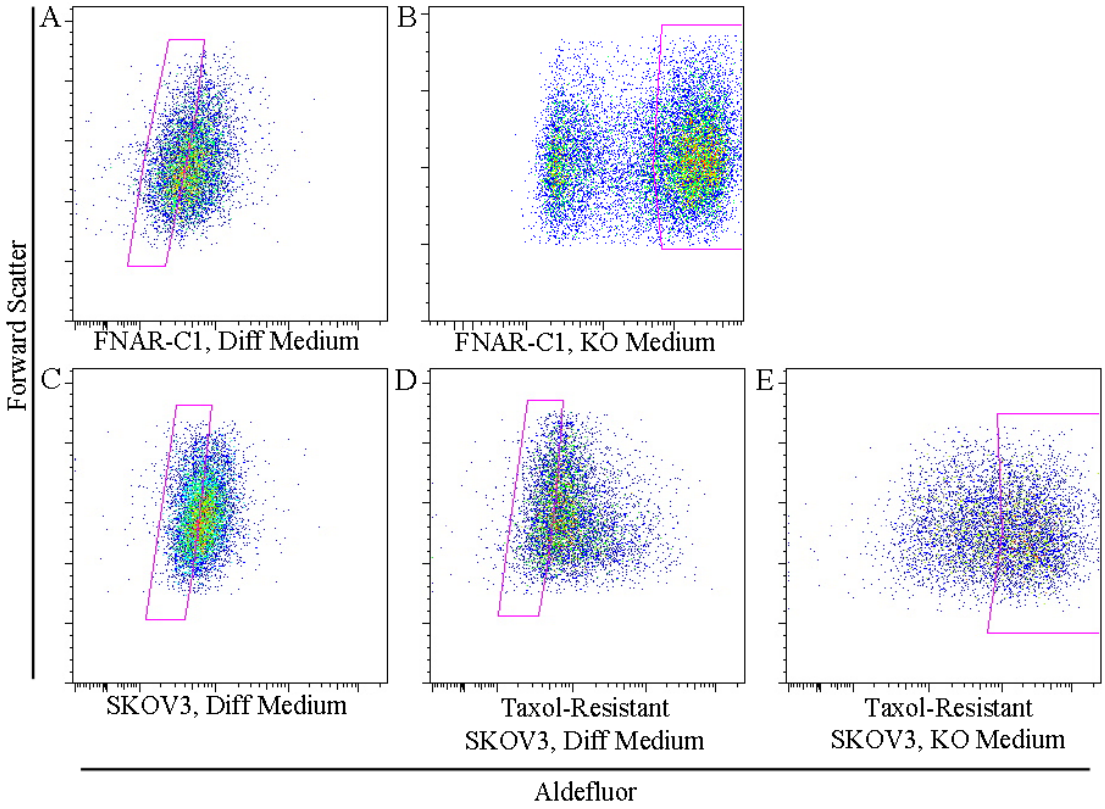

Representative samples of sorting gates are shown. All gating used DEAB as a negative control. (A) FNAR-C1 cells grown in differentiation medium were sorted for the Aldefluor low population. (B) FNAR-C1 cells grown in KnockOut medium were sorted for the Aldefluor high population. (C) SKOV3 cells grown in differentiation medium were sorted for the Aldefluor low population. (D) Taxol-resistant SKOV3 cells grown in differentiation medium were sorted for the Aldefluor low population. (E) Taxol-resistant SKOV3 cells grown in KnockOut medium were sorted for the Aldefluor high population.

Therefore, in order to study the biology of both $ALDH^{high}$ and $ALDH^{low}$ populations, two different culture conditions were used. When stained with Aldefluor, FNAR-C1 cells cultured in differentiation medium were predominantly $ALDH^{low}$ (Figure 4.1A). Occasional $ALDH^{high}$ cells were seen, but they were scattered and diffuse and did not appear to represent a distinct population (mean = 2.05%, range = 0.23 – 9.3%). When FNAR-C1 cells were grown in KnockOut medium, two clearly defined populations were seen, with $ALDH^{high}$ cells representing approximately half of the cells (Figure 4.1B; mean = 56.88%, range = 15.7 – 86.5%). It was hypothesized that $ALDH^{high}$ cells from KnockOut medium would represent a primitive stem-like population and $ALDH^{low}$ cells from differentiation medium would represent a differentiated cell population. Therefore, these were the two populations analyzed.

Like FNAR-C1 cells, SKOV3 cells cultured in differentiation medium showed few $ALDH^{high}$ cells (Figure 4.1C; mean = 2.12%, range = 0.18 – 6.28%). In contrast to the FNAR-C1 cells, culture of SKOV3 cells in KnockOut medium did not substantially change the percentage of $ALDH^{high}$ cells (data not shown). However, when SKOV3 cells obtained taxol-resistance, a distinct $ALDH^{high}$ population emerged in differentiation medium (Figure 4.1D; mean = 3.25%, range = 1.18 – 12.1%). Furthermore, culturing taxol-resistant SKOV3 cells in KnockOut medium resulted in a predominantly $ALDH^{high}$ population (Figure 4.1E; mean = 20.22, range = 10.0% to 42.2%). The cancer stem cell model proposes that cancer stem cells are relatively drug-resistant. Therefore, it was hypothesized that $ALDH^{high}$ taxol-resistant SKOV3

cells from KnockOut medium might represent a stem cell-like population and ALDH^{low} SKOV3 cells from differentiation medium could represent a differentiated population, and so these were the principal populations studied.

In order to test these hypotheses, each distinct ALDH population was examined for commonly accepted stem cell properties. These properties included nonadherent growth, quiescence, a lack of contact inhibition, size, the ability to regenerate the phenotypic diversity of the cell line, tumorigenicity and drug resistance[127-133]. Finally, expression patterns consistent with a stem cell phenotype were analyzed.

ALDH^{high} Cells Share Morphological and Growth Characteristics With Cancer Stem Cells

Commonly accepted properties of stem cells include non-adherent growth and the absence of contact inhibition[128]. FNAR-C1 cells grow adherently on plastic. Upon reaching confluency, ALDH^{low} cells showed substantial death, which resulted in large areas devoid of cells (data not shown). ALDH^{high} FNAR-C1 cells failed to undergo growth arrest upon achieving confluency and instead formed large three-dimensional clusters of cells, termed nodules (Figure 4.2A). These data suggest that ALDH^{low} cells retained contact inhibition, but ALDH^{high} cells lacked contact inhibition. In addition to forming nodules, a portion of ALDH^{high} FNAR-C1 cells grew as nonadherent clusters, termed spheroids (Figure 4.2B). Supernatant from ALDH^{low} FNAR-C1 cell cultures only showed apoptotic cells and cellular debris,

without any viable cell aggregates (data not shown). ALDH^{high} taxol-resistant SKOV3 cells also displayed nonadherent growth through the formation of spheroids (Figure 4.2C), which was not observed in ALDH^{low} SKOV3 cells (data not shown). Consistent with a stem cell phenotype, ALDH^{high} cells lack contact inhibition and possess the capacity for nonadherent growth, which are features not observed in ALDH^{low} cells.

Figure 4.2: Nodules and Spheroids

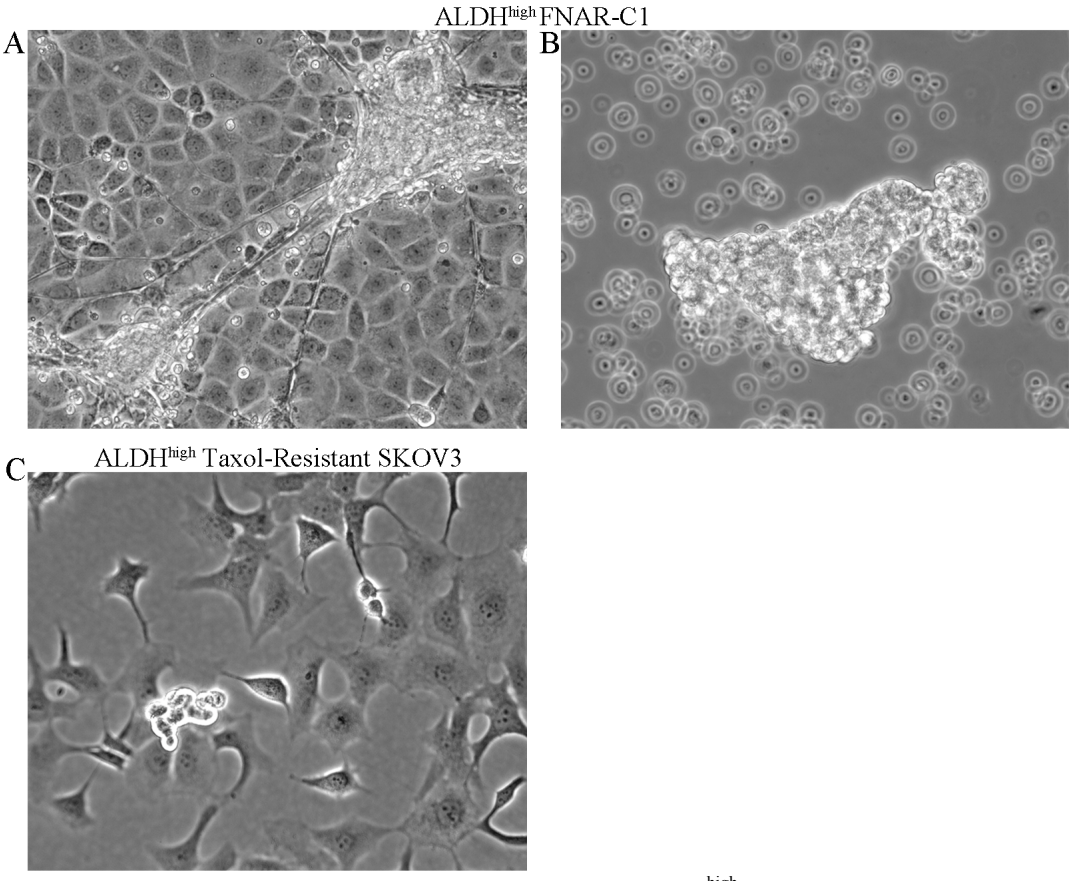

Pictomicrographs showing nodules (A) and spheroid (B) in ALDH^{high} FNAR-C1 cells and spheroid in ALDH^{high} taxol-resistant SKOV3 cells (C). For photography of ALDH^{high} FNAR-C1 spheroids, the supernatant was moved to an empty well. All images used a 20x phase contrast objective.

Figure 4.3: Cell Size

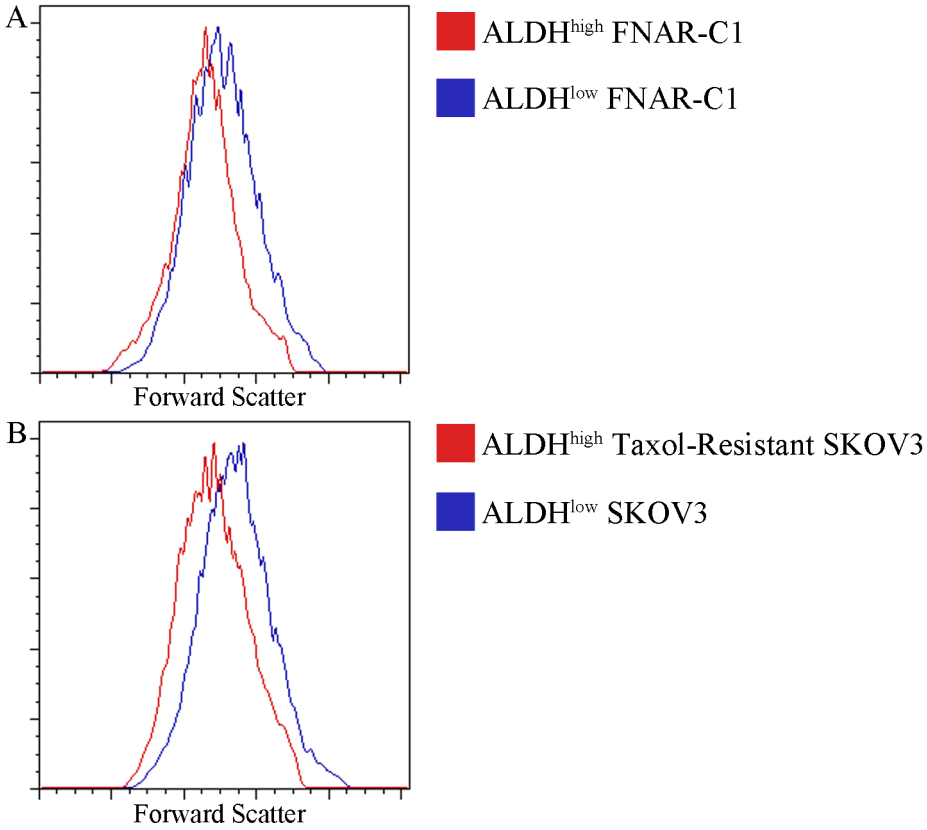

Unsorted cells were stained for Aldefluor and gated on the population of interest using DEAB as a negative control. The forward scatter, or size, of these cells was then displayed. (A) FNAR-C1 cells are shown with ALDH^{high} in red and ALDH^{low} in blue. (B) SKOV3 cells are shown. ALDH^{high} taxol-resistant SKOV3 cells are in red and ALDH^{low} SKOV3 cells are in blue.

Stem cells are typically smaller in size than their differentiated counterparts[127, 129]. Consistent with this, ALDH^{high} cells from both FNAR-C1 and taxol-resistant SKOV3 cells were smaller than ALDH^{low} cells from FNAR-C1 and SKOV3 cells, respectively (Figure 4.3). This smaller size is often attributed to the relative

quiescence of stem cells[132, 133]. ALDH^{high} FNAR-C1 cells had a doubling time of 32.2 hours compared to a doubling time of 15.6 hours for ALDH^{low} cells (Figure 4.4A).

Figure 4.4: Growth Curves

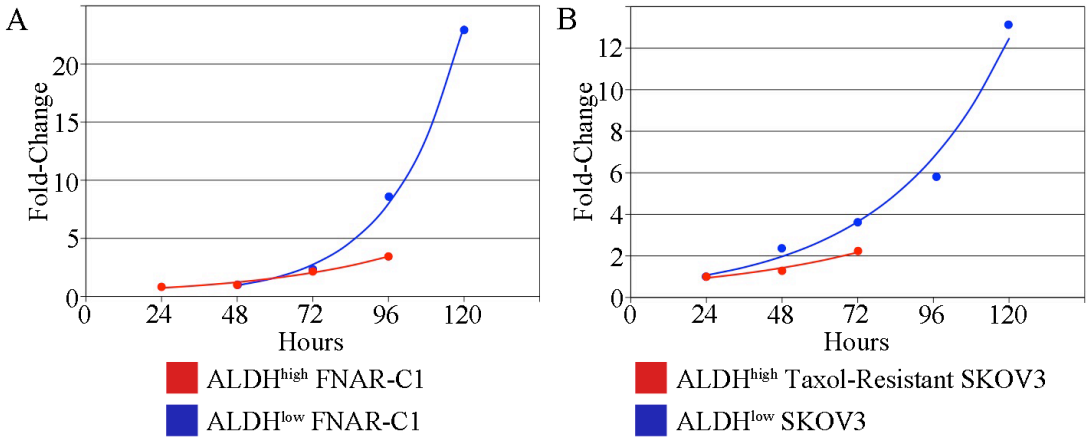

Sorted cells were counted at 24-hour intervals. (A) FNAR-C1 cells are shown with ALDH^{high} in red and ALDH^{low} in blue. (B) SKOV3 cells are shown. ALDH^{high} taxol-resistant SKOV3 cells are in red and ALDH^{low} SKOV3 cells are in blue.

ALDH^{high} taxol-resistant SKOV3 cells showed a similarly increased doubling time of 39.6 hours relative to 27.0 hours in ALDH^{low} SKOV3 cells (Figure 4.4B). These data reveal a slower growth rate in the ALDH^{high} cells of both models. This difference could be attributed to decreased proliferation or increased apoptosis. Cell cycle analysis distinguished between these two possibilities. ALDH^{high} FNAR-C1 cells had fewer dividing cells than ALDH^{low} FNAR-C1 cells with 52.8% of ALDH^{high} cells in the G1/G0 phase of the cell cycle versus 30.5% of ALDH^{low} cells (Figure 4.5A, B). This observation was confirmed in the SKOV3 model with 53.4% of ALDH^{high} taxol-resistant SKOV3 cells in the G1/G0 phase but only 42.2% of ALDH^{low} SKOV3

(Figure 4.5C, D). None of the populations showed a substantial sub-G1 cell population that would indicate apoptosis. Therefore, the increased doubling times of ALDH^{high} cells are the result of decreased proliferation.

Figure 4.5: Cell Cycle Analysis

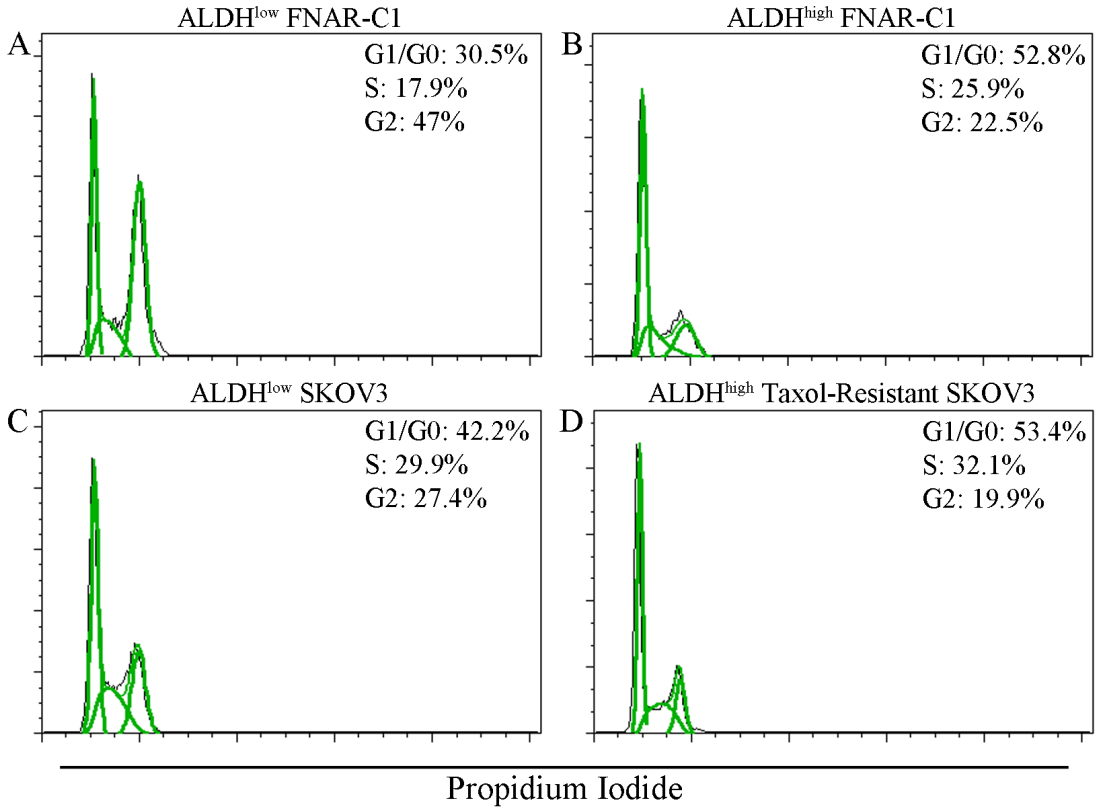

Representative cell cycle analyses using propidium iodide are shown: (A) ALDH^{low} FNAR-C1 cells, (B) ALDH^{high} FNAR-C1 cells, (C) ALDH^{low} SKOV3 cells, (D) ALDH^{high} taxol-resistant SKOV3 cells.

Microarray data showed that the decreased proliferation of ALDH^{high} cells is due to a block at the G1/S checkpoint. ALDH^{high} FNAR-C1 cells had downregulation of genes important for progression from G1 to S phase relative to ALDH^{low} FNAR-C1 cells (Figure 4.6). ALDH^{high} FNAR-C1 cells showed 3.512-fold (3.922-fold by PCR)

downregulation of c-myc and 5.704-fold downregulation of neuregulin 1, both of which promote cell cycle progression[134, 135]. Cyclin D1 stimulates the G1/S transition by complexing with cyclin dependent kinases 4 or 6 and was downregulated 2.503-fold (2.227-fold by PCR) in ALDH^{high} FNAR-C1 cells[136]. Additionally, cyclin D1 may play a role in exiting quiescence[137]. Downregulation of these crucial components of the G1/S checkpoint in ALDH^{high} FNAR-C1 cells suggests a block in cell cycle progression.

Differential regulation of genes in ALDH^{high} taxol-resistant SKOV3 cells compared to ALDH^{low} SKOV3 cells supports the same conclusion (Figure 4.7). ALDH^{high} taxol-resistant SKOV3 cells showed 2.22-fold downregulation (2.532-fold by PCR) of cyclin dependent kinase 6, which complexes with cyclin D1 to trigger the G1/S transition[138]. Transcription factor DP-1 (TFDP1) and ABL1 are components of the Rb/E2F pathway that is required for progression from G1 to S phase[139-142]. TFDP1 was downregulated 1.58-fold (1.526-fold by PCR) and ABL1 was 2.10-fold downregulated (3.086-fold by PCR) in ALDH^{high} taxol-resistant SKOV3 cells. In addition to downregulation of components of the G1/S checkpoint, ALDH^{high} taxol-resistant SKOV3 cells showed 2.28-fold overexpression (2.741-fold by PCR) of cyclin-dependent kinase inhibitor 1A (CDKN1A). CDKN1A inhibits cyclin dependent kinases 2 and 4, which are important components of the G1/S transition[143]. Overall, ALDH^{high} cells show a block at the G1/S checkpoint that results in fewer cycling cells and a decreased growth rate.

Figure 4.6: G1/S Arrest of ALDH^{high} FNAR-C1 Cells

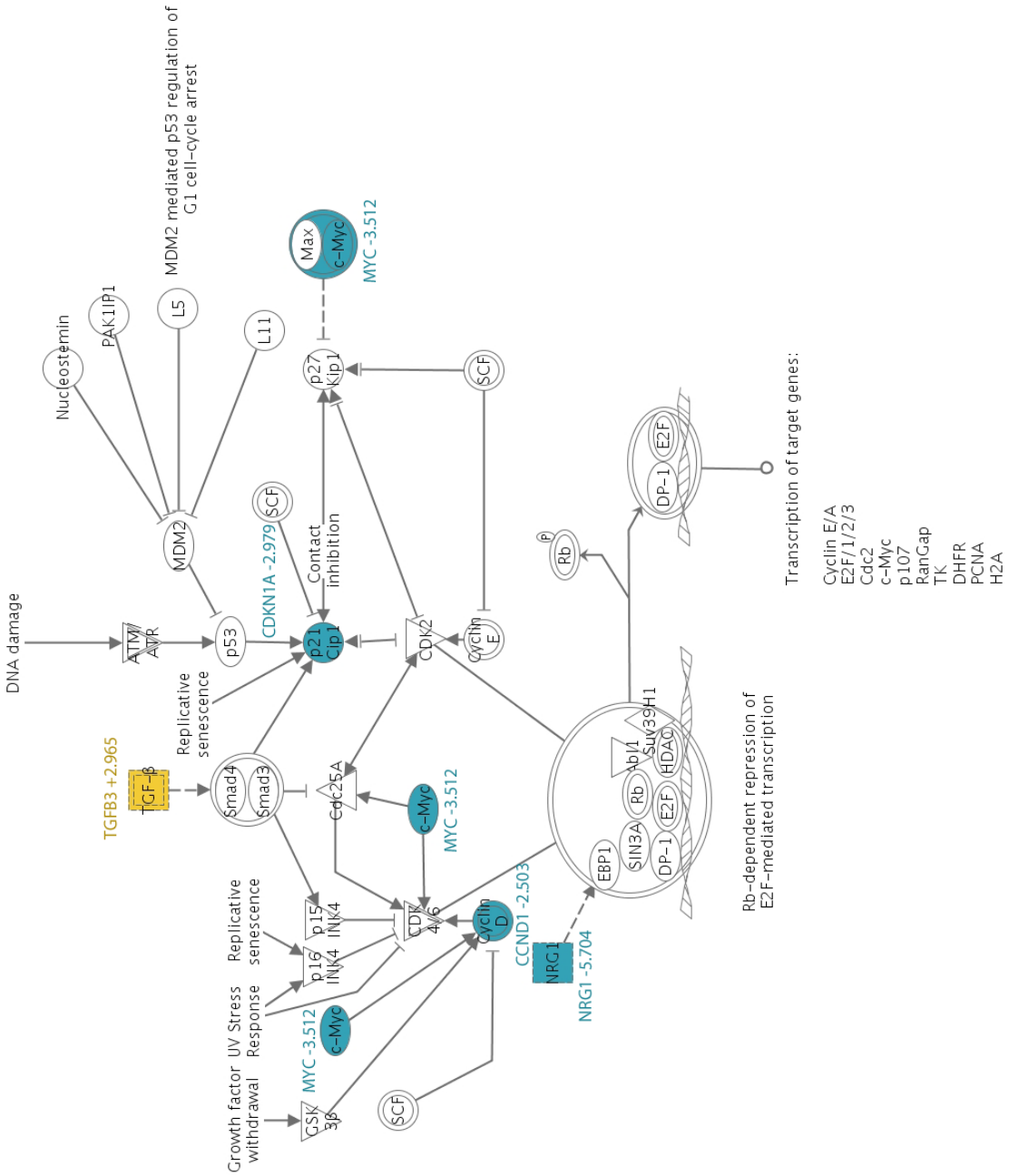

Pathway analysis of microarray data. Data is presented as ALDH^{high} FNAR-C1 cells relative to ALDH^{low} FNAR-C1 cells. Genes shaded in yellow were upregulated and genes shaded in blue were downregulated.

Figure 4.7: G1/S Arrest of ALDH^{high} Taxol-Resistant SKOV3 Cells

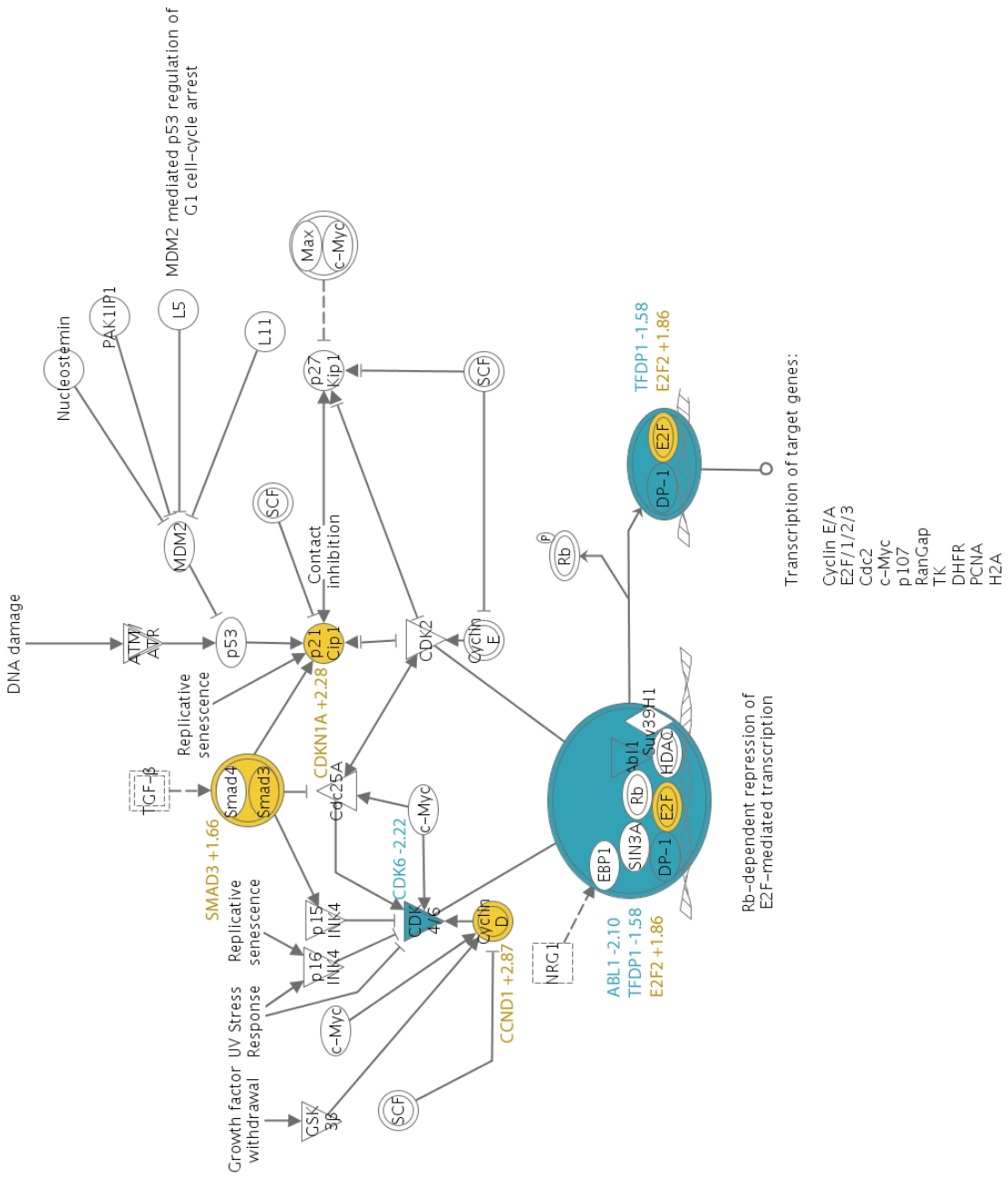

Pathway analysis of microarray data. Data is presented as ALDH^{high} taxol-resistant SKOV3 cells relative to ALDH^{low} SKOV3 cells. Genes shaded in yellow were upregulated and genes shaded in blue were downregulated.

ALDH^{high} Cells Are Capable of Regenerating the Phenotypic Diversity of the Cell Line and Are Tumorigenic *In Vivo*

Cancer stem cells should reconstitute the phenotypic heterogeneity of the tumor, while differentiated cells would not be expected to do so[128, 130-133]. ALDH^{low} FNAR-C1 (Figure 4.8C, D) and SKOV3 (Figure 4.9C, D) cells only produced ALDH^{low} cells *in vitro*, even when cultured in KnockOut medium that supports the growth of ALDH^{high} cells. Conversely, ALDH^{high} FNAR-C1 (Figure 4.8A, B) and taxol-resistant SKOV3 (Figure 4.9A, B) cells remained ALDH^{high} when cultured in KnockOut medium but rapidly generated ALDH^{low} cells in differentiation medium.

Figure 4.8: Regeneration of Phenotypic Diversity in FNAR-C1 Cells

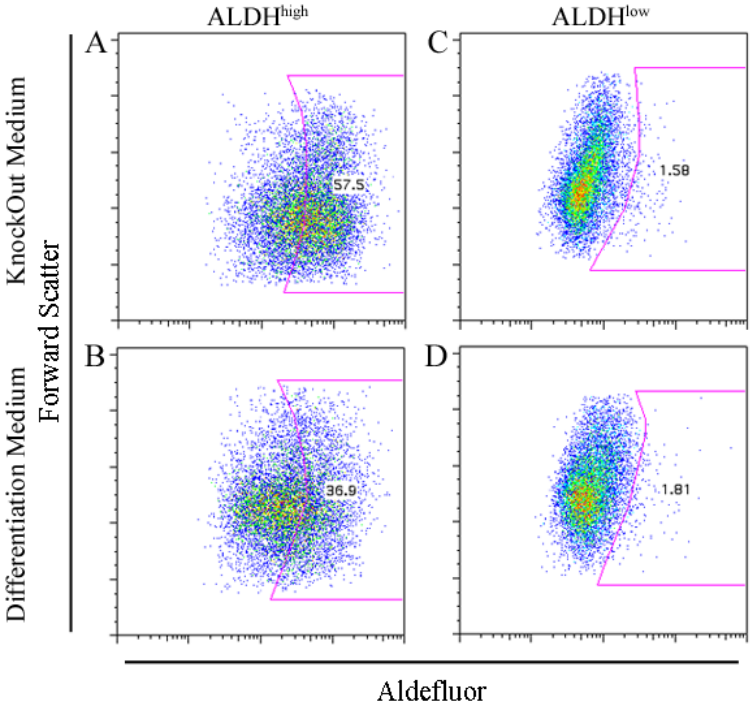

Sorted ALDH^{high} (A, B) and ALDH^{low} (C, D) FNAR-C1 cells were plated in either KnockOut medium (A, C) or differentiation medium (B, D) for four days and then stained for Aldefluor.

Accordingly, ALDH^{high}, but not ALDH^{low}, cells regenerate the phenotypic diversity of the cell lines, suggesting that ALDH^{high} cells represent a less differentiated phenotype than ALDH^{low} cells.

Figure 4.9: Regeneration of Phenotypic Diversity in SKOV3 Cells

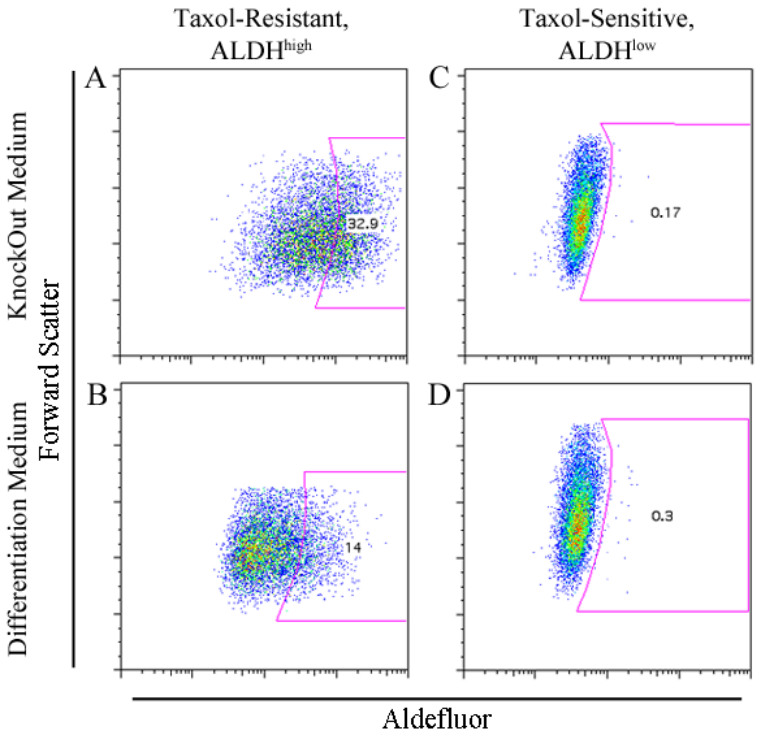

Sorted ALDH^{high} taxol-resistant SKOV3 cells (A, B) and ALDH^{low} SKOV3 cells (C, D) were plated in either KnockOut medium (A, C) or differentiation medium (B, D) for four days and then stained for Aldefluor.

The gold standard assay for cancer stem cells is increased *in vivo* tumorigenicity[128, 131-133]. In order to test the tumorigenicity of ALDH^{high} and ALDH^{low} cells, graded numbers of sorted FNAR-C1 cells were injected intraperitoneally into immunocompetent Lewis rats (Table 4.1). The only rats to develop tumors were those receiving ALDH^{high} cells. None of the rats injected with ALDH^{low} cells developed tumors. This provides *in vivo* support for the conclusion that ALDH^{high} cells represent the tumorigenic population within FNAR-C1 cells.

Table 4.1: *In Vivo* Tumorigenicity of FNAR-C1 Cells

	100,000 cells	1,000 cells
$ALDH^{high}$	3/16 (148, 177, 222)	1/12 (222)
$ALDH^{low}$	0/8	0/9

This table shows the number of rats that formed abdominal tumors out of the total number injected with sorted FNAR-C1 cells. In parenthesis are days post-injection until tumors were detected.

Figure 4.10: Drug Sensitivity

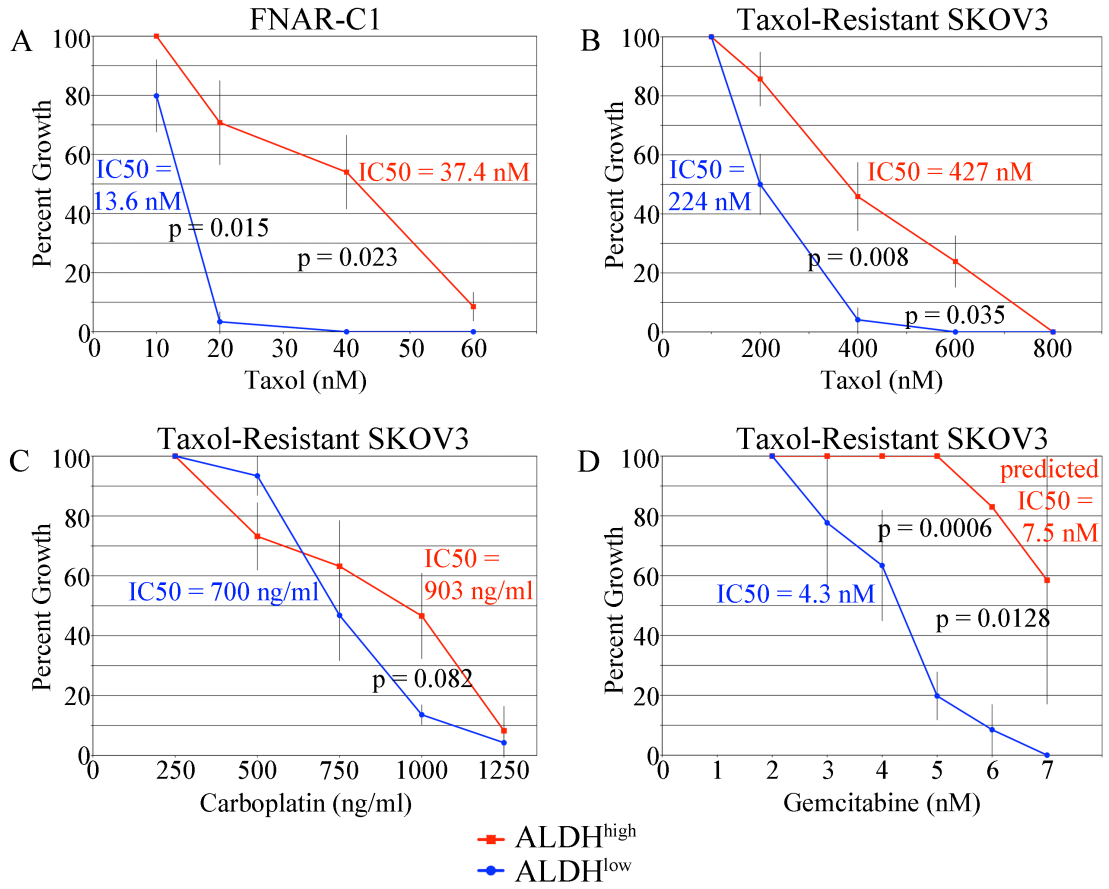

Sorted cells were assayed for their ability to grow in increasing concentrations of drugs. $ALDH^{high}$ cells grown are shown in red, and $ALDH^{low}$ cells are shown in blue. Error bars show the standard error. (A) FNAR-C1 cells cultured with taxol. (B-D) Taxol-resistant SKOV3 cells cultured in: (B) taxol, (C) carboplatin and (D) gemcitabine.

ALDH^{high} Cells Display Multi-Drug Resistance

The cancer stem cell hypothesis proposes that cancer stem cells are more resistant to chemotherapy and are therefore responsible for relapse[131-133]. To test the relative drug sensitivities of ALDH^{high} and ALDH^{low} populations, cells were incubated with increasing doses of drugs and examined for growth. ALDH^{high} FNAR-C1 cells showed increased resistance to taxol with an IC50 of 37.4 nM versus an IC50 of 13.6 nM for ALDH^{low} FNAR-C1 cells (Figure 4.10A). The differences in drug sensitivity were statistically significant at the 20 nM ($p = 0.015$) and 40 nM ($p = 0.023$) doses. When examining the sensitivities of SKOV3 cells, it was inappropriate to compare taxol-resistant cells to taxol-sensitive cells. Not only would this comparison produce invalid results for taxol, but also taxol-resistant cells were continuously cultured in the presence of taxol and would therefore be exposed to combination drug treatment when examining carboplatin and gemcitabine sensitivities. For these reasons, ALDH^{high} taxol-resistant SKOV3 cells grown in KnockOut medium were compared to ALDH^{low} taxol-resistant SKOV3 cells grown in differentiation medium. Taxol, carboplatin and gemcitabine were chosen because they each have different mechanisms of action and resistance. ALDH^{high} taxol-resistant SKOV3 cells showed increased resistance to taxol with an IC50 of 427 nM compared to an IC50 of 224 nM for ALDH^{low} taxol-resistant cells (Figure 4.10B). The observed differences in sensitivity were statistically significant at two doses (400 nM, $p=0.008$; 600 nM, $p=0.035$). These results were unexpected since both populations are grown in taxol. ALDH^{high} taxol-

resistant SKOV3 cells also showed a trend towards increased carboplatin resistance. The IC50 of $ALDH^{high}$ taxol-resistant SKOV3 cells was 903 ng/ml and the IC50 of $ALDH^{low}$ taxol-resistant SKOV3 cells was 700 ng/ml (Figure 4.10C). These results approached statistical significance with a p-value of 0.08 at the 1 μg/ml carboplatin dose. Finally, gemcitabine resistance was also demonstrated in $ALDH^{high}$ taxol-resistant SKOV3 cells. $ALDH^{low}$ taxol-resistant SKOV3 cells had an IC50 of 4.3 nM, but $ALDH^{high}$ taxol-resistant SKOV3 cells had more than 50% growth at all doses tested and so the IC50 was predicted to be 7.5 nM (Figure 4.10D). The differential sensitivities were statistically significant at two doses (5 nM, $p = 0.0006$; 6 nM, $p = 0.0128$). Therefore, $ALDH^{high}$ cells displayed resistance to chemotherapy drugs with different mechanisms of resistance, consistent with the multi-drug resistance of stem cells.

As an additional measure of drug resistance, the change in percentage of $ALDH^{high}$ cells after exposure to taxol was determined. When unsorted FNAR-C1 cells in differentiation medium were exposed to taxol, the percentage of $ALDH^{high}$ cells increased from a mean of 1.1% to 4.1% ($p = 0.04$; Figure 4.11A). Similarly, taxol-resistant SKOV3 cells in differentiation medium had an increased $ALDH^{high}$ population (mean = 4.1%) compared to taxol-sensitive SKOV3 cells cultured in differentiation medium (mean = 0.4%, $p = 0.024$; Figure 4.11B). This suggests that drug treatment enriches for $ALDH^{high}$ cells, likely due to selective elimination of $ALDH^{low}$ cells, and that this occurs even under conditions that do not support the

growth of stem cells. The increased resistance of ALDH^{high} cells was associated with upregulation of the multi-drug resistance 1 (MDR1) gene (ABCB1 in humans and ABCB1B in rats), which is an ATP-binding cassette transporter that functions in drug efflux and is a primary mechanism of taxol resistance[144]. ALDH^{high} FNAR-C1 cells displayed 16.797-fold upregulation (24.603-fold by PCR) of ABCB1B compared to ALDH^{low} FNAR-C1 cells (Table 4.2, pg. 98). ABCB1 was 3.743-fold upregulated (374.276-fold by PCR) in ALDH^{high} taxol-resistant SKOV3 cells compared to ALDH^{low} SKOV3 cells (Table 4.2, pg. 98). Therefore, increased expression of the MDR1 gene may contribute to taxol resistance in ALDH^{high} cells and their enrichment after taxol treatment. However, MDR1 plays no role in gemcitabine or carboplatin resistance.

Figure 4.11: Percentage of ALDH^{high} Cells After Taxol Treatment

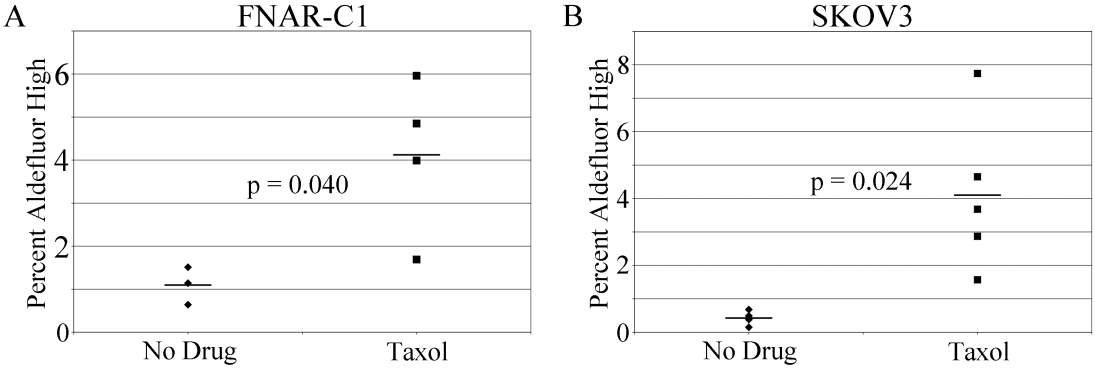

Unsorted FNAR-C1 (A) and SKOV3 (B) cells were cultured in differentiation medium with or without taxol. The percentage of ALDH^{high} cells was then measured.

ALDH^{high} Cells' Gene Expression Is Consistent With a Stem Cell Phenotype

Microarray analysis examined gene expression patterns consistent with a stem cell phenotype. The embryonic stem cell pluripotency pathway in FNAR-C1 cells is shown in Figure 4.12 (pg. 62). Data are presented as ALDH^{high} FNAR-C1 cells versus ALDH^{low} FNAR-C1 cells. ALDH^{high} FNAR-C1 cells showed upregulation of WNT2B (92.03-fold by microarray, 581.598-fold by PCR), WNT4 (10.745-fold by microarray, 18.296-fold by PCR) and WNT11 (8.719-fold by microarray, 15.722-fold by PCR)[145]. Each of these WNT genes has been shown to play important roles in stem cells. Embryonic stem cells express WNT2B[146]. Additionally, WNT2B is associated with metastasis and chemoresistance in ovarian cancer[147]. WNT4 is important in progenitor cell expansion[148, 149]. Finally, WNT11 has been shown to maintain proliferating stem cells in the presence of retinoic acid[150]. Also in the Wnt/β-catenin pathway is the TCF/LEF complex that is important for stem cell self-renewal[151, 152]. ALDH^{high} FNAR-C1 cells exhibited 3.225-fold upregulation (88.626-fold by PCR) of LEF1 and 4.192-fold upregulation (6.754-fold by PCR) of TCF7L1.

In addition to WNT family members, other stem cell associated genes were upregulated in ALDH^{high} FNAR-C1 cells. Platelet-derived growth factor β, which is involved in stem cell maintenance, was upregulated 3.192-fold (12.254-fold by PCR) in ALDH^{high} FNAR-C1 cells[153, 154]. Brain-derived neurotrophic factor was 5.886-fold (6.567-fold by PCR) upregulated in ALDH^{high} FNAR-C1 cells and can induce stem cell proliferation[155]. Stem cells express high levels of neurotrophin 3, and ALDH^{high}

FNAR-C1 cells demonstrated 3.18-fold upregulation[156]. Fibroblast growth factor receptors (FGFR) 1 and 2 are required for the maintenance of a diverse array of stem cells[157, 158]. FGFR1 was 3.736-fold upregulated (24.101-fold by PCR) and FGFR2 was 22.621-fold upregulated (33.065-fold by PCR) in ALDH^{high} FNAR-C1 cells. Bone morphogenetic protein 7, which was 4.44-fold upregulated (3.329-fold by PCR) in ALDH^{high} FNAR-C1 cells, is important for the survival and proliferation of progenitor cells[159]. Accordingly, ALDH^{high} FNAR-C1 cells showed upregulation of numerous genes that serve crucial functions in the maintenance, self-renewal and proliferation of stem cells.

The embryonic stem cell pluripotency pathway in Figure 4.13 (pg. 63) displays genes differentially regulated in ALDH^{high} taxol-resistant SKOV3 cells relative to ALDH^{low} SKOV3 cells. Despite some dissimilarity with ALDH^{high} FNAR-C1 cells, ALDH^{high} taxol-resistant SKOV3 cells also demonstrated an expression pattern consistent with a stem cell phenotype. ALDH^{high} taxol-resistant SKOV3 cells showed 1.58-fold upregulation of the regulatory subunit of phosphoinositide-3-kinase, which is important in breast cancer stem cells[160]. SMAD3 signaling maintains stem cell pluripotency and was upregulated 1.66-fold in ALDH^{high} taxol-resistant SKOV3 cells[161]. Self-renewal of stem cells is strongly influenced by bone morphogenetic protein 4 (BMP4)[162]. Accordingly, ALDH^{high} taxol-resistant SKOV3 cells demonstrated 5.67-fold upregulation of BMP4. Bone morphogenetic protein 5 has the capacity to increase the number of stem cells and ALDH^{high} taxol-resistant SKOV3

cells displayed 3.01-fold (117.407-fold by PCR) upregulation versus ALDH^{low} SKOV3 cells[163]. In addition to upregulation of stem cell associated genes, ALDH^{high} taxol-resistant SKOV3 cells showed downregulation of a gene associated with differentiation: bone morphogenetic protein 1 (1.55-fold downregulation)[164]. Similar to ALDH^{high} FNAR-C1 cells, ALDH^{high} taxol-resistant SKOV3 cells exhibited upregulation of genes that control vital properties of stem cells and downregulation of a gene involved in differentiation.

ALDH^{high} cells additionally showed differential regulation of genes in the OCT4 pathway consistent with a stem cell phenotype. Figure 4.14 (pg. 64) shows ALDH^{high} FNAR-C1 cells compared to ALDH^{low} FNAR-C1 cells. NR2F1 was 2.625-fold upregulated in ALDH^{high} FNAR-C1 cells and has been reported to induce quiescence[165]. CDX2 induces differentiation and was downregulated 12.968-fold in ALDH^{high} FNAR-C1 cells[166]. Therefore, differential expression of genes in the OCT4 pathway suggests that ALDH^{high} FNAR-C1 cells exhibit a more primitive phenotype than their ALDH^{low} counterparts. Figure 4.15 (pg. 65) presents the OCT4 pathway in ALDH^{high} taxol-resistant SKOV3 calls relative to ALDH^{low} SKOV3 cells. ALDH^{high} taxol-resistant SKOV3 cells displayed 3.74-fold upregulation (3.298-fold by PCR) of the downstream effector secreted phosphoprotein 1, which is highly expressed in stem and progenitor cells[167]. Observations in both models suggest the OCT4 pathway plays a role in the maintenance of a stem cell phenotype in ALDH^{high} cells.

Figure 4.12: FNAR-C1 Embryonic Stem Cell Pluripotency

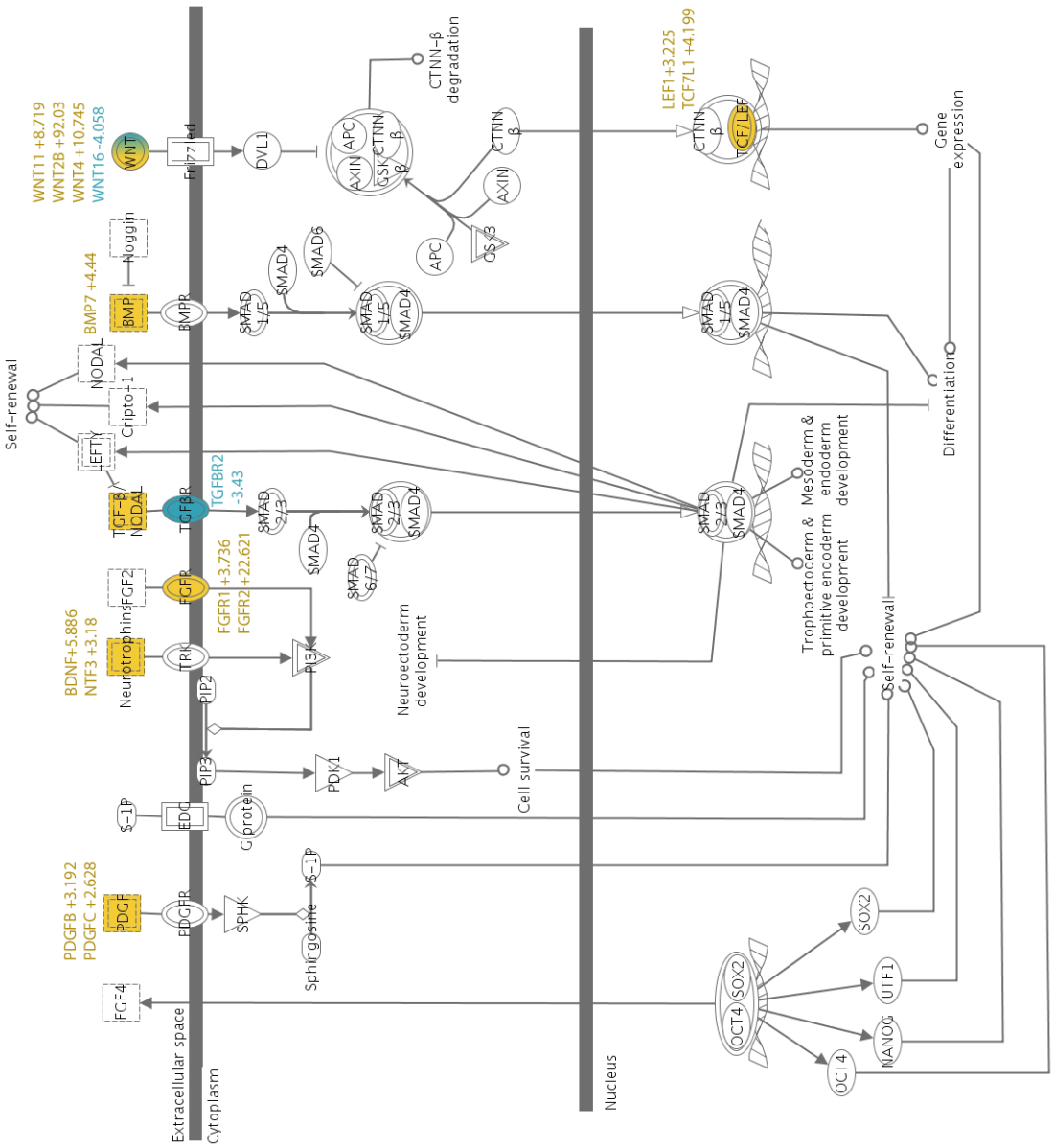

Pathway analysis of microarray data. Data is presented as ALDH^{high} FNAR-C1 cells relative to ALDH^{low} FNAR-C1 cells. Genes shaded in yellow were upregulated and genes shaded in blue were downregulated.

Figure 4.13: SKOV3 Embryonic Stem Cell Pluripotency

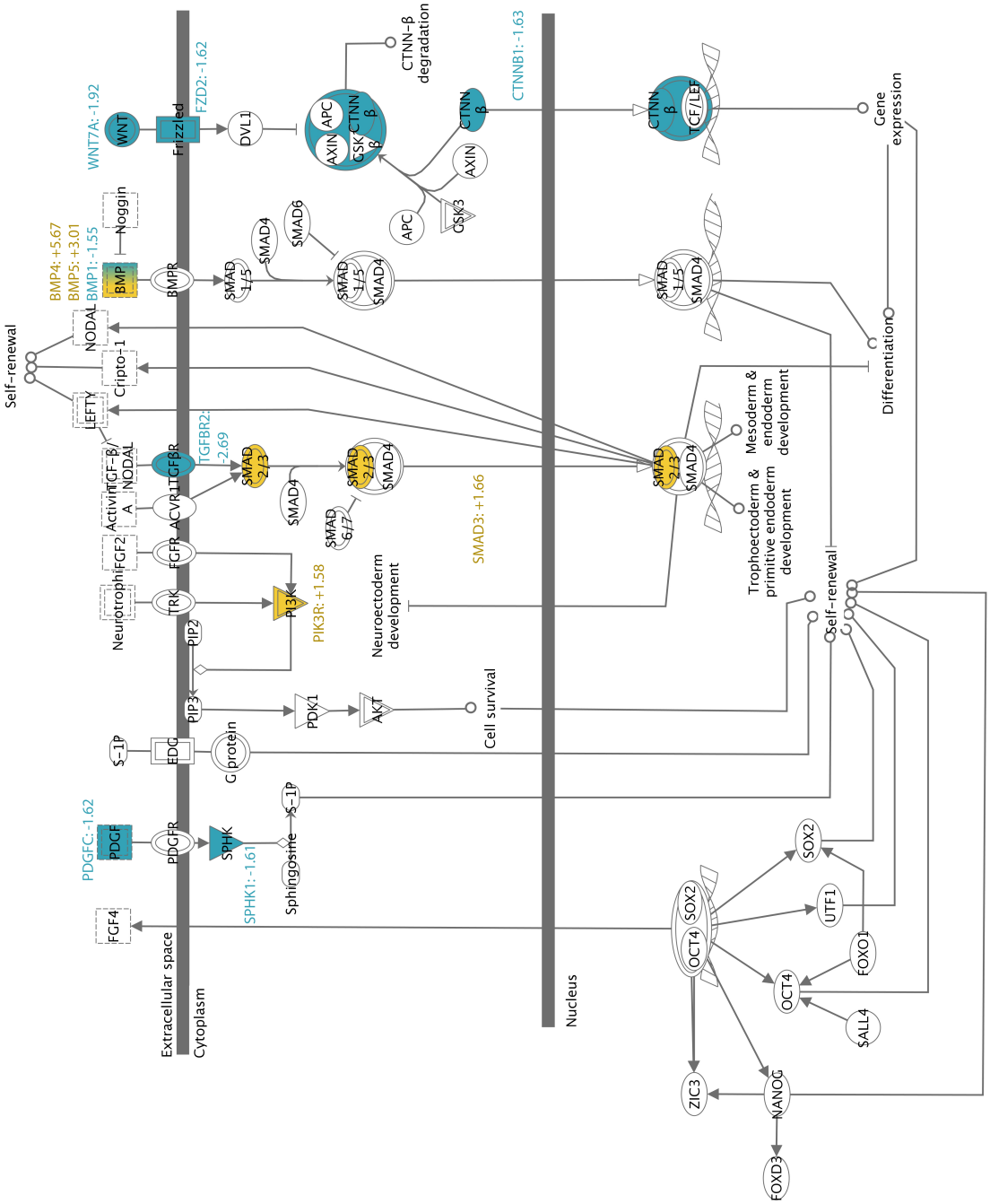

Pathway analysis of microarray data. Data is presented as $ALDH^{high}$ taxol-resistant SKOV3 cells relative to $ALDH^{low}$ SKOV3 cells. Genes shaded in yellow were upregulated and genes shaded in blue were downregulated.

Figure 4.14: FNAR-C1 Oct4 in Mammalian Embryonic Stem Cell Pluripotency

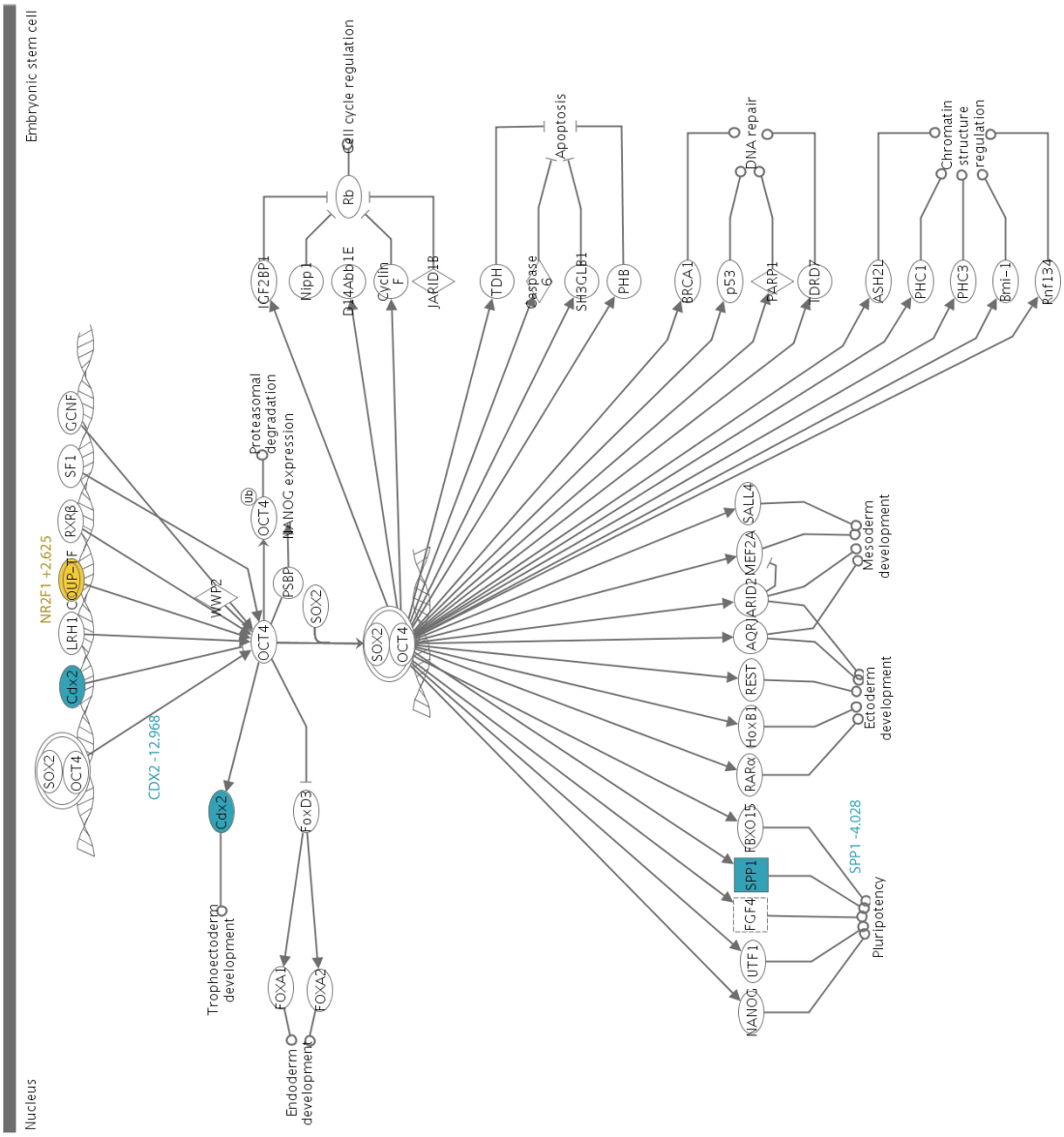

Pathway analysis of microarray data. Data is presented as $ALDH^{high}$ FNAR-C1 cells relative to $ALDH^{low}$ FNAR-C1 cells. Genes shaded in yellow were upregulated and genes shaded in blue were downregulated.

Figure 4.15: SKOV3 Oct4 in Mammalian Embryonic Stem Cell Pluripotency

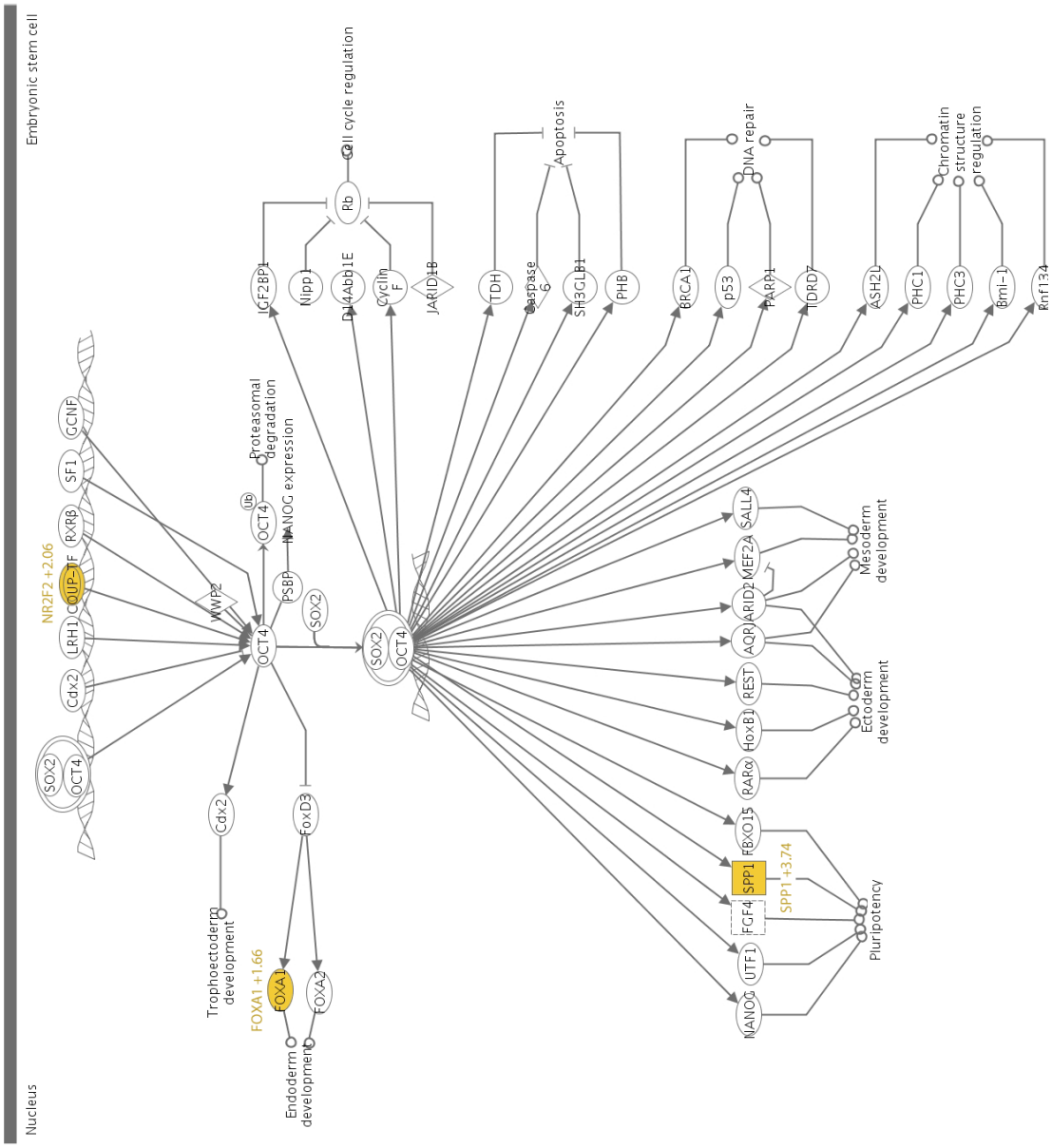

Pathway analysis of microarray data. Data is presented as ALDH^{high} taxol-resistant SKOV3 cells relative to ALDH^{low} SKOV3 cells. Genes shaded in yellow were upregulated and genes shaded in blue were downregulated.

ALDH^{high} Cells Represent a Biologically Distinct Population

Data presented thus far show that ALDH^{high} cells represent a stem cell-like population within ovarian cancer. Therefore, studying gene expression differences in these cells should reveal biological properties of ovarian cancer stem cells. The FNAR-C1 and SKOV3 models represent different ovarian cancer subtypes. By examining microarray data for those features that are consistently differentially regulated in the ALDH^{high} cells of both models, it may be possible to identify properties of ovarian cancer stem cells that would be representative of all patients, rather than those with a specific subtype.

For microarray analysis, cells were isolated based on different levels of Aldefluor staining. In order to validate the Aldefluor staining patterns in isolated cells with aldehyde dehydrogenase 1 (ALDH1) expression, the expression levels of ALDH1 family members were examined. The enzymes of the ALDH1 family are also known as retinaldehyde dehydrogenases. Although the precise function of ALDH1 enzymes in stem-cell biology is unclear, the major biological function of the ALDH1 family appears to be the biosynthesis of retinoic acid, the active metabolite of vitamin A (retinol). ALDH1 catalyzes the final step of this process, the oxidation of retinaldehyde to retinoic acid[168]. There are three known members of the family, ALDH1A1, A2, and A3, with somewhat redundant expression and function. In ALDH^{high} FNAR-C1 cells, there was 86.522-fold upregulation (325.761-fold by PCR) of ALDH1A2 relative to ALDH^{low} FNAR-C1 cells (Table 4.2, pg. 98). ALDH^{high}

taxol-resistant SKOV3 cells expressed ALDH1A1 at a 23.699-fold greater level (44.494-fold by PCR) than $ALDH^{low}$ SKOV3 cells (Table 4.2, pg. 98). Not only does this confirm that Aldefluor high cells have the expected increased expression of ALDH1, it suggests that there may be species differences with regard to specific isoenzyme expression.

Tight junctions form barriers that prevent diffusion of molecules between epithelial cells. Additionally, signaling through tight junction proteins regulates cellular behavior. Both models exhibited upregulation of tight junction genes in $ALDH^{high}$ cells suggesting a role for this pathway in ovarian cancer stem cells. Figure 4.16 presents the expression of tight junction genes in $ALDH^{high}$ FNAR-C1 cells relative to $ALDH^{low}$ FNAR-C1 cells, and Figure 4.17 represents $ALDH^{high}$ taxol-resistant SKOV3 cells compared to $ALDH^{low}$ SKOV3 cells. Claudin genes, the primary proteins that form tight junctions and regulate their permeability, were upregulated in $ALDH^{high}$ cells (FNAR-C1: claudin 23; SKOV3: claudins 1 and 3, confirmed by PCR). A second class of tight junction genes, junctional adhesion molecules (JAM), exhibited differential regulation in $ALDH^{high}$ FNAR-C1 cells with 2.96-fold upregulation of JAM3 (4.882-fold by PCR). Both models also showed upregulation of multiple intracellular signaling components. Although it is clear that $ALDH^{high}$ cells have the capacity for increased tight junction formation and intracellular signaling, the strength of the barriers formed is less certain.

Figure 4.16: FNAR-C1 Tight Junction Signaling

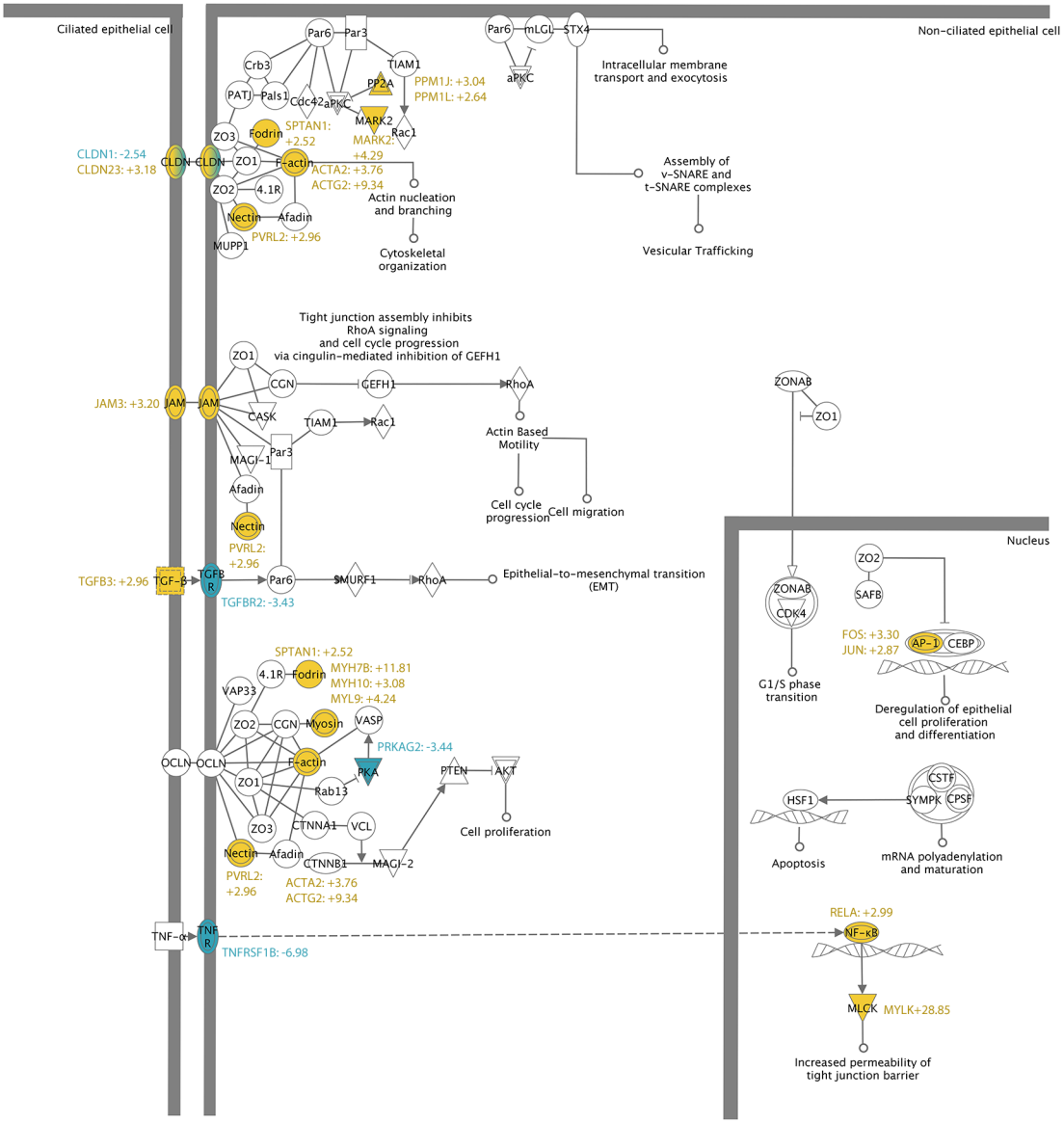

Pathway analysis of microarray data. Data is presented as ALDH^{high} FNAR-C1 cells relative to ALDH^{low} FNAR-C1 cells. Genes shaded in yellow were upregulated and genes shaded in blue were downregulated.

Figure 4.17: SKOV3 Tight Junction Signaling

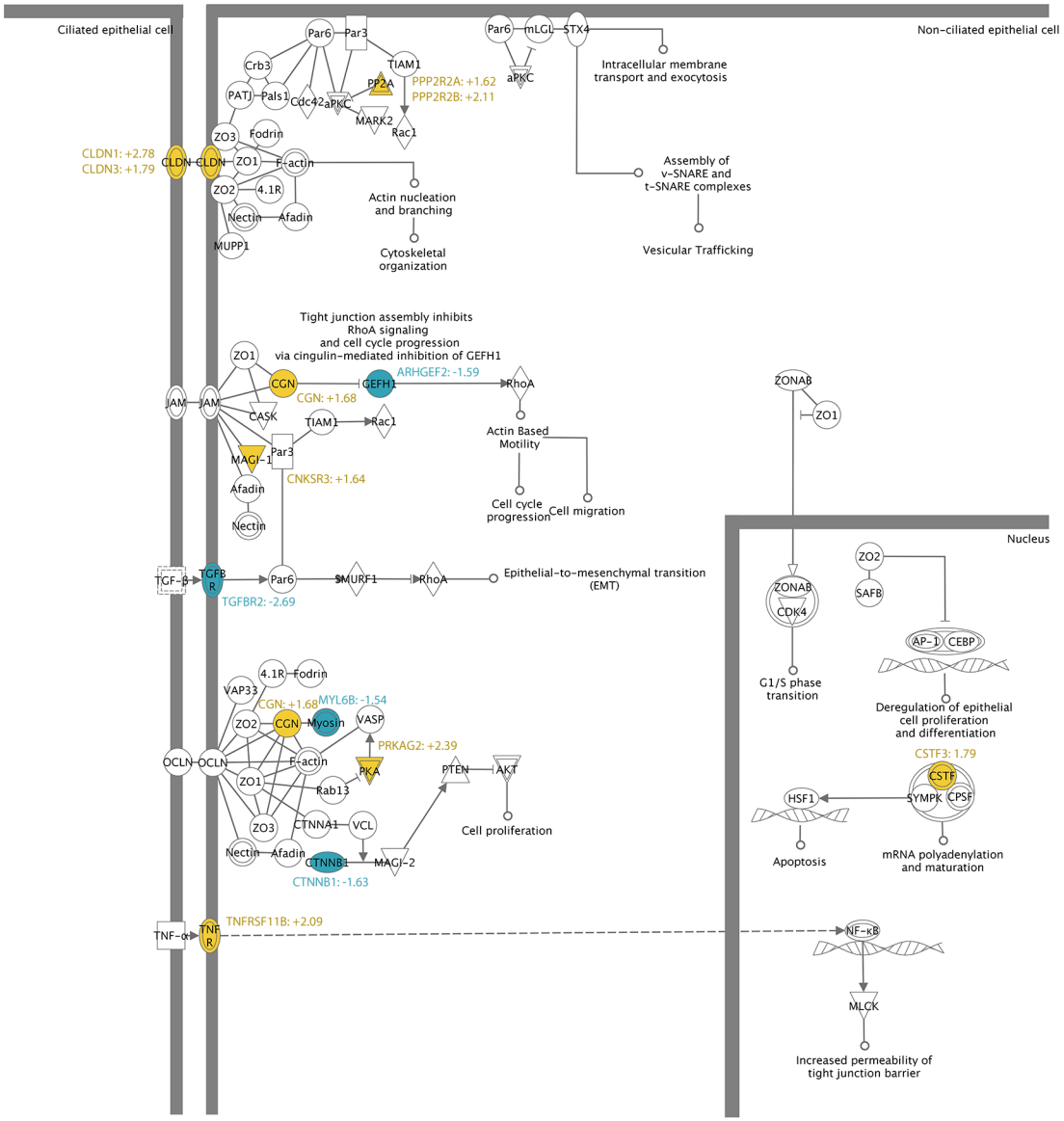

Pathway analysis of microarray data. Data is presented as ALDH^{high} taxol-resistant SKOV3 cells relative to ALDH^{low} SKOV3 cells. Genes shaded in yellow were upregulated and genes shaded in blue were downregulated.

Not present in the pathway analysis is CXADR, which is important for tight junction integrity and was upregulated in ALDH^{high} cells of both models (Table 4.2, pg. 98)[169, 170]. This would suggest that ALDH^{high} cells form robust barriers. However, ALDH^{high} cells also displayed upregulation of several genes that increase tight junction permeability, including protein phosphatase 2A (PP2A) family members in both models and myosin light chain kinase in FNAR-C1 cells (MYLK: 89.956-fold by PCR)[171, 172]. While the integrity of tight junctions formed by ALDH^{high} cells is uncertain, it is apparent that tight junction signaling may play an important role in ALDH^{high} cells. Additionally, the tendency of ALDH^{high} cells to grow as clusters and form spheroids may be due to increased formation of tight junctions.

Differential gene expression suggests that ALDH^{high} cells may represent tumor initiating cells. Tumor suppressors in the kruppel-like factor, S100 calcium binding protein and epithelial membrane protein families were downregulated in ALDH^{high} cells (Table 4.4, pg. 102)[173-178]. ALDH^{high} cells also appear to have an increased capacity for invasion. ALDH^{high} FNAR-C1 cells displayed upregulation of bone morphogenetic protein 7, cadherin 11, protein tyrosine kinase 7, matrix metallopeptidase 2 and matrix metallopeptidase 14 (Table 4.4, pg. 102)[179-182]. Different members of the same gene families were upregulated in ALDH^{high} taxol-resistant SKOV3 cells, comprising bone morphogenetic protein 4, protein tyrosine kinase 2 and matrix metallopeptidase 7 (Table 4.4, pg. 102)[183-185]. These genes have been shown to induce migration and invasion, so upregulation implies that ALDH^{high}

cells represent the invasive population of tumor cells. Further supporting this conclusion is downregulation of inhibitors of extracellular matrix degradation. SERPINB2 was downregulated in ALDH^{high} FNAR-C1 cells, as was SERPINE1 in ALDH^{high} taxol-resistant SKOV3 cells (Table 4.4, pg. 103)[186, 187]. Not only do ALDH^{high} cells have an increased capacity for invasion, but this process is aided by reduced deposition of the extracellular matrix. Collagen components of the basement membrane exhibited reduced expression in ALDH^{high} cells (Table 4.4, pg. 103)[188-191]. Additionally, the transmembrane collagen COL17A1 was downregulated in ALDH^{high} cells of both models (Table 4.3, pg. 100)[192]. The formation of mature collagen fibers requires processing of procollagen molecules. ALDH^{high} cells showed downregulation of PCOLCE2, which binds to procollagen to enhance its cleavage, and downregulation of P4HA2, which is a component of the key collagen synthesis enzyme prolyl 4-hydroxylase (Table 4.3, pg. 100)[193, 194]. In addition to reduced collagen expression and processing, laminin components of the basement membrane were also downregulated in ALDH^{high} cells, including LAMB3 and LAMC2 (Table 4.3, pg. 100)[195]. The apparent reduced extracellular matrix deposition seen in ALDH^{high} cells would facilitate invasion by diminishing the amount of extracellular matrix degradation required. These observations suggest that ALDH^{high} cells display an increased capacity for migration and invasion, potentially indicating a role in metastasis.

Expression patterns in both models suggest decreased coagulation in ALDH^{high} cells. Figure 4.18 displays the expression of coagulation genes in ALDH^{high} FNAR-C1 cells compared to ALDH^{low} FNAR-C1 cells, and Figure 4.19 shows ALDH^{high} taxol-resistant SKOV3 cells relative to ALDH^{low} SKOV3 cells. In ALDH^{high} cells, coagulation was primarily inhibited via upregulation of tissue factor pathway inhibitor (TFPI), which blocks the extrinsic pathway of the coagulation cascade (Table 4.2, pg. 98)[196]. Additionally, ALDH^{high} taxol-resistant SKOV3 cells exhibited 1.87-fold downregulation of fibrin, further reducing clot formation[197]. Inhibition of the extrinsic coagulation pathway has intriguing implications in ovarian cancer. The extrinsic pathway is activated by tissue damage, which is likely to result if cancer cells disrupt the integrity of blood vessels during invasion[198]. If coagulation were allowed to proceed under these circumstances, it would sequester migrating cancer cells. Therefore, inhibition of the extrinsic coagulation pathway could permit widespread cancer dissemination. The inhibited coagulation in ALDH^{high} cells along with the increased capacity for invasion further supports the conclusion that ALDH^{high} cells represent the population that initiates metastasis.

Figure 4.18: FNAR-C1 Coagulation System

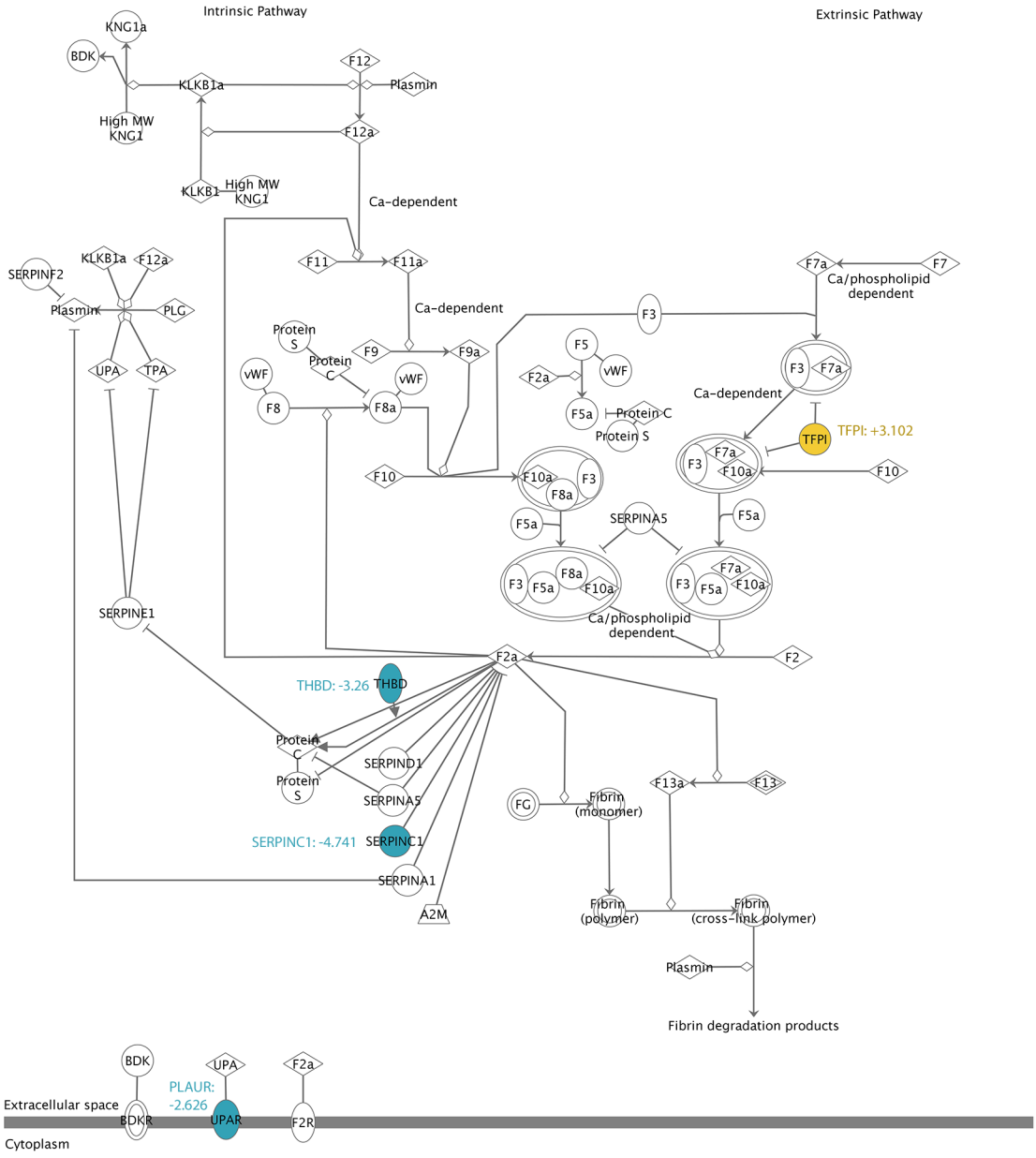

Pathway analysis of microarray data. Data is presented as ALDH^{high} FNAR-C1 cells relative to ALDH^{low} FNAR-C1 cells. Genes shaded in yellow were upregulated and genes shaded in blue were downregulated.

Figure 4.19: SKOV3 Coagulation System

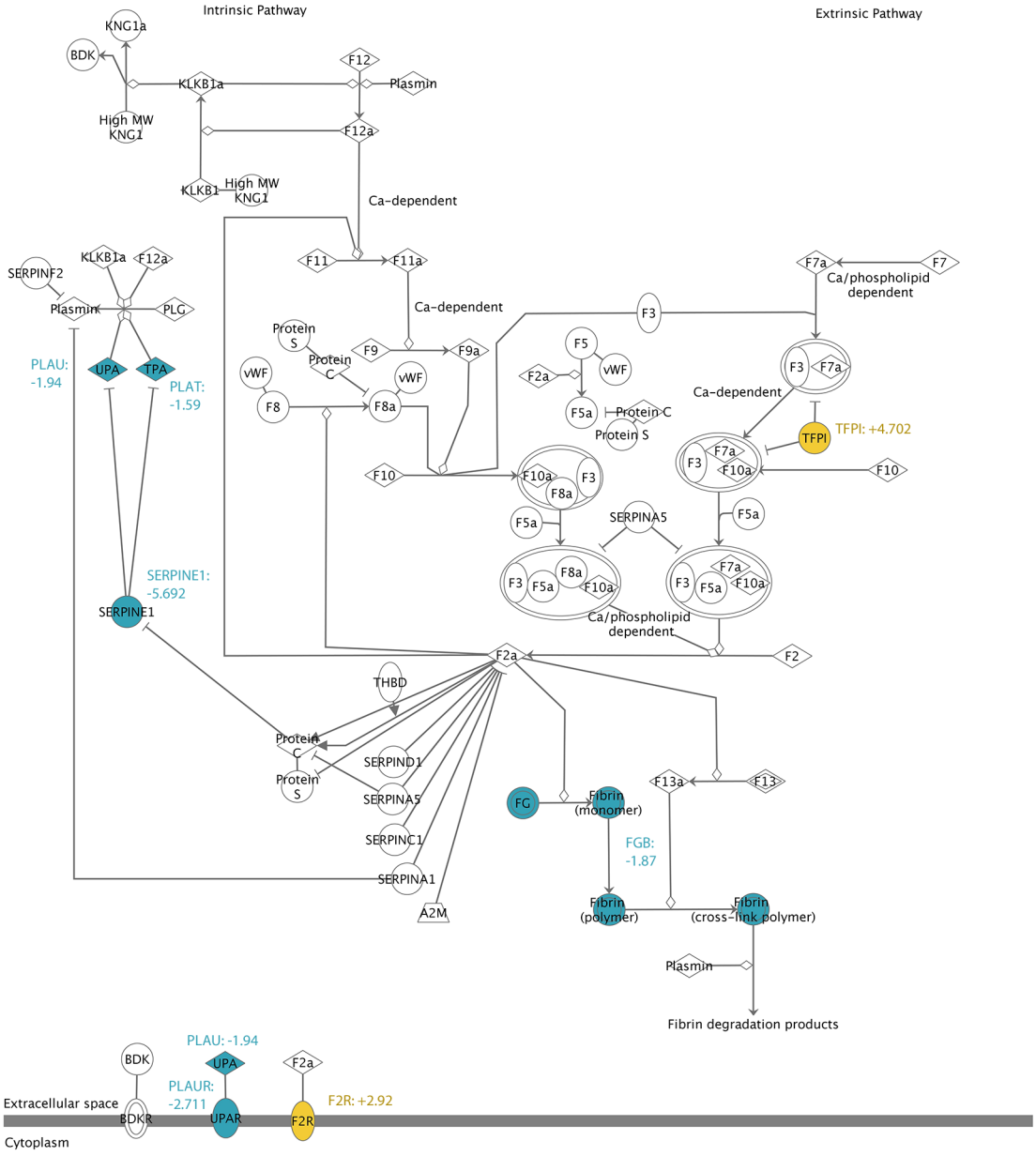

Pathway analysis of microarray data. Data is presented as ALDH^{high} taxol-resistant SKOV3 cells relative to ALDH^{low} SKOV3 cells. Genes shaded in yellow were upregulated and genes shaded in blue were downregulated.

Inconsistent Expression of Previously Reported Ovarian Cancer Stem Cell Markers in ALDH^{high} Cells

In addition to ALDH1, several different markers have been proposed to enrich for ovarian cancer stem cells, including CD24, CD44, KIT and CD133. However, most studies only examined one marker. Because of this, it is not known if these markers identify the same cell population. Gene expression analysis of ALDH^{high} and ALDH^{low} cells allowed for examination of alternative ovarian cancer stem cell makers to determine coexpression. By assessing two distinct ovarian cancer subtypes, those makers with consistent coexpression could be identified.

While CD24 has been proposed as an ovarian cancer stem cell marker, disagreements exist concerning whether ovarian cancer stem cells express it to a greater or lesser degree than differentiated cells[46, 59]. ALDH^{high} taxol-resistant SKOV3 cells exhibited substantial downregulation of CD24 relative to ALDH^{low} SKOV3 cells (Table 4.5, pg. 108). ALDH^{high} FNAR-C1 cells also showed downregulation of CD24, but to a lesser degree than in SKOV3 cells (Table 4.5, pg. 108). Therefore, ovarian cancer stem cells may express lower levels of CD24 than differentiated cells. However, all populations expressed considerable levels of CD24, potentially limiting its usefulness as a marker for isolation.

High expression of CD44 has been reported to enrich for ovarian cancer stem cells[28, 29]. In opposition to these reports, ALDH^{high} FNAR-C1 cells exhibited substantial downregulation of CD44 relative to ALDH^{low} FNAR-C1 cells (Table 4.5,

pg. 108). However, there was no difference in CD44 expression between ALDH^{high} taxol-resistant SKOV3 cells and ALDH^{low} SKOV3 cells (Table 4.5, pg. 108). Additionally, both SKOV3 populations showed very high levels of expression. While these results contradict previous reports using CD44 positivity to isolate ovarian cancer stem cells, there are reports of tumorigenic ovarian cancer cells lacking CD44 expression[36, 37]. The data presented here indicates variable expression of CD44 in ALDH^{high} cells, which challenges the use of CD44 as a universal ovarian cancer stem cell marker.

Published reports of ovarian cancer stem cells demonstrate stark variability in KIT expression, which is reflected in this study[25, 29, 34, 61]. In FNAR-C1 cells, KIT expression was too low for differences to be reliably detected by microarray. PCR data showed that KIT expression was largely confined to the ALDH^{high} population (Table 4.5, pg. 108). ALDH^{high} taxol-resistant SKOV3 cells exhibited the opposite pattern with expression of KIT only reliably detected in ALDH^{low} SKOV3 cells (Table 4.5, pg. 108). In conjunction with previously published results, these findings indicate dynamic expression of KIT in ovarian cancer stem cells.

Ovarian cancer stem cells have been isolated based on CD133 positivity[49, 55]. CD133 expression was too low to be reliably detected in FNAR-C1 cells using microarray analysis. PCR analysis showed possible downregulation of CD133 in ALDH^{high} FNAR-C1 cells (Table 4.5, pg. 108). CD133 was undetectable in the ALDH^{high} population but appeared to be expressed at a very low level in the ALDH^{low}

fraction. In ALDH^{high} taxol-resistant SKOV3 and ALDH^{low} SKOV3 cells, CD133 expression was too low for reliable detection by either assay (Table 4.5, pg. 108). Therefore, ALDH^{high} cells do not express higher levels of CD133. Furthermore, none of the tested populations displayed robust expression of CD133. This is consistent with findings of CD133 expression in only 30% of ovarian tumors, which limits the potential of CD133 for isolation of ovarian cancer stem cells[57].

Multiple markers of ovarian cancer stem cells have been proposed and each marker has been shown to identify a population of ovarian cancer cells with stem cell properties. Published studies have generally only examined one marker. This does not allow for comparison of the different markers, and so it is not known if these markers identify the same cell population. The data presented here suggests overlap between cells with high expression of ALDH1 and decreased expression of CD24. The remaining markers (CD44, KIT and CD133) do not exhibit consistent differential expression in ALDH^{high} cells indicating that these markers identify different cell populations than ALDH1.

No Consistent Differential Regulation of Hormone Receptors in ALDH^{high} Cells

Steroid hormones and their receptors have been implicated in the pathogenesis of ovarian cancer, and hormone receptor status serves as a prognostic indicator. Therefore, it is important to evaluate differential expression of hormone receptors in ovarian cancer stem cells. Expression of estrogen receptor α (ESR1) was too low to

reliably detect differences by microarray. PCR data indicated downregulation of ESR1 in $ALDH^{high}$ FNAR-C1 cells compared to $ALDH^{low}$ FNAR-C1 cells (Table 4.5, pg. 108). $ALDH^{high}$ taxol-resistant SKOV3 cells, however, exhibited upregulation of ESR1 relative to $ALDH^{low}$ SKOV3 cells (Table 4.5, pg. 108). In FNAR-C1 cells, progesterone receptor (PGR) expression appeared to be predominantly confined to $ALDH^{high}$ cells (Table 4.5, pg. 108). In SKOV3 cells, the opposite pattern was seen. $ALDH^{high}$ taxol-resistant SKOV3 cells did not express detectable levels of PGR, but very low levels of expression were detected in $ALDH^{low}$ SKOV3 cells (Table 4.5, pg. 108). In all populations tested, expression of androgen receptor was too low to reliably detect differences. Overall, no consistent differences in hormone receptor expression were found between $ALDH^{high}$ and $ALDH^{low}$ cells, suggesting no reliable association exists between hormone receptor expression and ovarian cancer stem cells.

Gonadotropins have been proposed to play a role in the progression of ovarian cancer, and therapies targeting gonadotropin receptors have been tested. Therefore, the expression of gonadotropin receptors in ovarian cancer stem cells may be relevant to therapeutics. Modest expression of follicle stimulating hormone receptor (FSHR) was measured in $ALDH^{high}$ and $ALDH^{low}$ FNAR-C1 cells by microarray (Table 4.5, pg. 108). FSHR could not be detected by PCR, but the clear expression by microarray suggests that this is likely a technical rather than biological phenomenon (Table 4.5, pg. 108). $ALDH^{high}$ taxol-resistant SKOV3 and $ALDH^{low}$ SKOV3 cells did not appear to express FSHR when measured by microarray (Table 4.5, pg. 108). Luteinizing

hormone/choriogonadotropin receptor (LHCGR) did not appear to be expressed in any population tested (Table 4.5, pg. 108). Overall, gonadotropin receptors do not appear to be consistently expressed in ALDH^{high} cells, which could have important implications for gonadotropin receptor targeted therapies.

Although her-2/neu and CA125 are not hormone receptors, their prognostic importance in ovarian cancer necessitates evaluation of expression levels in ovarian cancer stem cells. High levels of her-2/neu (ERBB2) expression were detected in all populations tested, but no reliable differences were found between ALDH^{high} and ALDH^{low} cells (Table 4.5, pg. 108). Therefore, ERBB2 does not appear to be consistently differentially regulated in ALDH^{high} ovarian cancer cells. Modest expression of CA125 (MUC16) was detected in all populations studied. ALDH^{high} FNAR-C1 cells showed upregulation of MUC16 relative to ALDH^{low} FNAR-C1 cells (Table 4.5, pg. 108). In contrast, no differences were seen between ALDH^{high} taxol-resistant SKOV3 cells and ALDH^{low} SKOV3 cells (Table 4.5, pg. 108). This indicates consistent expression of MUC16 in ovarian cancer stem cells.

Upregulation of MDR1, But Not Other ABC Transporters, in ALDH^{high} Cells

Increased expression of ATP-binding cassette (ABC) transporters leads to resistance to a wide array of drugs, possibly causing multi-drug resistance in stem cells[199]. The only ABC transporter that showed strong upregulation in ALDH^{high} cells of both models was the multidrug resistance protein 1 (MDR1), which is designated ABCB1 in humans and ABCB1B in rats (Table 4.2, pg. 98). Resistance to taxol

primarily results from increased expression of MDR1. Because the human model compares taxol-resistant to taxol-sensitive SKOV3 cells, upregulation of MDR1 may be associated with the acquisition of taxol resistance. Members of the multidrug resistance-associated protein subfamily (ABCC_) also induce multi-drug resistance. In $ALDH^{high}$ and $ALDH^{low}$ FNAR-C1 cells, high expression of ABCC1 was seen with the highest expression in $ALDH^{low}$ cells (Table 4.5, pg. 108). In contrast, similar levels of modest ABCC1 expression were detected in $ALDH^{high}$ taxol-resistant SKOV3 cells and $ALDH^{low}$ SKOV3 cells (Table 4.5, pg. 108). ABCC3 was upregulated in $ALDH^{high}$ taxol-resistant SKOV3 cells but was still highly expressed in both populations (Table 4.5, pg. 108). Conversely, both populations of FNAR-C1 cells showed similarly low levels of ABCC3 expression (Table 4.5, pg. 108). Side population is one proposed method to enrich for stem cells and is commonly attributed to ABCG2 expression[38, 39]. Similarly high levels of ABCG2 expression were seen in $ALDH^{high}$ and $ALDH^{low}$ FNAR-C1 cells with no apparent difference between the two populations (Table 4.5, pg. 108). However, ABCG2 was found to be upregulated in $ALDH^{high}$ taxol-resistant SKOV3 cells relative to $ALDH^{low}$ SKOV3 cells (Table 4.5, pg. 108). Although expression of ABCG2 varied in $ALDH^{low}$ cells, consistent expression was seen in the $ALDH^{high}$ population. No other ABC transporters associated with a stem cell phenotype or drug resistance were differentially regulated in either model. Overall, these data suggest that expression of ABC transporters may

not be consistently differentially regulated between ovarian cancer stem cells and their differentiated counterparts.

Telomerase Is Not Upregulated in ALDH^{high} Cells

Cells that undergo repeated cell division must maintain telomere length. Accordingly, elevated telomerase activity has been reported in a variety of cancer stem cells, and so expression of telomerase genes was examined[200-202]. Both ALDH^{high} and ALDH^{low} populations of FNAR-C1 cells showed comparably modest levels of TERC expression (Table 4.5, pg. 108). Modest expression of TERC was also detected in ALDH^{high} taxol-resistant SKOV3 and ALDH^{low} SKOV3 cells, but with slight upregulation in the ALDH^{high} population (Table 4.5, pg. 108). Relative to expression levels of TERC, FNAR-C1 cells expressed higher levels of TERT, but SKOV3 cells expressed lower levels of TERT. TERT was not differentially expressed in ALDH^{high} FNAR-C1 compared to ALDH^{low} FNAR-C1 cells (Table 4.5, pg. 108). In contrast, TERT was downregulated in ALDH^{high} taxol-resistant SKOV3 cells versus ALDH^{low} SKOV3 cells (Table 4.5, pg. 108). All populations tested exhibited very high expression of DKC1 with possible slight downregulation in ALDH^{high} cells compared to ALDH^{low} cells in both models (Table 4.5, pg. 108). FNAR-C1 cells expressed high levels of TEP1 with no apparent differences between ALDH^{high} and ALDH^{low} populations (Table 4.5, pg. 108). However, SKOV3 cells showed low expression of TEP1 with downregulation in ALDH^{high} taxol-resistant SKOV3 cells. Overall, no consistent upregulation of telomerase genes was observed in ALDH^{high} cells.

Additionally, the specific telomerase genes displayed highly variable levels of expression within the same populations. This suggests that telomerase activity is not responsible for telomere maintenance in these models.

Developmental Pathways Are Not Consistently Active In ALDH^{high} Cells

Developmental pathways not only regulate embryonic development, but various reports suggest that they also play an important role in ovarian cancer stem cells. Proliferation of ovarian cancer stem cells depends on NFκB signaling[203]. The Wnt/β-catenin pathway regulates tumor-initiating capacity and chemoresistance in ovarian cancer stem cells[204, 205]. Ovarian cancer stem cell survival involves Notch signaling[35]. Although no data specific to ovarian cancer stem cells exists at this time, Hedgehog signaling has been reported in cancer stem cells and chemoresistant ovarian cancer cells[54, 206]. Because of the reported importance of developmental pathways in ovarian cancer stem cells, gene expression patterns for the NFκB, Wnt/β-catenin, Notch and Hedgehog pathways were examined in ALDH^{high} cells.

Analysis of the NFκB pathway revealed upregulation of many genes in ALDH^{high} FNAR-C1 cells relative to ALDH^{low} FNAR-C1 cells (Figure 4.20). Receptors often serve as a primary level of pathway regulation. Accordingly, ALDH^{high} cells expressed higher levels of several NFκB pathway receptors. Toll-like receptor 3, which activates the NFκB pathway in response to double-stranded RNA, showed 2.51-fold upregulation[207]. Activating growth factor receptors also exhibited

upregulation, including: fibroblast growth factor receptors 1 and 2 (FGFR1: 3.82-fold, 24.101-fold by PCR; FGFR2: 22.67-fold, 33.065-fold by PCR), fms-related tyrosine kinase 1 (3.13-fold), and growth hormone receptor (4.65-fold)[208-210]. In addition to receptors, intracellular kinases regulate pathway activity. $ALDH^{high}$ cells showed 4.18-fold upregulation of mitogen-activated protein kinase kinase 6, which triggers a signaling cascade that activates NFκB[211]. Finally, $ALDH^{high}$ cells displayed 2.99-fold (3.553-fold by PCR) upregulation of a component of the NFκB complex, RELA[212]. Although not differentially regulated, both $ALDH^{high}$ and $ALDH^{low}$ FNAR-C1 cells strongly expressed NFκB. Overall, upregulation of receptors, an activating kinase and a component of the NFκB complex indicates increased NFκB pathway activity in $ALDH^{high}$ FNAR-C1 cells.

Conversely, $ALDH^{high}$ taxol-resistant SKOV3 cells showed downregulation of the NFκB pathway compared to $ALDH^{low}$ SKOV3 cells (Figure 4.21). Differential expression of receptors served as the primary level of regulation. TNFRSF11B and interleukin 1 receptor type II (IL1R2) are decoy receptors that lack intracellular signaling motifs, thereby inhibiting pathway activation[213, 214]. $ALDH^{high}$ cells displayed 2.09-fold upregulation of TNFRSF11B and 2.40-fold upregulation of IL1R2. Furthermore, the activating receptor TGFBR2 exhibited 2.69-fold (12.987-fold by PCR) downregulation[215]. The observed downregulation of a signaling receptor and upregulation of decoy receptors suggests reduced activity of the NFκB pathway in $ALDH^{high}$ taxol-resistant SKOV3 cells.

Figure 4.20: FNAR-C1 NFκB Signaling

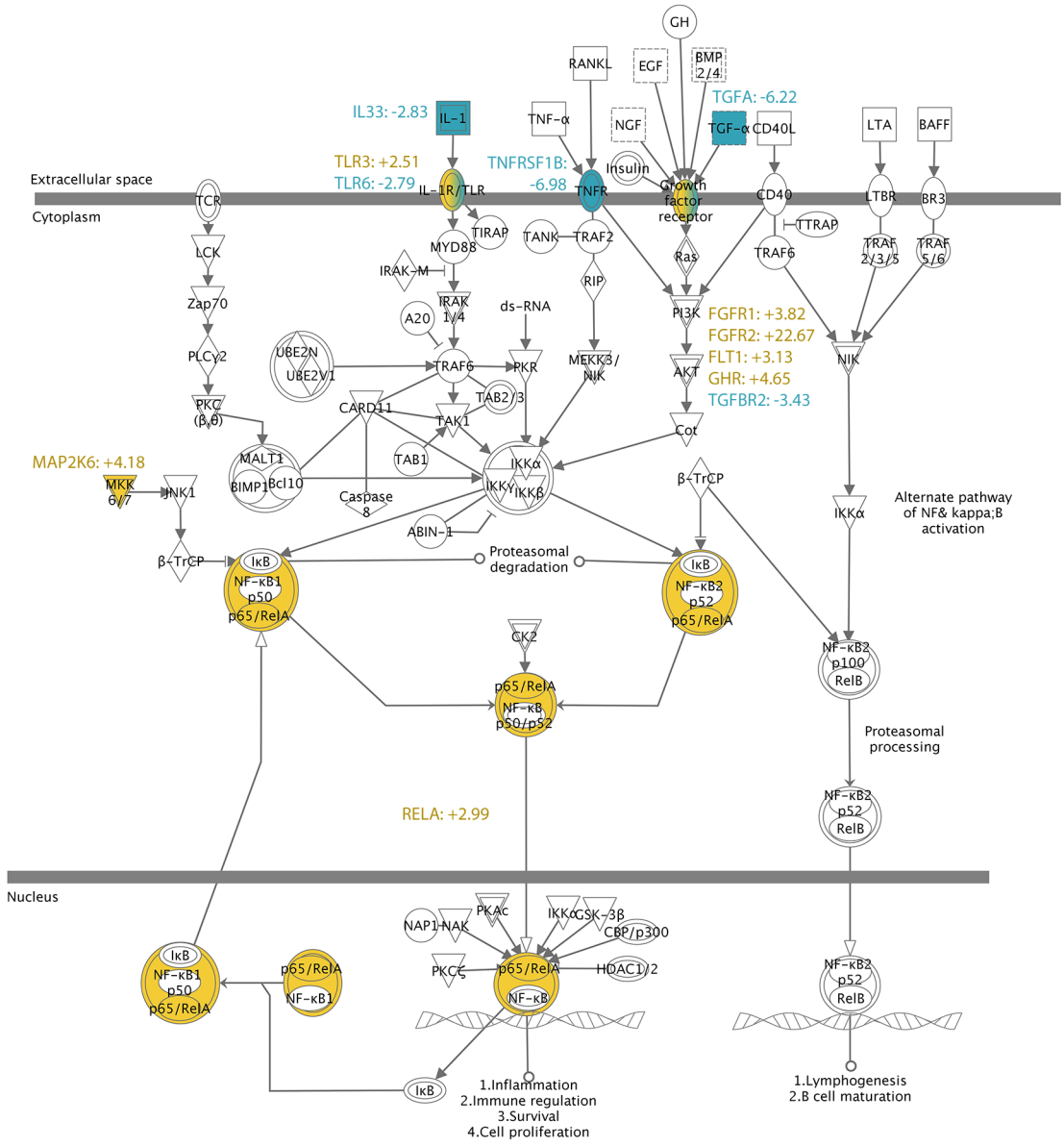

Pathway analysis of microarray data. Data is presented as ALDH^{high} FNAR-C1 cells relative to ALDH^{low} FNAR-C1 cells. Genes shaded in yellow were upregulated and genes shaded in blue were downregulated.

Figure 4.21: SKOV3 NFκB Signaling

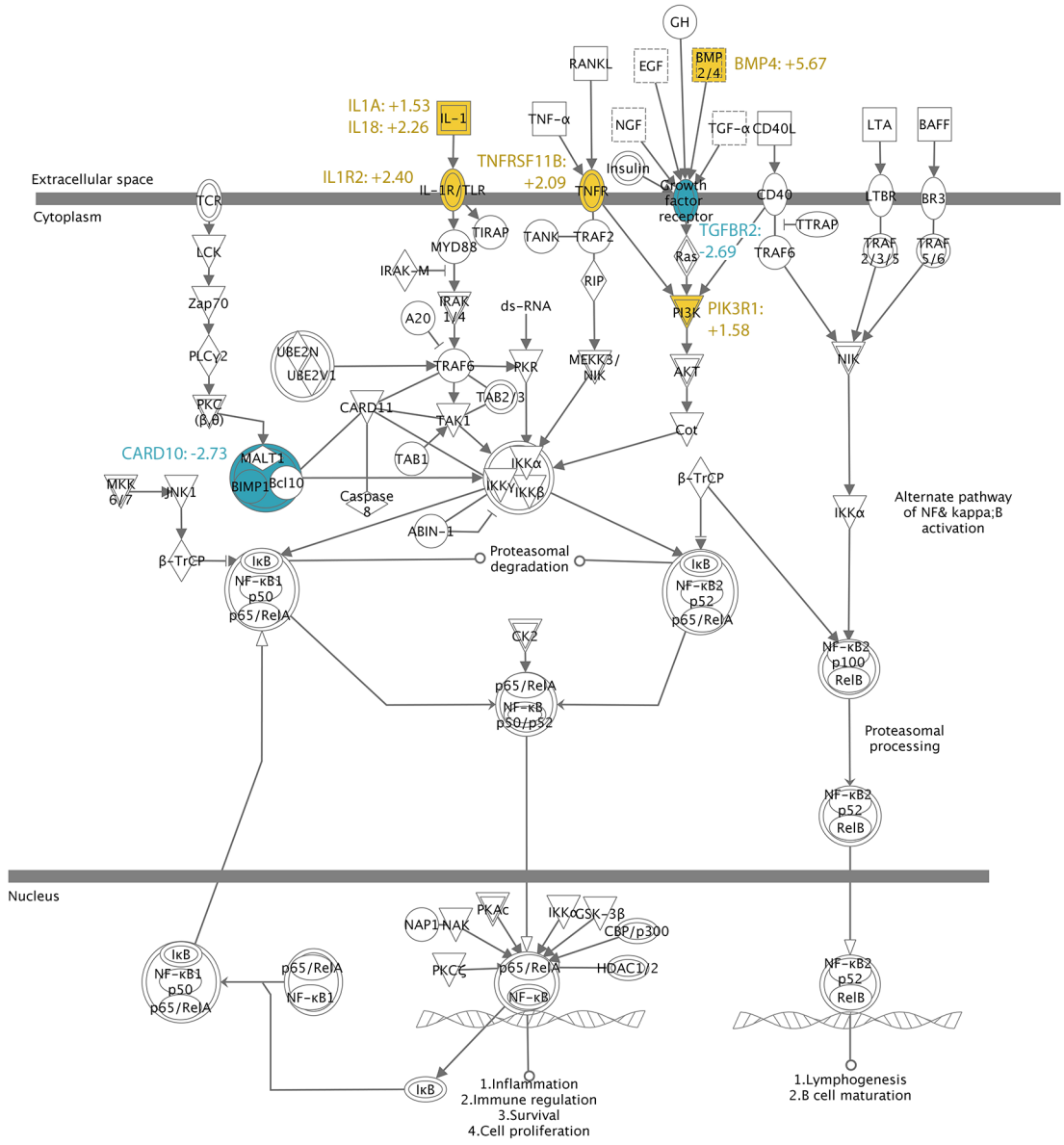

Pathway analysis of microarray data. Data is presented as ALDH^{high} taxol-resistant SKOV3 cells relative to ALDH^{low} SKOV3 cells. Genes shaded in yellow were upregulated and genes shaded in blue were downregulated.

The Wnt/β-catenin pathway exhibited substantial differential regulation in $ALDH^{high}$ FNAR-C1 cells relative to $ALDH^{low}$ FNAR-C1 cells (Figure 4.22). $ALDH^{high}$ cells showed upregulation of multiple WNT genes, including: WNT2B (93.69-fold, 581.598-fold by PCR), WNT4 (10.79-fold, 18.296-fold by PCR), WNT10A (2.56-fold), and WNT11 (10.75-fold, 15.722-fold by PCR). Although secreted WNT proteins can act in an autocrine or paracrine manner, upregulation of intracellular pathway components in $ALDH^{high}$ cells suggests increased Wnt/β-catenin activity in this population. MARK2 promotes nuclear translocation of β-catenin and exhibited 4.29-fold upregulation (5.212-fold by PCR) in $ALDH^{high}$ cells[216]. However, observation of nuclear β-catenin in unsorted cells cultured in differentiation medium suggests that nuclear β-catenin may not be restricted to the $ALDH^{high}$ population (Figure 2.4). Transcription of β-catenin target genes requires the LEF/TCF complex in addition to nuclear β-catenin[217]. $ALDH^{high}$ cells displayed 3.31-fold upregulation (88.626-fold by PCR) of LEF1 and 4.20-fold upregulation (6.754-fold by PCR) of TCF7L1. Additionally, $ALDH^{low}$ cells did not express detectable levels of LEF1. This implies that transcription of β-catenin target genes can only take place in $ALDH^{high}$ cells. Therefore, $ALDH^{high}$ FNAR-C1 cells have increased Wnt/β-catenin pathway activity versus $ALDH^{low}$ cells.

Figure 4.22: FNAR-C1 Wnt/β-Catenin Signaling

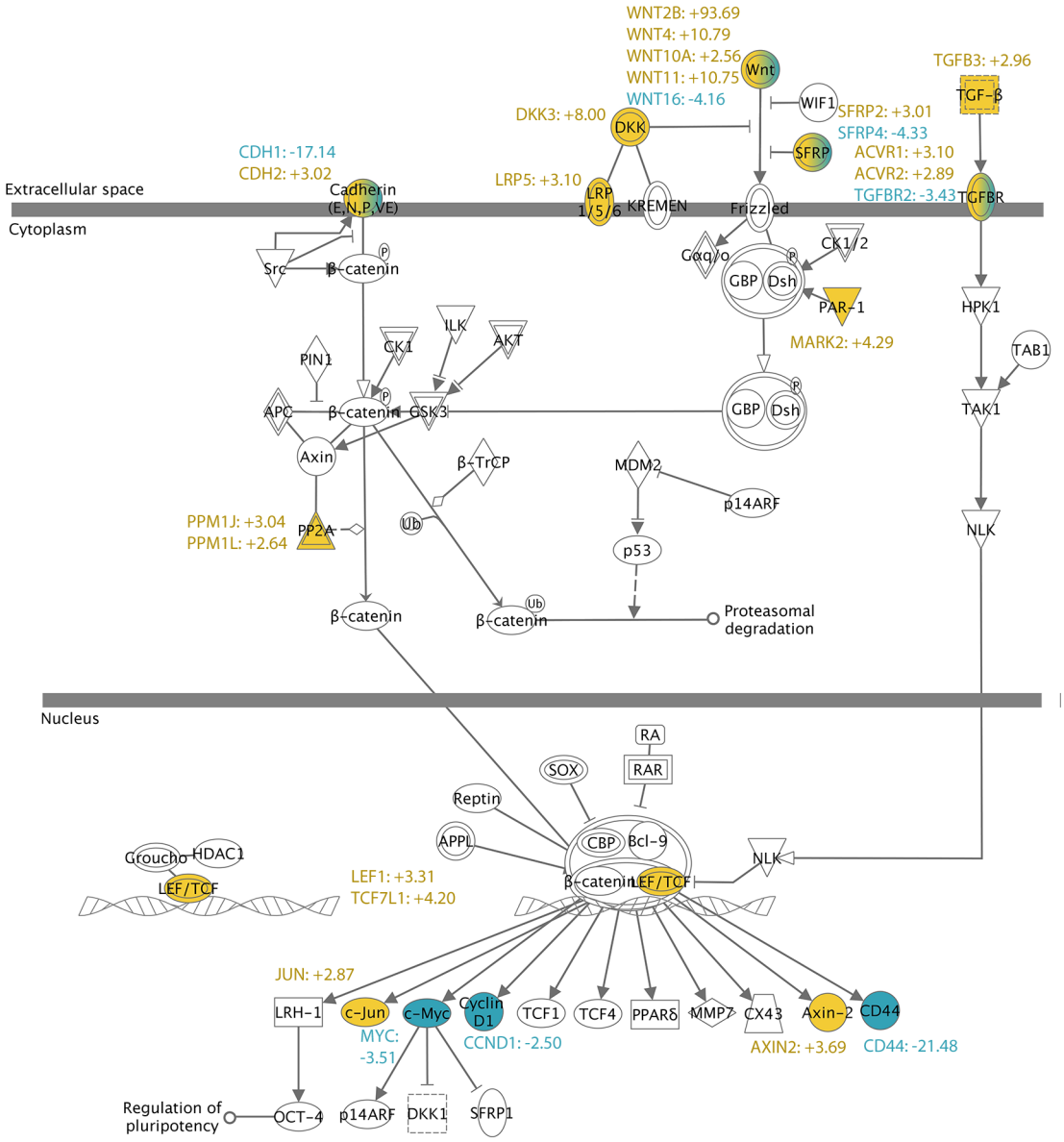

Pathway analysis of microarray data. Data is presented as ALDH^{high} FNAR-C1 cells relative to ALDH^{low} FNAR-C1 cells. Genes shaded in yellow were upregulated and genes shaded in blue were downregulated.

Figure 4.23: SKOV3 Wnt/β-Catenin Signaling

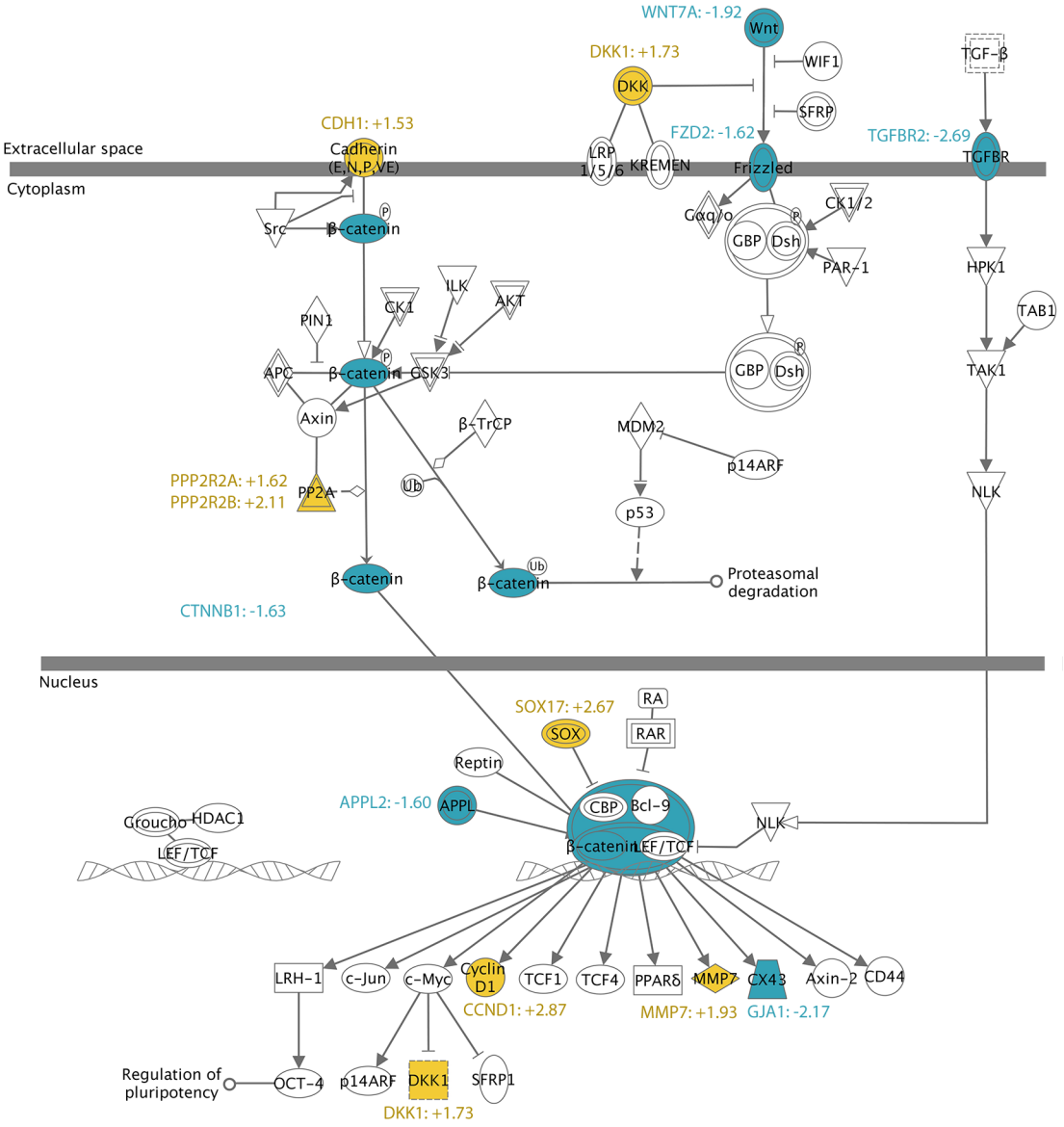

Pathway analysis of microarray data. Data is presented as ALDH^{high} taxol-resistant SKOV3 cells relative to ALDH^{low} SKOV3 cells. Genes shaded in yellow were upregulated and genes shaded in blue were downregulated.

In contrast, ALDH^{high} taxol-resistant SKOV3 cells showed downregulation of the Wnt/β-catenin pathway relative to ALDH^{low} SKOV3 cells (Figure 4.23). ALDH^{high} cells exhibited 1.63-fold downregulation (2.519-fold by PCR) of β-catenin (CTNNB1). In addition to downregulation of this crucial transcriptional coregulator, frizzled family receptor 2 (FZD2), the predominant frizzled receptor expressed in these cells, displayed 1.62-fold downregulation in ALDH^{high} cells. Additional reduction of pathway activity in ALDH^{high} cells was suggested by 2.67-fold upregulation of the inhibitor SOX17 and 1.60-fold downregulation of the activator APPL2[218, 219]. Based on downregulation of the preponderant receptor, downregulation of β-catenin, and differential regulation of genes that modulate pathway activity, the Wnt/β-catenin pathway appears to be less active in ALDH^{high} taxol-resistant SKOV3 cells than in ALDH^{low} SKOV3 cells.

Although few genes of the Notch pathway were differentially regulated in ALDH^{high} FNAR-C1 cells compared to ALDH^{low} FNAR-C1 cells, those that were differentially expressed serve as important regulators of pathway activity (Figure 4.24). ALDH^{high} cells exhibited downregulation of the Notch ligands jagged 1 (JAG1, 1.85-fold) and jagged 2 (JAG2, 6.14-fold), which would primarily impact signaling in adjacent cells. However, the endocytosis of Notch ligands bound to cleaved Notch also alters signaling in the ligand-expressing cell[220]. Manic fringe (MFNG) inhibits jagged 1 activation of Notch signaling and showed 3.66-fold upregulation in ALDH^{high} cells[221]. Overall, ALDH^{high} FNAR-C1 cells displayed differential regulation of genes

that suggests reduced Notch signaling, but this effect may not be limited to the $ALDH^{high}$ population.

Differential regulation of Notch pathway genes in $ALDH^{high}$ taxol-resistant SKOV3 cells versus $ALDH^{low}$ SKOV3 cells suggests altered Notch signaling (Figure 4.25). The only intracellular pathway component to exhibit differential regulation was nicastrin (NCSTN), which is a component of the γ-secretase complex. γ-Secretase cleaves the intracellular domain of Notch to permit signaling[222]. Although nicastrin showed 1.52-fold downregulation in $ALDH^{high}$ cells, the gene was still highly expressed in both $ALDH^{high}$ and $ALDH^{low}$ cells, and the other known components of γ-secretase were expressed at similar levels in both populations. Therefore, γ-secretase is likely active in both populations. Altered Notch signaling appeared to be primarily due to 2.12-fold downregulation of lunatic fringe (LFNG) in $ALDH^{high}$ cells. Lunatic fringe inhibits jagged 1 signaling through Notch 1, and so downregulation would increase Notch signaling[223]. Differential regulation of genes in $ALDH^{high}$ taxol-resistant SKOV3 cells suggests increased Notch signaling, however this altered signaling may impact other cell populations as well.

Figure 4.24: FNAR-C1 Notch Signaling

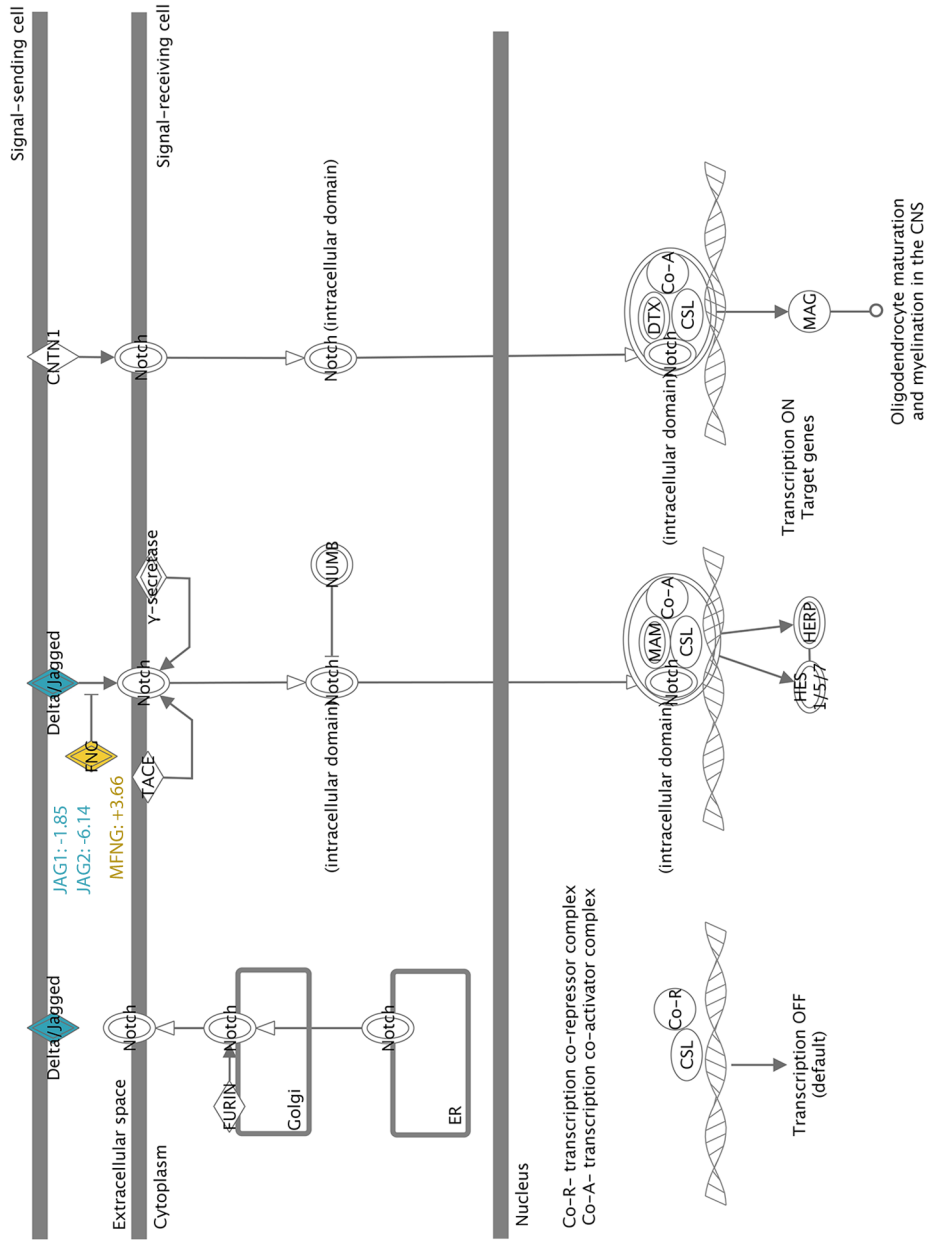

Pathway analysis of microarray data. Data is presented as $ALDH^{high}$ FNAR-C1 cells relative to $ALDH^{low}$ FNAR-C1 cells. Genes shaded in yellow were upregulated and genes shaded in blue were downregulated.

Figure 4.25: SKOV3 Notch Signaling

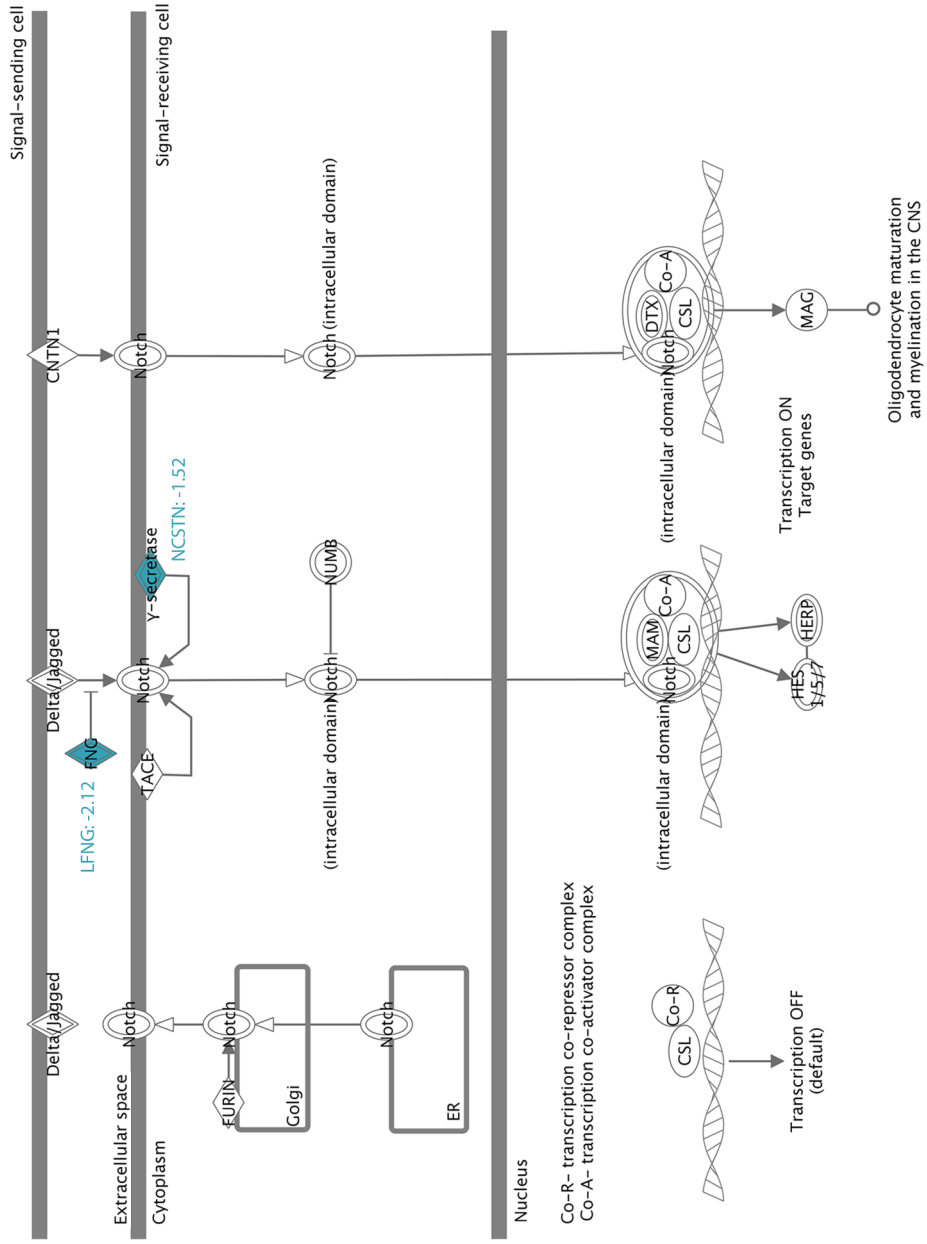

Pathway analysis of microarray data. Data is presented as ALDH^{high} taxol-resistant SKOV3 cells relative to ALDH^{low} SKOV3 cells. Genes shaded in yellow were upregulated and genes shaded in blue were downregulated.

The data presented here indicates inconsistent developmental pathway activity in ovarian cancer stem cells from different sources. $ALDH^{high}$ FNAR-C1 cells displayed upregulation of the NFκB and Wnt/β-catenin pathways but downregulation of Notch signaling. $ALDH^{high}$ taxol-resistant SKOV3 cells demonstrated the opposite pattern with upregulated Notch signaling but downregulated NFκB and Wnt/β-catenin pathways. The only consistency between the two models was that neither model exhibited differential regulation of the Hedgehog pathway. While this data indicates a role for developmental pathways in ovarian cancer stem cells, their significance is not consistent.

Potential Therapeutic Targets to Eliminate $ALDH^{high}$ Cells

The primary purpose of studying ovarian cancer stem cells was to identify potential therapies. If the cancer stem cell hypothesis is accurate, eliminating ovarian cancer stem cells should lead to durable remission for patients. Microarray data identified gene expression profiles in $ALDH^{high}$ cells that could be exploited for cancer stem cell-targeted therapy. These potential therapeutic targets include the mTOR pathway, her-2/neu, CD47 and FGF18.

Differential gene expression of $ALDH^{high}$ cells from both models indicates increased mTOR signaling. Figure 4.26 shows the mTOR pathway in $ALDH^{high}$ FNAR-C1 cells compared to $ALDH^{low}$ FNAR-C1 cells. The mTOR pathway in $ALDH^{high}$ taxol-resistant SKOV3 cells relative to $ALDH^{low}$ SKOV3 cells is displayed in Figure 4.27. The primary mechanism of increased mTOR signaling involved

modulation of the tuberous sclerosis complex (TSC), which inhibits mTOR activation through RHEB[224]. ALDH^{high} FNAR-C1 cells inhibited TSC complex activity through 4.61-fold upregulation of insulin receptor substrate 1 (IRS1)[225]. Inhibition of the TSC complex in ALDH^{high} taxol-resistant SKOV3 cells was achieved with 1.58-fold upregulation of PI3K[226]. ALDH^{high} cells of both models additionally blocked TSC inhibition of the mTOR pathway through upregulation of RPS6KB2 (FNAR-C1: 3.23-fold; SKOV3: 1.55-fold)[227]. Not shown in the pathway analysis is ras-related GTP binding D (RRAGD), which stimulates the mTOR pathway[228]. ALDH^{high} cells from both models exhibited upregulation of RRAGD (Table 4.2, pg. 98). The increased activity of the mTOR pathway in ALDH^{high} cells of both models suggests that inhibition of mTOR signaling could eliminate ovarian cancer stem cells. The mTOR inhibitor rapamycin has been administered clinically for more than a decade. Because the clinical safety of rapamycin is well established, clinical testing for the treatment of ovarian cancer could proceed rapidly.

Ovarian cancer specimens commonly express her-2/neu (ERBB2)[229]. Accordingly, expression of ERBB2 was detected in both models. FNAR-C1 cells showed strong expression in both ALDH^{high} and ALDH^{low} fractions (Table 4.5, pg. 108). SKOV3 cells expressed ERBB2 at a sufficiently high level as to suggest overexpression. Furthermore, ALDH^{high} taxol-resistant SKOV3 cells displayed a slight, but consistent, upregulation of ERBB2 relative to ALDH^{low} SKOV3 cells (Table 4.5, pg. 108). Because both ALDH^{high} populations expressed ERBB2, ERBB2-

targeted therapy could potentially eliminate ovarian cancer stem cells in patients with detectable expression. Several drugs targeting ERBB2 are currently clinically available, which would reduce the time necessary for clinical testing.

Figure 4.26: FNAR-C1 mTOR Signaling

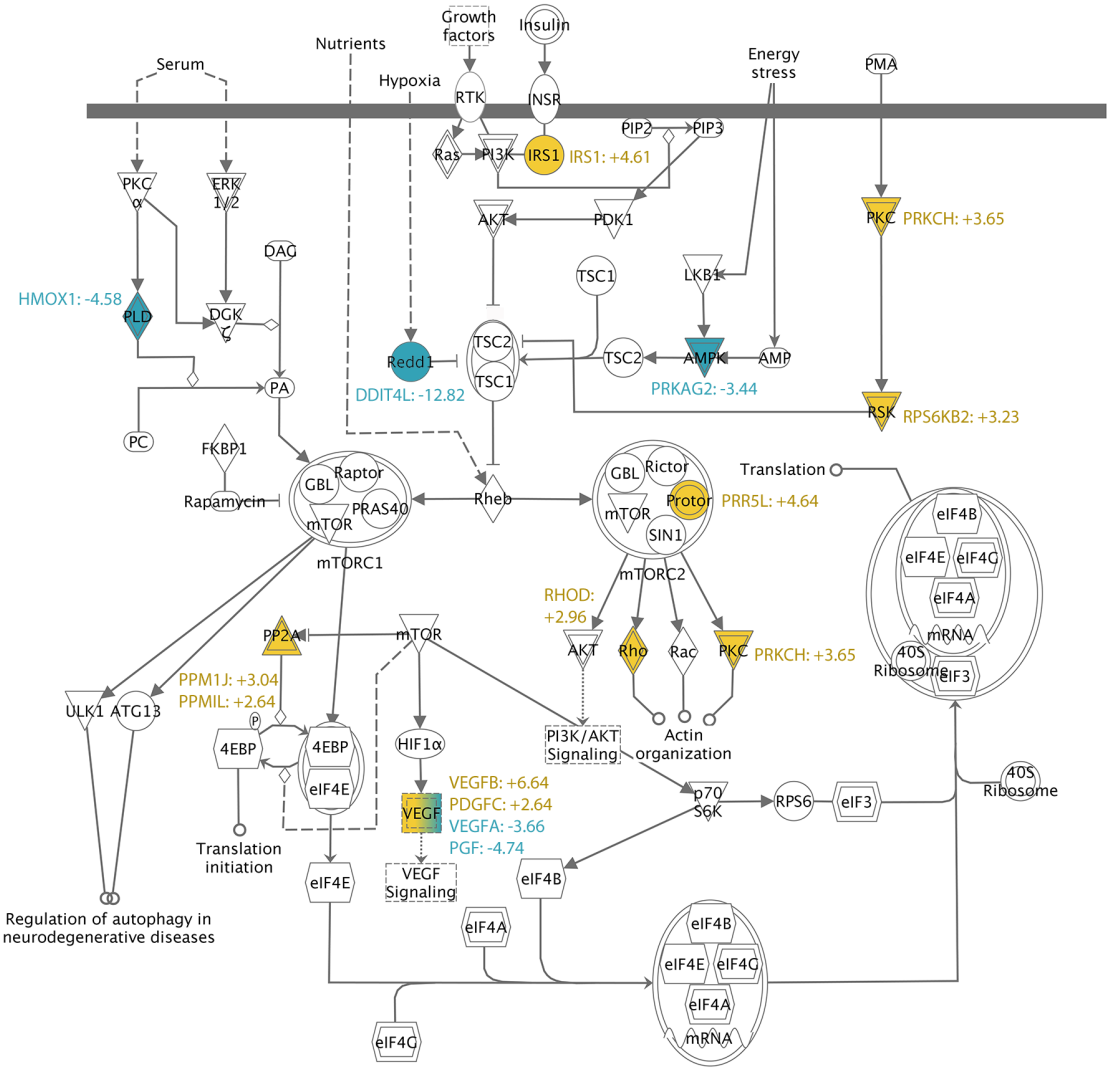

Pathway analysis of microarray data. Data is presented as ALDH^{high} FNAR-C1 cells relative to ALDH^{low} FNAR-C1 cells. Genes shaded in yellow were upregulated and genes shaded in blue were downregulated.

Figure 4.27: SKOV3 mTOR Signaling

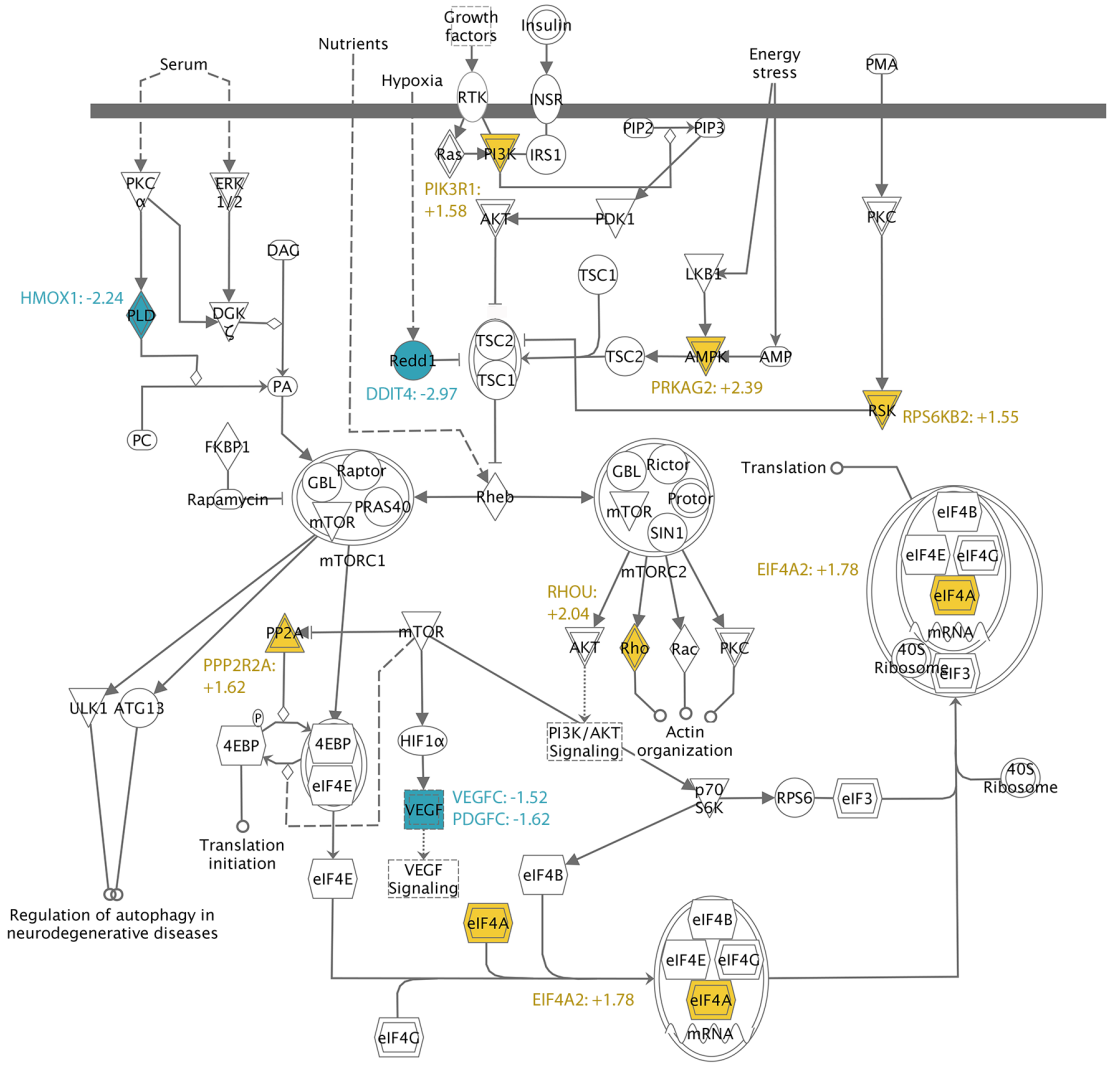

Pathway analysis of microarray data. Data is presented as ALDH^{high} taxol-resistant SKOV3 cells relative to ALDH^{low} SKOV3 cells. Genes shaded in yellow were upregulated and genes shaded in blue were downregulated.

CD47 prevents phagocytosis by macrophages and is highly expressed in normal and malignant stem cells[230, 231]. ALDH^{high} cells of both models expressed higher levels of CD47 than their ALDH^{low} counterparts (Table 4.2, pg. 99).

Accordingly, therapy targeting CD47 could potentially eradicate ovarian cancer stem cells. Preclinical studies suggest that CD47-specific antibodies could effectively treat a broad range of cancers, including ovarian cancer[232]. Should this treatment strategy proceed to clinical use, it may successfully eliminate all populations of ovarian cancer cells.

Both $ALDH^{high}$ populations exhibited upregulation of fibroblast growth factor 18 versus their $ALDH^{low}$ counterparts (FGF18; Table 4.2, pg. 98). FGF18 primarily signals through fibroblast growth factor receptor 3 (FGFR3), which was expressed in all populations tested[233]. Therefore, FGF18 signaling may serve an important role in all populations of ovarian cancer cells, and FGFR3 inhibition might successfully treat ovarian cancer stem cells. Encouragingly, several small molecule inhibitors of FGFR3 are in clinical development for cancer treatment.

Table 4.2: Common Upregulated Genes (continued on next page)

Gene Symbol	FNAR-C1 Microarray	FNAR-C1 PCR	SKOV3 Microarray	SKOV3 PCR
NOV	100.842		2.226	
ALDH1A2	86.522	325.761		
ALDH1A1			23.699	44.494
FBN2	32.256		1.592	
ANGPTL4	17.557	31.900	2.621	3.511
ABCB1B (MDR1)	16.797	24.603		
ABCB1 (MDR1)			3.743	374.276
FRAS1	5.665		2.143	
TM7SF2	5.444		2.105	
MAL2	5.390		10.221	
PLCE1	5.294		1.620	
CTSC	4.447		1.521	
HIST3H2A	4.349		1.647	
CHKA	4.302		2.703	
SUV420H1	3.948		1.531	
OLR1	3.869		2.859	
CXADR	3.734		4.441	
RRAGD	3.467		2.309	
RPS6KB2	3.225		1.551	
NDUFV1	3.187		1.616	
KRT19	3.183		2.153	
TFPI	3.102	3.850	4.702	5.129
EDN2	3.082		2.318	
CFH	3.030		2.867	
COX8A	3.007		1.785	
FGF18	2.912	3.793	1.778	3.775
CFB	2.848		1.515	
DAB2	2.834		2.320	
TRPT1	2.789		1.617	
SPRY1	2.786		2.012	
PXDN	2.776		2.431	
ASNS	2.768		2.191	

Table 4.2 Continued: Common Upregulated Genes

Gene Symbol	FNAR-C1 Microarray	FNAR-C1 PCR	SKOV3 Microarray	SKOV3 PCR
AGRN	2.757		1.789	
EYA4	2.746		1.704	
WBP5	2.679		2.955	
MTUS1	2.655		1.580	
COL5A2	2.603		2.384	
ECH1	2.600		1.795	
CTSD	2.582		2.282	
RTN3	2.568		1.791	
ANXA1	2.557	2.745	1.576	1.488
NGFRAP1	2.373		1.865	
NAPRT1	2.353		1.705	
FLOT1	2.311		1.699	
CTTN	2.295		1.571	
RHOBTB3	2.282		3.038	
SDPR	2.274		4.977	
GCA	2.257		1.771	
IL1R2	2.176		2.398	
PIK3R1	2.119		1.580	
STX3	2.090		1.627	
CD47	2.088	1.961	1.827	2.079
PPP2R2B	2.074		2.108	183.615
ITPKA	2.072		1.605	
EIF4A2	2.064		1.780	
HEXB	2.034		1.692	
APLP2	2.025		1.996	
AIF1L	2.018		1.546	
MRPL23	2.003		1.620	

This table lists all genes that were upregulated in both models along with fold-change values from microarray and PCR analyses. Empty cells signify that the gene was not tested with that assay. FNAR-C1 data is presented as $ALDH^{high}$ FNAR-C1 cells versus $ALDH^{low}$ FNAR-C1 cells. SKOV3 data is presented as $ALDH^{high}$ taxol-resistant SKOV3 cells versus $ALDH^{low}$ SKOV3 cells.

Table 4.3: Common Downregulated Genes (continued on next page)

Gene Symbol	FNAR-C1 Microarray	FNAR-C1 PCR	SKOV3 Microarray	SKOV3 PCR
LAMB3	-30.654		-1.682	
KCNN4	-25.750		-2.313	
PLAC8	-18.015		-2.993	
NQO1	-14.447		-1.821	
LAMC2	-11.326		-3.648	
CDA	-8.878		-6.756	-776.822
TUBB3	-8.845	-20.000	-6.735	-10.526
ANXA8/ANXA8L1	-7.870		-1.951	
TGFBI	-6.848	-6.250	-25.686	-90.909
SFN	-6.696		-3.786	-11.494
COL17A1	-5.623		-3.033	
SCD	-5.517		-1.649	
ALDH4A1	-5.182		-1.553	
ANKRD37	-5.095		-1.517	
UAP1	-5.000		-1.574	
SGK1	-4.978		-6.039	
HMOX1	-4.582	-5.155	-2.241	-18.868
PCOLCE2	-4.360		-1.977	
P4HA2	-4.167		-2.509	
TSPAN13	-4.007		-1.933	
GCNT1	-3.678		-2.538	
CCDC92	-3.672		-1.948	
TGFBR2	-3.432	-2.114	-2.691	-12.987
HSPB1	-3.391		-1.994	
FSTL3	-3.277	-12.500	-1.936	-3.115
ALDOC	-3.224		-1.858	
PTHLH	-3.211		-1.910	
CLIC3	-3.191		-2.056	
HOMER2	-3.112		-1.631	
MT2A	-3.107		-2.094	
PFKP	-3.098		-1.904	
TUBA4A	-3.070	-3.030	-6.257	-33.333

Table 4.3 Continued: Common Downregulated Genes

Gene Symbol	FNAR-C1 Microarray	FNAR-C1 PCR	SKOV3 Microarray	SKOV3 PCR
UBL3	-3.031		-1.758	
SLC2A1	-2.958		-3.406	
SNAI2	-2.909		-4.370	
VIM	-2.901	-3.300	-2.798	-4.000
SAT1	-2.896		-1.533	
ELL2	-2.721		-1.551	
PKM2	-2.684		-1.798	
NET1	-2.647		-1.513	
AK4	-2.634		-2.641	
PLAUR	-2.626	-2.667	-2.711	-9.346
RNPEP	-2.552		-1.825	
NUDT5	-2.509		-1.896	
FXYD5	-2.449	-2.096	-3.708	-4.630
PGK1	-2.369		-1.903	
PAQR4	-2.312		-1.721	
KRT17	-2.274		-2.321	
TBC1D2	-2.259		-2.100	
LDHA	-2.254		-2.096	
MAOA	-2.223		-1.622	
RGS2	-2.099		-2.161	
BNIP3	-2.068		-3.836	
UGT1A6	-2.053		-1.780	
HDGF	-2.030		-1.612	
ANKRD57	-2.018		-2.037	

This table lists all genes that were downregulated in both models along with fold-change values from microarray and PCR analyses. Empty cells signify that the gene was not tested with that assay. FNAR-C1 data is presented as $ALDH^{high}$ FNAR-C1 cells versus $ALDH^{low}$ FNAR-C1 cells. SKOV3 data is presented as $ALDH^{high}$ taxol-resistant SKOV3 cells versus $ALDH^{low}$ SKOV3 cells.

Table 4.4: Commonly Regulated Gene Families (continued on next 5 pages)

Gene	FNAR-C1	SKOV3	Function
Kruppel-Like Factor			
KLF2		-1.932	Differentiation
KLF4	-4.256		Differentiation; tumor suppressor
KLF6		-2.039	Tumor suppressor
S100 Calcium Binding Protein			
S100A2		-4.856	Tumor suppressor
S100A11		-1.814	
Epithelial Membrane Protein			
EMP2	-3.937		Cell proliferation; cell-cell interactions; tumor suppressor
EMP3		-4.642	
Bone Morphogenetic Protein			
BMP4		5.671	Cancer invasion
BMP7	4.454 (3.329)		
Cadherin			
CDH11	4.150		Cancer invasion
CDH16		-1.590	Functionally related cell-cell adhesion molecules
CDH17	-10.845		
Protein Tyrosine Kinase			
PTK2		1.538	Cell adhesion molecule; cell migration; proliferation and apoptosis; angiogenesis
PTK7	3.609		
Matrix Metallopeptidase			
MMP2	3.137 (↑)		Extracellular matrix degradation; cancer invasion
MMP7		1.927 (8.823)	
MMP14	2.610 (3.274)		
Insulin-Like Growth Factor Binding Protein			
IGFBP4	-5.651		Enhancer of apoptosis in malignant prostate cells
IGFBP3		-2.366	
ADAM Metallopeptidase Domain			
ADAM15	-4.114		Invasion and metastasis
ADAM19		-3.034	
ADAM23	-6.454		

Table 4.4 Continued: Commonly Regulated Gene Families

Gene	FNAR-C1	SKOV3	Function
Doublecortin-Like Kinase			
DCLK1		-1.544	Neuronal migration
DCLK3	-2.795		
Semaphorin			
SEMA3B		2.194	Tumor suppressor
SEMA3D	6.965		
Vascular Endothelial Growth Factor			
VEGFA	-3.660 (-5.348)		Vasculogenesis; angiogenesis; endothelial cell growth/migration
VEGFC		-1.524	
Serpin Peptidase Inhibitor			
SERPINB6	-2.640		Coagulation
SERPINB8	-4.538		
SERPINC1	-4.741 (-3.676)		
SERPINE1		-5.692 (-32.258)	
SERPINB2	-4.340 (-3.546)		Inhibition of extracellular matrix degradation
SERPINE1		-5.692 (-32.258)	
Collagen			
COL5A2	2.603	2.384	Regulation of type I collagen fibrillogenesis
COL24A1	2.778		
COL4A1		-2.016 (-3.333)	Basement membrane
COL4A4	-3.854		
COL7A1		-2.848 (-83.333)	
COL14A1	-4.909		
Cathepsin			
CTSL1		-3.390	Lysosomal proteinase
CTSH	-2.562		

Table 4.4 Continued: Commonly Regulated Gene Families

Gene	FNAR-C1	SKOV3	Function
Keratin			
KRT19	3.183	2.153	Structural integrity of epithelial cells
KRT15	11.738		
KRT34		-1.565	Structural constituent of cytoskeleton activity
KRT31	-3.487		
Kelch-Like Family Member			
KLHL2	2.538		Organizing the actin cytoskeleton of the brain cells
KLHL5		1.547	
Tubulin			
TUBA1A		-1.679	Constituent of microtubules
TUBA8	-3.601		
TUBA4A	-3.070 (-3.030)	-6.257 (-33.333)	Constituent of microtubules; GTPase
TUBB2A	-19.737		
TUBB3	-8.845 (-20.000)	-6.735 (-10.526)	GTPase
Tropomyosin			
TPM1		-1.628	
TPM2	-13.703		
TPM3		-1.908	
RAS Oncogene Family			
RAB1B	2.689		ER, Golgi transport
RAB36	5.053		
RAB38		1.527	
RAB7A		1.840	Endocytosis
RAB36	5.053		
RAB38		1.527	
RIN2	4.260		
RAB31		2.160	
RAS			
RASA1		-2.241	Inhibition of RAS
RASA4/RASA4B	-2.998		

Table 4.4 Continued: Commonly Regulated Gene Families

Gene	FNAR-C1	SKOV3	Function
Copine			
CPNE7	3.118		Calcium-dependent, phospholipid binding protein, membrane trafficking and in protein-protein interactions
CPNE8		1.559	
Cytochrome P450			
CYP1B1		1.552 (1.996)	Androgen metabolism; source of retinoic acid
CYP3A5	3.149		Metabolism of intra-prostatic androgens
CYP26B1	-12.803		Specific inactivation of all-trans-retinoic acid
DNA-Damage-Inducible Transcript			
DDIT4		-2.967	Inhibition of MTOR activity
DDIT4L	-12.820		
Nuclear Receptor Subfamily 1, Group H			
NR1H4	2.699		Cholesterol transport & metabolism
NR1H3		1.570	
ATP-Binding Cassette, Subfamily A			
ABCA1		-2.747	Lipid efflux
ABCA7	-2.862		
Solute Carrier Family			
SLC16A5		1.893	Monocarboxylic acid transporter
SLC16A11	3.183		
SLC22A1	-3.740		Organic cation transporter
SLC22A2		-1.677	
SLC22A18	-3.667		
Microsomal Glutathione S-Transferase			
MGST1	6.948		Protecting cells from cytostatic drugs
MGST2		2.919	Leukotriene biosynthesis
MGST3	2.737		
Glutathione S-Transferase			
GSTA2	2.609		Conjugating reduced glutathione to a wide mumber of exogenous and endogenous hydrophobic electrophiles
GSTM1		1.731 (**)	

Table 4.4 Continued: Commonly Regulated Gene Families

Gene	FNAR-C1	SKOV3	Function
Dimethylarginine Dimethylaminohydrolase			
DDAH1		1.690	Regulating cellular concentration of demethylargenines
DDAH2	3.598		
Phospholipase C			
PLCB1	2.764		Hydrolysis of phosphatidylinositol 4,5 biphosphate to generate diacylglycerol and inositol 1,4,5 triphosphate
PLCE1	5.294	1.620	
Caspase			
CASP3		1.686	Cysteine containing aspartate-specific protease; apoptosis
CASP4		1.606	
CASP7	2.677		
1-Acylglycerol-3-Phosphate O-Acyltransferase			
AGPAT4		-1.566	Phospholipid biosynthesis
AGPAT9	-2.604		
Dual-Specificity Tyrosine-(Y)-Phosphorylation Regulated Kinase			
DYRK2		-1.608	Serine/threonine and tyrosine kinase; phosphorylating histone H2B; cell growth and development
DYRK3	-3.081		
Hexokinase			
HK1		-1.609	Phosphorylating glucose to produce glucose-6-phosphate
HK2	-3.287		
Gap Junction Protein			
GJA1		-2.173 (-11.905)	Formation of gap junctions
GJA5	-3.752		
GJB2	-768.740		
Transglutaminase			
TGM2		-2.002	Cross-linking of proteins; signal transduction; guanosine triphosphate hydrolysis
TGM5	-3.813		
Glutathione Peroxidase			
GPX2	-4.330		Formation of glutathione disulfide
GPX8		-1.631	

Table 4.4 Continued: Commonly Regulated Gene Families

Gene	FNAR-C1	SKOV3	Function
Phosphodiesterase			
PDE5A	6.074		Inactivation of cGMP
PDE9A		1.887	
Receptor Tyrosine Kinase-Like Orphan Receptor			
ROR1		1.548	Functionally redundant
ROR2	4.119		
Cysteine and Glycine-Rich Protein			
CSRP2	3.871		
CSR2BP		1.576	

This table lists members of gene families with similar function that are consistently differentially regulated in both models by microarray. Fold change values from microarray analysis are presented and fold-change values from PCR analysis are shown in parenthesis. Arrows denote direction of change when fold-change values cannot be calculated because one sample is undetectable by PCR. ** Denotes genes undetectable by PCR in both samples. FNAR-C1 data is presented as $ALDH^{high}$ FNAR-C1 cells versus $ALDH^{low}$ FNAR-C1 cells. SKOV3 data is presented as $ALDH^{high}$ taxol-resistant SKOV3 cells versus $ALDH^{low}$ SKOV3 cells.

Table 4.5: Previously Reported Ovarian Cancer Stem Cell Markers, Hormone Receptors, ABC Transporters and Telomerase Genes

Gene	FNAR-C1 Microarray	FNAR-C1 PCR	SKOV3 Microarray	SKOV3 PCR
CD24	-1.763	-1.560	-9.458	-41.667
CD44	-21.481	-22.727	-1.188	-1.003
KIT	1.289	10.644	-1.968	-333.333
CD133 (PROM1)	-1.009	↓	-1.026	1.38
ESR1	1.062	-2.101	1.126	2.544
PGR	1.306	123.991	-1.032	↓
AR		3.073	1.029	-1.242
FSHR	1.140	**	1.022	
LHCGR	-1.008	**	1.036	
ERBB2 (her-2/neu)	-1.040	-1.147	1.320	1.308
MUC16 (CA125)	5.241	13.157	-1.078	
ABCC1	-2.120	-2.421	1.031	
ABCC3	-1.051		2.207	1.652
ABCG2	-1.462	-1.242	1.377	20.030
TERC	1.015		1.037	1.779
TERT	1.111	1.561	-1.046	-7.936
DKC1	-1.618		-1.355	
TEP1	-1.369	-1.179	1.014	-2.421

This table lists genes important in cancer stem cells or ovarian cancer along with fold-change values from microarray and PCR. FNAR-C1 data is presented as $ALDH^{high}$ FNAR-C1 cells versus $ALDH^{low}$ FNAR-C1 cells. SKOV3 data is presented as $ALDH^{high}$ taxol-resistant SKOV3 cells versus $ALDH^{low}$ SKOV3 cells. Arrows signify direction of change when gene was undetectable in one sample. ** Signifies that the gene was not detectable in either sample. Empty cells signify that the gene was not tested with that assay.

5 Discussion

ALDH^{high} Cells Represent Ovarian Cancer Stem Cells

The cancer stem cell hypothesis proposes that, although altered, the differentiation hierarchy of malignancies remains intact with rare stem cell populations giving rise to the differentiated progeny that comprise the bulk of the tumor. Cancer stem cells have been identified in many cancers, and these cells have been proposed to initiate metastases and relapse. This project identified putative ovarian cancer stem cells based on high aldehyde dehydrogenase 1 (ALDH1) activity in two models of ovarian cancer. The first model was the FNAR-C1 rat model of ovarian cancer, which most closely resembles an endometrioid carcinoma. One

benefit of this model is that it originated from a spontaneous tumor and therefore does not have artificial genetic manipulation. It can also be readily transplanted into immunocompetent Lewis rats, which may be more representative than xenografts into immunodeficient mice. Although the endometrioid subtype is a less aggressive subtype, it would be ideal to identify a marker that isolates ovarian cancer stem cells in all ovarian cancer subtypes[234].

In order to control for species or subtype differences, the human SKOV3 cell line was also studied. The initial report of the SKOV3 cell line did not describe the subtype[235]. Subsequent analyses described SKOV3 cells as both serous and clear cell subtypes[76, 77]. The serous subtype is the most common form of ovarian cancer, representing approximately 70% of cases[236]. Meanwhile, only 10% of ovarian cancer cases are of the clear cell subtype[236]. When stratified by stage, serous and clear cell subtypes have similar prognoses; however, patients with the serous subtype are much less likely to present in stage I than those with the clear cell subtype[236, 237]. Despite the uncertain histological subtype represented by SKOV3 cells, this model is distinct from the endometrioid subtype of FNAR-C1 cells. Therefore, the use of these two models should allow for identification of ovarian cancer stem cells across all subtypes.

High ALDH1 activity ($ALDH^{high}$) is strongly associated with stem cells and chemoresistant cells[62, 238, 239]. Additionally, multiple types of cancer stem cells have been reported to possess high ALDH1 enzyme activity[20, 63-65, 67, 74]. For these reasons, ovarian cancer cells were isolated based on ALDH1 activity and examined for stem

cell characteristics. Cells cultured in medium containing serum (referred to as differentiation medium) lacked a distinct $ALDH^{high}$ population (Figure 4.1A, C). In order to study $ALDH^{high}$ cells, it was necessary to culture cells in medium that supported the expansion of undifferentiated cells (KnockOut medium). FNAR-C1 cells maintained in KnockOut medium possessed a distinct $ALDH^{high}$ population (Figure 4.1B). SKOV3 cells, on the other hand, remained $ALDH^{low}$ (data not shown). Examination of a taxol-resistant SKOV3 subline showed a prominent $ALDH^{high}$ population (Figure 4.1D). To further expand this population, taxol-resistant SKOV3 cells were cultured in KnockOut medium (Figure 4.1E). Using these conditions permitted the comparison of $ALDH^{high}$ and $ALDH^{low}$ populations from both models.

A concern of comparing cells from distinct culture conditions is that differences between the two populations may be due to biology or the differing media. However, less than ten percent of differentially regulated genes were consistent between the two models. Because so few genes were consistently differentially regulated, the observed differences between $ALDH^{high}$ and $ALDH^{low}$ cells is likely to be due to the underlying biology of the cells. An additional concern is comparing taxol-resistant to taxol-sensitive SKOV3 cells, as this could identify differences due to drug resistance rather than a stem cell phenotype. To control for this, microarray data from the SKOV3 model was compared to the FNAR-C1 model, which had not undergone drug selection. Only those differences that were consistent between the two models were presented thus eliminating differences due to drug resistance alone.

Moreover, taxol-resistant SKOV3 cells displayed resistance to additional drugs with different mechanisms of resistance, which makes it unlikely that the taxol resistance per se was responsible for the observed biological differences

With the populations identified, it became possible to test the hypothesis that cells with high ALDH1 activity have a stem cell phenotype. The first category of stem cell properties examined was growth characteristics, which included nonadherent growth, relative quiescence and lacking contact inhibition. $ALDH^{high}$ cells displayed an absence of contact inhibition with the formation of nodules, which were not seen in $ALDH^{low}$ cells (Figure 4.2A). The capacity for nonadherent growth, as shown through the formation of spheroids, was also restricted to the $ALDH^{high}$ population (Figure 4.2B, C). Gene expression analysis showed a block at the G1/S checkpoint in $ALDH^{high}$ cells (Figures 4.6 and 4.7). Because of this, the $ALDH^{high}$ population contained fewer dividing cells than the $ALDH^{low}$ population (Figure 4.5) resulting in a slower growth rate (Figure 4.4). Taken together, $ALDH^{high}$ cells were more quiescent than their $ALDH^{low}$ counterparts. Overall, $ALDH^{high}$ cells possessed growth characteristics consistent with a stem cell phenotype.

Cancer stem cells are hypothesized to possess additional biological features, such as smaller size, the ability to regenerate the phenotypic diversity of the tumor, self-renewal, increased tumorigenicity, and drug resistance[127-133]. $ALDH^{high}$ cells were smaller in size than their $ALDH^{low}$ counterparts, which may be due to their relative quiescence (Figure 4.3). $ALDH^{high}$ cells were the only population able to produce

both $ALDH^{high}$ and $ALDH^{low}$ cells, thus regenerating the phenotypic diversity of the cell line (Figures 4.8 and 4.9). This indicates the loss of ALDH1 activity concurrent with differentiation. The expansion of $ALDH^{high}$ cells additionally suggests the capacity for self-renewal. Tumorigenicity was confined to the $ALDH^{high}$ population (Table 4.1). Exposure to drugs with different mechanisms of action and resistance revealed multi-drug resistance in $ALDH^{high}$ cells (Figure 4.10)[144, 240-247]. Additionally, culture with taxol increased the percentage of $ALDH^{high}$ cells (Figure 4.11). Therefore, $ALDH^{high}$ cells display biological characteristics of stem cells.

Gene expression patterns may also indicate a stem cell phenotype (Figures 4.12 to 4.15). $ALDH^{high}$ cells expressed higher levels of genes commonly restricted to stem cells and lower levels of genes associated with differentiation. Differential gene expression suggested the capacity for self-renewal in $ALDH^{high}$ cells. Genes associated with the maintenance of pluripotency were upregulated in $ALDH^{high}$ cells as were genes involved in quiescence. $ALDH^{high}$ cells also exhibited upregulation of genes important for stem or progenitor cell proliferation. Thus, differential gene expression in $ALDH^{high}$ cells further supports the conclusion that this population represents ovarian cancer stem cells.

Since $ALDH^{high}$ cells displayed numerous cancer stem cell properties, analysis of $ALDH^{high}$ cells may reveal properties of ovarian cancer stem cells. Because of its comprehensive nature, microarray analysis was employed to compare $ALDH^{high}$ and $ALDH^{low}$ cells, and real-time qRT-PCR of individual genes was performed to validate

the findings. By better understanding the biology of ovarian cancer stem cells, targeted therapeutics can be developed in order to improve patient outcomes.

ALDH^{high} Cells Represent a Biologically Distinct Population

Differential gene expression indicated increased tight junction signaling in ALDH^{high} cells (Figures 4.16 and 4.17). Transmembrane components of tight junctions were upregulated as well as intracellular signaling molecules. The increased tendency of ALDH^{high} cells to form tight junctions may explain the observed formation of spheroids by these cells (Figure 4.2B, C)[248, 249]. Decreased cell cycle progression appears to be one result of these junctions. Junctional adhesion molecule 3 (JAM3) binds cingulin, which inhibits cell cycle progression by binding to Rho/Rac guanine nucleotide exchange factor 2 (ARHGEF2)[250, 251]. Both models showed differential regulation of the components of these interactions. ALDH^{high} FNAR-C1 cells expressed increased levels of JAM3. Conversely, ALDH^{high} taxol-resistant SKOV3 cells exhibited upregulation of cingulin and downregulation of ARHGEF2. This signaling interaction may provide a mechanism for contact inhibition. Intriguingly, ALDH^{high} cells in nodules and spheroids continue to proliferate, albeit at a very slow rate, suggesting that some Aldefluor high cells escape this growth inhibition.

Ovarian cancer stem cells have been proposed to be responsible for invasion and metastasis. Differential gene expression in ALDH^{high} cells provides support for this hypothesis (Table 4.4). ALDH^{high} cells showed downregulation of multiple tumor

suppressor genes, indicating a more malignant phenotype with increased proliferation, migration and invasion[173, 177, 252-256]. In addition to the loss of tumor suppressor genes, ALDH^{high} cells exhibited upregulation of genes contributing to invasion, including enzymes responsible for extracellular matrix degradation. Not only were degradation enzymes upregulated, but inhibitors of degradation were also downregulated. Further permitting invasion, ALDH^{high} cells downregulated basement membrane deposition. Taken together, ALDH^{high} cells demonstrated an increased capacity for migration and invasion compared to ALDH^{low} cells. One route for dissemination of cancer cells is the vascular system. Activation of the extrinsic pathway of the coagulation cascade could potentially inhibit this migration. Tissue factor pathway inhibitor (TFPI) inhibits the initiation of the extrinsic pathway and was upregulated in ALDH^{high} cells (Table 4.2, Figure 4.18 and Figure 4.19). Combined with increased invasiveness, the prevention of coagulation observed in ALDH^{high} cells indicates an ability to enter the blood and lead to distant metastases. Overall, differential gene expression in ALDH^{high} cells supports the hypothesis that ovarian cancer stem cells are more malignant than their differentiated counterparts and represent the cell population capable of migration, invasion and metastasis.

ALDH^{high} Cells Have Inconsistent Expression of Previously Reported Ovarian Cancer Stem Cell Markers

In addition to high ALDH1 activity, other markers have been reported to identify ovarian cancer stem cells, including CD24, CD44, KIT and CD133. Because

most studies only examine one marker, it is not known if these varied markers identify the same cell population. This project permitted the evaluation of marker expression levels in $ALDH^{high}$ and $ALDH^{low}$ cells from two different ovarian cancer subtypes. CD24 was the only marker to show consistent differential expression between the two models (Table 4.5). Previous reports disagree as to whether ovarian cancer stem cells express CD24 to a greater or lesser degree than their differentiated progeny[46, 59]. Data presented here indicated reduced CD24 expression in ovarian cancer stem cells. However, all populations showed strong expression of CD24, potentially limiting the usefulness of this marker for isolation. Variable expression of CD44 and KIT have been reported for putative ovarian cancer stem cells and this study confirmed previously reported variability[29, 35, 37, 61]. CD44 was downregulated in $ALDH^{high}$ FNAR-C1 cells but unchanged in $ALDH^{high}$ taxol-resistant SKOV3 cells. KIT was upregulated in $ALDH^{high}$ FNAR-C1 cells but downregulated in $ALDH^{high}$ taxol-resistant SKOV3 cells. Despite reports of CD133 expression on ovarian cancer stem cells, only 30-70% of ovarian cancer specimens express detectable levels of CD133[55, 56]. Expression of CD133 could not be reliably detected in any population tested. Therefore, the only previously reported ovarian cancer stem cell marker to be consistently differentially regulated in $ALDH^{high}$ cells was CD24.

The differentiation hierarchy of normal solid tissues is poorly understood, which complicates studies of cancer stem cells in solid tumors. The reason for such varied reports of ovarian cancer stem cell markers is unclear. It is possible that

differentiation proceeds through several stages and each marker identifies a particular stage. Furthermore, ovarian cancer is a collection of diseases with different subtypes, and some markers may be subtype-specific. This project benefits from the study of two distinct subtypes to control for this possibility. Alternatively, heterogeneity between patients may yield inconsistent results. Further study is necessary to distinguish between the potential explanations for marker variability.

No Consistent Differential Regulation of Hormone Receptors in ALDH^{high} Cells

Steroid hormones are often used as prognostic indicators in ovarian cancer, and hormone therapy has been proposed as a treatment strategy. Therefore, expression of hormone receptors in ovarian cancer stem cells could have implications for clinical evaluation and treatment. Estrogen receptor α (ESR1) was differentially regulated in both models, but in opposite directions (Table 4.5). Although expression was low overall, both ALDH^{high} populations expressed detectable levels of ESR1. This indicates variability in ESR1 expression in ovarian cancer stem cells relative to differentiated cells. However, ovarian cancer stem cells likely express ESR1 at sufficient levels for hormone therapy to be effective. Like ESR1, progesterone receptor (PGR) showed conflicting directions of differential regulation in the two models (Table 4.5). In contrast to ESR1, PGR did not show detectable expression in ALDH^{high} taxol-resistant SKOV3 cells suggesting that PGR may not be expressed in all ovarian cancer stem cells. Androgen receptor (AR) expression could not be

reliably detected in any population (Figure 4.5). It is not clear why FNAR-C1 cells showed expression of AR by flow cytometry but not by PCR (Figure 2.3). However, due to upregulation of cytochrome P450 genes that inactivate testosterone, it appears that androgen signaling may not be active in $ALDH^{high}$ cells (CYP3A5 in FNAR-C1 and CYP1B1 in SKOV3; Table 4.4, pg. 104)[257, 258]. Overall, no consistent differences in hormone receptor expression were seen in $ALDH^{high}$ cells, which indicates variable expression in ovarian cancer stem cells.

Gonadotropin signaling has been implicated in ovarian cancer progression, and gonadotropin-targeted therapies have been proposed. Consequently, gonadotropin receptor expression in ovarian cancer stem cells may have clinical implications. Gonadotropin receptors were infrequently expressed and when expressed did not show differential expression in $ALDH^{high}$ cells. Follicle stimulating hormone receptor (FSHR) was only detected in FNAR-C1 cells (Table 4.5). Luteinizing hormone/choriogonadotropin receptor (LHCGR) was not expressed in any population tested (Table 4.5). Therefore, any therapy targeting gonadotropin receptors would be unlikely to reliably eliminate ovarian cancer stem cells.

Although not hormone or gonadotropin receptors, her-2/neu (ERBB2) and CA125 (MUC16) have implications for ovarian cancer prognosis, necessitating evaluation of their expression in ovarian cancer stem cell. Similarly high levels of ERBB2 expression were detected in $ALDH^{high}$ and $ALDH^{low}$ FNAR-C1 cells (Table 4.5). SKOV3 cells exhibited extremely high levels of ERBB2 expression, suggesting

overexpression. Additionally, ALDH^{high} taxol-resistant SKOV3 cells displayed a slight, but consistent, upregulation of ERBB2 (Table 4.5). Overall, these data suggest that ovarian cancer stem cells consistently express ERBB2 at a similar level as the rest of the tumor. Therefore, any prognostic or therapeutic application for ERBB2 should be unaffected by the presence of ovarian cancer stem cells. CA125 is used clinically to evaluate response to therapy and relapse. FNAR-C1 cells showed modest expression of CA125 with upregulation in ALDH^{high} cells (Table 4.5). Both populations of SKOV3 cells showed consistent, low levels of CA125 expression (Table 4.5). This implies that ovarian cancer stem cells express CA125 and should not interfere with clinical measurements.

Upregulation of MDR1, But Not Other ABC Transporters, In ALDH^{high} Cells

Expression of ATP-binding cassette (ABC) transporters has been proposed as a specific feature of stem cells. The only ABC transporter that was consistently upregulated in ALDH^{high} cells was multidrug resistance protein 1 (MDR1; ABCB1B in rats, ABCB1 in humans; Table 4.2). MDR1 prevents the intracellular accumulation of a broad class of drugs, including taxol, which may account for the observed taxol resistance in ALDH^{high} cells. The multidrug resistance-associated protein subfamily (ABCC_) also causes drug resistance. ABCC1 was downregulated in ALDH^{high} FNAR-C1 cells, but still highly expressed (Table 4.5). SKOV3 cells, on the other hand, showed similar, low levels of ABCC1 expression in both populations (Table 4.5). Conversely, both populations of SKOV3 cells showed high levels of ABCC3

expression, despite upregulation in ALDH^{high} taxol-resistant SKOV3 cells (Table 4.5). Both ALDH^{high} and ALDH^{low} FNAR-C1 cells exhibited modest ABCC3 expression without differential regulation (Table 4.5). Therefore, each model showed strong expression with differential regulation of one member of the multidrug resistance-associated protein subfamily, but neither of these differentially regulated genes were consistent between the two models. The side population phenotype that is often used to enrich for stem cells is attributed to ABCG2 expression. Only ALDH^{high} taxol-resistant SKOV3 cells showed upregulation of ABCG2 (Table 4.5). Similarly high levels of ABCG2 expression were observed in both populations of FNAR-C1 cells (Table 4.5). Accordingly, expression of ABCG2 was consistently found in ALDH^{high} cells, but variable in ALDH^{low} cells. Overall, ovarian cancer stem cells likely express variable levels of ABC transporters and those that are consistent may be clinically relevant.

Telomere Maintenance Is Due To Alternative Lengthening of Telomeres

The gene components of telomerase showed variable levels of expression and inconsistent differential regulation (Table 4.5). This suggests that telomerase is unlikely to be responsible for telomere maintenance in ALDH^{high} cells. Instead, microarray data suggested that alternative lengthening of telomeres might be the mechanism for telomere maintenance (data not shown). Many genes reportedly involved in alternative lengthening of telomeres showed high levels of expression in all populations studied, including the MRN complex (MRE11A, RAD50 and NBN),

proteins that prevent telomere shortening (FEN1, MUS81 and FANCD2), and additional components (TERF1, TERF2, TINF2 and TERF2IP)[259-263]. ALDH^{high} FNAR-C1 cells showed some upregulation of these genes, including SMC5 (3.226-fold), FEN1 (3.295-fold) and MUS81 (2.058-fold). Functionally though, alternative lengthening of telomeres likely occurs in both ALDH^{high} and ALDH^{low} cells. Because all cells were expanded *in vitro*, all populations required maintenance of telomere length. In order to determine mechanisms of telomere maintenance in ovarian cancer stem cells, primary tumors must be analyzed.

Developmental Pathways Are Not Consistently Active In ALDH^{high} Cells

While the importance of developmental pathways in embryonic development has been well established, recent evidence indicates a role for developmental pathways in normal and malignant adult stem cells as well[264-271]. The NFκB, Wnt/β-catenin and Notch pathways showed differential regulation in both models, but with different effects. Differential regulation in ALDH^{high} FNAR-C1 cells indicated active NFκB and Wnt/β-catenin pathways but decreased Notch signaling (Figures 4.20, 4.22 and 4.24). In contrast, ALDH^{high} taxol-resistant SKOV3 cells exhibited increased Notch signaling but downregulated NFκB and Wnt/β-catenin signaling (Figures 4.21, 4.23 and 4.25). Neither model displayed differential regulation of the Hedgehog pathway. This suggests that developmental pathways may have the dual functions of stem cell maintenance or differentiation depending on the context of the cell.

Potential Ovarian Cancer Stem Cell-Targeted Therapy

The ultimate goal of cancer research is to improve patient outcomes. The cancer stem cell hypothesis proposes that eliminating cancer stem cells will lead to durable remission. This study identified potential therapeutic targets on the basis of gene expression, including the mTOR pathway, ERBB2, CD47 and FGF18. Because two distinct subtypes were studied, the results found here are more likely to be representative of all ovarian cancer stem cells.

Of the identified potential therapeutic targets, only the mTOR pathway and CD47 are expected to be specific for ovarian cancer stem cells. $ALDH^{high}$ cells showed increased mTOR activity and upregulation of CD47 compared to $ALDH^{low}$ cells. In contrast, ERBB2 was highly expressed in all populations. Although FGF18 was upregulated in $ALDH^{high}$ cells, the secreted protein could act on either $ALDH^{high}$ or $ALDH^{low}$ cells, both of which express the specific receptor FGFR3. While targeting ERBB2 or FGFR3 would potentially eliminate ovarian cancer stem cells, these treatments would likely also target the differentiated population.

The potential treatment strategies also differ in clinical drug availability. Drugs targeting the mTOR pathway and ERBB2 are already in clinical use, thereby permitting a more rapid application of these treatment schemes. However, ERBB2-targeted therapy has only been used against cells that overexpress ERBB2, and so it remains to be determined if this therapy would also be effective against cells without overexpression. Several FGFR3 inhibitors are in clinical trials, but none has

completed phase 3 trials. Therapy targeting CD47 is still undergoing preclinical testing. Therefore, therapy targeting FGFR3 or CD47 would proceed much more slowly than mTOR- or ERBB2-targeted therapies.

Implications and Future Directions

This project contributes a valuable research model for the study of ovarian cancer. The FNAR-C1 model arose from a spontaneous ovarian tumor, so it lacks artificial genetic manipulation that may not be representative of the human disease. The tumor can be propagated *in vitro*, allowing for more detailed analysis of the cells. The tumor can also be transplanted *in vivo* into immunocompetent animals, permitting investigation of immune system interactions with the cancer. Additionally, recent controversy concerning evaluation of tumorigenicity in immunocompromised animals is circumvented with this model. Finally, the FNAR-C1 model is phenotypically consistent with human endometrioid ovarian cancer, making it a reliable model for this disease. Because the endometrioid subtype is not as common or aggressive as the serous subtype, fewer models of this subtype exist[234]. This project provides a model of endometrioid ovarian cancer with the potential to improve understanding of this disease.

In addition to contributing a novel research model, this project further validates the existence of ovarian cancer stem cells as well as the use of high aldehyde dehydrogenase activity as an ovarian cancer stem cell marker. Further research is required to elucidate the reason for the variety of proposed ovarian cancer stem cell

markers. This project begins to resolve this concern by demonstrating inconsistent expression of all markers except CD24. This represents the first analysis of multiple markers in different subtypes and helps to clarify the value of reported markers. Further comparisons remain necessary, ideally in a large cohort of patient samples, in order to fully characterize ovarian cancer stem cell markers.

Furthermore, this project provides the first comprehensive gene expression analysis of ovarian cancer stem cells from two discrete subtypes. This analysis illustrated the variability within ovarian cancer stem cells. In some cases, each achieved the same function but via alternative genes. In other cases, pathways were altered in divergent manners producing diverse properties. Rarely were gene expression differences consistent in both models. By identifying those genes and pathways with consistent expression, potential therapeutic targets were identified. Few studies have proposed targets for ovarian cancer stem cell eradication. Moreover, the few treatments that have been presented were not based on thorough analysis of independent ovarian cancer stem cell samples and therefore may not be consistently effective. In contrast, the treatments proposed by this analysis would likely target ovarian cancer stem cells across multiple subtypes.

While this project provides further understanding of ovarian cancer stem cells, additional research is necessary. Gene expression differences require validation via functional assays. These differences must also be confirmed in patient samples, ideally in a large cohort that includes all subtypes. Finally, proposed therapeutic

targets need to be tested for effectiveness against ovarian cancer stem cells. Should additional research confirm the results of this study, therapy targeting ovarian cancer stem cells may provide durable remission for patients.

References:

1. Bryan, Cyril P., *The Papyrus Ebers*. 1 ed. Vol. 1. 1930, Letchworth: The Garden City Press LTD. 167.
2. Pusey, Wm. Allen. *Report of Cases Treated with Roentgen Rays.* The Journal of the American Medical Association 1902;38(15):911-919.
3. Aronson, Stanley M. *Arsenic and Old Myths.* Rhode Island Medicine 1994;77233-234.
4. Gilman, Alfred. *Therapeutic applications of chemical warfare agents.* Federation Proceedings 1946;5285-292.
5. Jemal, Ahmedin, Rebecca Siegel, et al. *Cancer Statistics, 2009.* CA: A Cancer Journal for Clinicians 2009;59(4):225-249.
6. Ashley, D. J. B. *The two "hit" and multiple "hit" theories of carcinogenesis.* British Journal of Cancer 1969;23(2):313-328.
7. Richards, B. M. *Deoxyribose Nucleic Acid Values in Tumour Cells with Reference to the Stem-cell Theory of Tumour Growth.* Nature 1955;175(4449):259-261.
8. Makino, Sajiro. *The role of tumor stem-cells in regrowth of the tumor following drastic applications.* Acta Unio Int Contra Cancrum 1959;15(Suppl 1)(Suppl 1):196-198.
9. Killmann, S. A., E. P. Cronkite, et al. *Estimation of Phases of the Life Cycle in Leukemic Cells from Labeling in Human Beings in Vivo with Tritiated Thymidine.* Laboratory Investigation 1963;12(7):671-684.
10. Gavosto, Felice. *The proliferative kinetics of the acute leukemias.* European journal of clinical and biological research 1970;15(10):1042-1047.
11. Kohler, G. and C. Milstein. *Continuous cultures of fused cells secreting antibody of predefined specificity.* Nature 1975;256(5517):495-497.
12. Sabbath, Kert D., Edward D. Ball, et al. *Heterogeneity of clonogenic cells in acute myeloblastic leukemia.* Journal of Clinical Investigation 1985;75(2):746-753.
13. Lapidot, Tsvee, Christian Sirard, et al. *A cell initiating human acute myeloid leukaemia after transplantation into SCID mice.* Nature 1994;367(6464):645-648.
14. Bonnet, Dominique and John E. Dick. *Human acute myeloid leukemia is organized as a hierarchy that originates from a primitive hematopoietic cell.* Nature Medicine 1997;3730-737.
15. Sarry, Jean-Emmanuel, Kathleen Murphy, et al. *Human acute myelogenous leukemia stem cells are rare and heterogeneous when assayed in NOD/SCID/IL2Rgammac-deficient mice.* Journal of Clinical Investigation 2011;121(1):384-395.

16. Gerber, Jonathan M., B. Douglas Smith, et al. *A clinically relevant population of leukemic CD34+CD38- cells in acute myeloid leukemia.* Blood 2012;119(15):3571-3577.
17. Petzer, Andreas L., Connie J. Eaves, et al. *Characterization of primitive subpopulations of normal and leukemic cells present in the blood of patients with newly diagnosed as well as established chronic myeloid leukemia.* Blood 1996;88(6):2162-2171.
18. Gerber, Jonathan M., Lu Qin, et al. *Characterization of chronic myeloid leukemia stem cells.* American Journal of Hematology 2011;86(1):31-37.
19. Matsui, William, Carol Ann Huff, et al. *Characterization of clonogenic multiple myeloma cells.* Blood 2004;103(6):2332-2336.
20. Matsui, William, Qiuju Wang, et al. *Clonogenic Multiple Myeloma Progenitors, Stem Cell Properties, and Drug Resistance.* Cancer Research 2008;68(1):190-197.
21. Ikegame, A., S. Ozaki, et al. *Small molecule antibody targeting HLA class I inhibits myeloma cancer stem cells by repressing pluripotency-associated transcription factors.* Leukemia 2012.
22. Jones, Richard J., Christopher D. Gocke, et al. *Circulating clonotypic B cells in classic Hodgkin lymphoma.* Blood 2009;113(23):5920-5926.
23. Al-Hajj, Muhammad, Max S. Wicha, et al. *Prospective identification of tumorigenic breast cancer cells.* Proceedings of the National Academy of Sciences 2003;100(7):3983-3988.
24. Cannistra, Stephen A. *Cancer of the Ovary.* New England Journal of Medicine 1993;329(21):1550-1559.
25. Bapat, Sharmila A., Avinash M. Mali, et al. *Stem and Progenitor-Like Cells Contribute to the Aggressive Behavior of Human Epithelial Ovarian Cancer.* Cancer Research 2005;65(8):3025-3029.
26. Alvero, Ayesha B., Rui Chen, et al. *Molecular phenotyping of human ovarian cancer stem cells unravels the mechanisms for repair and chemoresistance.* Cell Cycle 2009;8(1):158-166.
27. Wei, Xiaolong, David Dombkowski, et al. *Mullerian inhibiting substance preferentially inhibits stem/progenitors in human ovarian cancer cell lines compared with chemotherapeutics.* Proceedings of the National Academy of Sciences 2010;107(44):18874-18879.
28. Wang, Lijuan, Roman Mezencev, et al. *Isolation and characterization of stem-like cells from a human ovarian cancer cell line.* Molecular and Cellular Biochemistry 2012;363(1-2):257-268.
29. Zhang, Shu, Curt Balch, et al. *Identification and Characterization of Ovarian Cancer-Initiating Cells from Primary Human Tumors.* Cancer Research 2008;68(11):4311-4320.

30. Abelson, Sagi, Yeela Shamai, et al. *Intratumoral Heterogeneity in the Self-Renewal and Tumorigenic Differentiation of Ovarian Cancer.* Stem Cells 2012;30(3):415-424.
31. Liang, Dongming, Yuanyuan Ma, et al. *The hypoxic microenvironment upgrades stem-like properties of ovarian cancer cells.* BMC Cancer 2012;12(1):201-211.
32. Steffensen, Karina Dahl, Ayesha B. Alvero, et al. *Prevalence of epithelial ovarian cancer stem cells correlates with recurrence in early-stage ovarian cancer.* Journal of Oncology 2011;2011(29):620523.
33. Liu, Ming, Gil Mor, et al. *High Frequency of Putative Ovarian Cancer Stem Cells With CD44/CK19 Coexpression Is Associated With Decreased Progression-Free Intervals In Patients With Recurrent Epithelial Ovarian Cancer.* Reproductive Sciences 2012.
34. Szotek, Paul P., Rafael Pieretti-Vanmarcke, et al. *Ovarian cancer side population defines cells with stem cell-like characteristics and Mullerian Inhibiting Substance responsiveness.* Proceedings of the National Academy of Sciences 2006;103(30):11154-11159.
35. Vathipadiekal, Vinod, Deepa Saxena, et al. *Identification of a Potential Ovarian Cancer Stem Cell Gene Expression Profile from Advanced Stage Papillary Serous Ovarian Cancer.* PLoS ONE 2012;7(1):e29079.
36. Hu, L., C. McArthur, and R. B. Jaffe. *Ovarian cancer stem-like side-population cells are tumourigenic and chemoresistant.* British Journal of Cancer 2010;102(8):1276-1283.
37. Latifi, Ardian, Rodney B. Luwor, et al. *Isolation and Characterization of Tumor Cells from the Ascites of Ovarian Cancer Patients: Molecular Phenotype of Chemoresistant Ovarian Tumors.* PLoS ONE 2012;7(10):e46858.
38. Zhou, Sheng , John D. Schuetz, et al. *The ABC transporter Bcrp1/ABCG2 is expressed in a wide variety of stem cells and is a molecular determinant of the side-population phenotype.* Nature Medicine 2001;7(9):1028-1034.
39. Scharenberg, Christian W., Michael A. Harkey, and Beverly Torok-Storb. *The ABCG2 transporter is an efficient Hoechst 33342 efflux pump and is preferentially expressed by immature human hematopoietic progenitors.* Blood 2002;99(2):507-512.
40. Dou, Jun, Cuilian Jiang, et al. *Using ABCG2-molecule-expressing side population cells to identify cancer stem-like cells in a human ovarian cell line.* Cell Biology International 2011;35(3):227-234.
41. Rizzo, Siân, Jenny M. Hersey, et al. *Ovarian Cancer Stem Cell-Like Side Populations Are Enriched Following Chemotherapy and Overexpress EZH2.* Molecular Cancer Therapeutics 2011;10(2):325-335.

42. Gao, Quanli, Li Geng, et al. *Identification of Cancer Stem-like Side Population Cells in Ovarian Cancer Cell Line OVCAR-3.* Ultrastructural Pathology 2009;33(4):175 - 181.
43. Yo, Yi-Te, Ya-Wen Lin, et al. *Growth Inhibition of Ovarian Tumor-Initiating Cells by Niclosamide.* Molecular Cancer Therapeutics 2012;11(8):1703-1712.
44. Liu, Te, Weiwei Cheng, et al. *Characterization of primary ovarian cancer cells in different culture systems.* Oncology Reports 2010;23(5):1277-1284.
45. Moserle, Lidia, Stefano Indraccolo, et al. *The Side Population of Ovarian Cancer Cells Is a Primary Target of IFN-{alpha} Antitumor Effects.* Cancer Research 2008;68(14):5658-5668.
46. Shi, M., J. Jiao, et al. *Identification of cancer stem cell-like cells from human epithelial ovarian carcinoma cell line.* Cellular and Molecular Life Sciences 2010;67(22):3915-3925.
47. Durand, Ralph E. and Peggy L. Olive. *Cytotoxicity, Mutagenicity and DNA damage by Hoechst 33342.* Journal of Histochemistry and Cytochemistry 1982;30(2):111-116.
48. Ferrandina, G., G Bonanno, et al. *Expression of CD133-1 and CD133-2 in ovarian cancer.* International Journal of Gynecological Cancer 2008;18(3):506-514.
49. Baba, T., P. A. Convery, et al. *Epigenetic regulation of CD133 and tumorigenicity of CD133+ ovarian cancer cells.* Oncogene 2009;209-218.
50. Curley, Michael D., Vanessa A. Therrien, et al. *CD133 Expression Defines a Tumor Initiating Cell Population in Primary Human Ovarian Cancer.* Stem Cells 2009;27(12):2875-2883.
51. Kryczek, Ilona, Suling Liu, et al. *Expression of aldehyde dehydrogenase and CD133 defines ovarian cancer stem cells.* International Journal of Cancer 2012;130(1):29-39.
52. Ma, Li, Dongmei Lai, et al. *Cancer stem-like cells can be isolated with drug selection in human ovarian cancer cell line SKOV3.* Acta Biochimica et Biophysica Sinica 2010;42(9):593-602.
53. Guo, Rongjiao, Qiuhua Wu, et al. *Description of the CD133+ subpopulation of the human ovarian cancer cell line OVCAR3.* Oncology Reports 2011;25(1):141-146.
54. Steg, Adam D., Kerri S. Bevis, et al. *Stem Cell Pathways Contribute to Clinical Chemoresistance in Ovarian Cancer.* Clinical Cancer Research 2012;18(3):869-881.
55. Zhang, Jing, Xiaoqing Guo, et al. *CD133 expression associated with poor prognosis in ovarian cancer.* Modern Pathology 2012;25(3):456-464.
56. Silva, Ines A., Shoumei Bai, et al. *Aldehyde Dehydrogenase in Combination with CD133 Defines Angiogenic Ovarian Cancer Stem Cells That Portend Poor Patient Survival.* Cancer Research 2011;71(11):3991-4001.

57. Ferrandina, Gabriella, Enrica Martinelli, et al. *CD133 antigen expression in ovarian cancer.* BMC Cancer 2009;9(1):221-229.
58. Qin, Q., Y. Sun, et al. *Expression of putative stem marker nestin and CD133 in advanced serous ovarian cancer.* Neoplasma 2012;59(3):310-316.
59. Gao, M. Q., Y. P. Choi, et al. *CD24+ cells from hierarchically organized ovarian cancer are enriched in cancer stem cells.* Oncogene 2010;292672-2680.
60. Koh, Jiae, Saet-byul Lee, et al. *Susceptibility of CD24+ ovarian cancer cells to anti-cancer drugs and natural killer cells.* Biochemical and Biophysical Research Communications 2012;427(2):373-378.
61. Luo, Lijing, Jianfang Zeng, et al. *Ovarian cancer cells with the CD117 phenotype are highly tumorigenic and are related to chemotherapy outcome.* Experimental and Molecular Pathology 2011;91(2):596-602.
62. Hess, David A., Todd E. Meyerrose, et al. *Functional characterization of highly purified human hematopoietic repopulating cells isolated according to aldehyde dehydrogenase activity.* Blood 2004;104(6):1648-1655.
63. Ginestier, Christophe, Min Hee Hur, et al. *ALDH1 Is a Marker of Normal and Malignant Human Mammary Stem Cells and a Predictor of Poor Clinical Outcome.* Cell Stem Cell 2007;1555-567.
64. Huang, Emina H., Mark J. Hynes, et al. *Aldehyde Dehydrogenase 1 Is a Marker for Normal and Malignant Human Colonic Stem Cells (SC) and Tracks SC Overpopulation during Colon Tumorigenesis.* Cancer Research 2009;69(8):3382-3389.
65. Jiang, Feng, Qi Qiu, et al. *Aldehyde Dehydrogenase 1 Is a Tumor Stem Cell-Associated Marker in Lung Cancer.* Molecular Cancer Research 2009;7(3):330-338.
66. Rasheed, Zeshaan A., Jie Yang, et al. *Prognostic Significance of Tumorigenic Cells With Mesenchymal Features in Pancreatic Adenocarcinoma.* Journal of the National Cancer Institute 2010;102(5):340-351.
67. Rasper, Michael, Andrea Schäfer, et al. *Aldehyde dehydrogenase 1 positive glioblastoma cells show brain tumor stem cell capacity.* Neuro-oncology 2010;12(10):1024-1033.
68. Zhi, Qiao Ming, Xue Hua Chen, et al. *Salinomycin can effectively kill ALDHhigh stem-like cells on gastric cancer.* Biomedicine & Pharmacotherapy 2011;65(7):509-515.
69. Deng, Shan, Xiaojun Yang, et al. *Distinct Expression Levels and Patterns of Stem Cell Marker, Aldehyde Dehydrogenase Isoform 1 (ALDH1), in Human Epithelial Cancers.* PLoS ONE 2010;5(4):e10277.
70. Landen, Charles N., Blake Goodman, et al. *Targeting Aldehyde Dehydrogenase Cancer Stem Cells in Ovarian Cancer.* Molecular Cancer Therapeutics 2010;9(12):3186-3199.

71. Wang, Yu-Chi, Yi-Te Yo, et al. *ALDH1-Bright Epithelial Ovarian Cancer Cells Are Associated with CD44 Expression, Drug Resistance, and Poor Clinical Outcome.* The American Journal of Pathology 2012;180(3):1159-1169.
72. Shank, Jessica J., Kun Yang, et al. *Metformin targets ovarian cancer stem cells in vitro and in vivo.* Gynecologic Oncology 2012;127(2):390-397.
73. Whitworth, Jenny M., Angelina I. Londo√±o-Joshi, et al. *The impact of novel retinoids in combination with platinum chemotherapy on ovarian cancer stem cells.* Gynecologic Oncology 2012;125(1):226-230.
74. Chang, Bin, Guangzhi Liu, et al. *ALDH1 expression correlates with favorable prognosis in ovarian cancers.* Modern Pathology 2009.
75. Kusumbe, Anjali P., Avinash M. Mali, and Sharmila A. Bapat. *CD133-Expressing Stem Cells Associated with Ovarian Metastases Establish an Endothelial Hierarchy and Contribute to Tumor Vasculature.* Stem Cells 2009;27(3):498-508.
76. Novetsky, Akiva P., Dominic M. Thompson, et al. *Lithium chloride and inhibition of glycogen synthase kinase 3β as a potential therapy for serous ovarian cancer.* International Journal of Gynecological Cancer 2013;23(2):361-366.
77. Shaw, Tanya J., Mary K. Senterman, et al. *Characterization of Intraperitoneal, Orthotopic, and Metastatic Xenograft Models of Human Ovarian Cancer.* Molecular Therapy 2004;10(6):1032-1042.
78. Jones, Richard J., James P. Barber, et al. *Assessment of aldehyde dehydrogenase in viable cells.* Blood 1995;85(10):2742-2746.
79. Jemal, Ahmedin, Ram C. Tiwari, et al. *Cancer Statistics, 2004.* CA: A Cancer Journal for Clinicians 2004;54(1):8-29.
80. Cannistra, S. A. *Cancer of the ovary.* The New England Journal of Medicine 1993;3291550-1559.
81. Armstrong, Deborah K., Brian Bundy, et al. *Intraperitoneal Cisplatin and Paclitaxel in Ovarian Cancer.* New England Journal of Medicine 2006;354(1):34-43.
82. Garson, Kenneth, Tanya J. Shaw, et al. *Models of ovarian cancer--Are we there yet?* Molecular and Cellular Endocrinology 2005;239(1-2):15-26.
83. Vanderhyden, Barbara, Tanya Shaw, and Jean-Francois Ethier. *Animal models of ovarian cancer.* Reproductive Biology and Endocrinology 2003;1(1):67.
84. Beamer, Wesley G., Peter C. Hoppe, and Wesley K. Whitten. *Spontaneous Malignant Granulosa Cell Tumors in Ovaries of Young SWR Mice.* Cancer Research 1985;45(11 Part 2):5575-5581.
85. Walsh, Kathleen M. and James Poteracki. *Spontaneous Neoplasms in Control Wistar Rats.* Fundamental and Applied Toxicology 1994;22(1):65-72.
86. Fredrickson, T. N. *Ovarian Tumors of the Hen.* Environmental Health Perspectives 1987;7335-51.

87. Godwin, Andrew K., Joseph R. Testa, et al. *Spontaneous Transformation of Rat Ovarian Surface Epithelial Cells: Association With Cytogenetic Changes and Implications of Repeated Ovulation in the Etiology of Ovarian Cancer.* Journal of the National Cancer Institute 1992;84(8):592-601.
88. Connolly, Denise C., Rudi Bao, et al. *Female Mice Chimeric for Expression of the Simian Virus 40 TAg under Control of the MISIIR Promoter Develop Epithelial Ovarian Cancer.* Cancer Research 2003;63(6):1389-1397.
89. Flesken-Nikitin, Andrea, Kyung-Chul Choi, et al. *Induction of Carcinogenesis by Concurrent Inactivation of p53 and Rb1 in the Mouse Ovarian Surface Epithelium.* Cancer Research 2003;63(13):3459-3463.
90. Orsulic, Sandra, Yi Li, et al. *Induction of ovarian cancer by defined multiple genetic changes in a mouse model system.* Cancer Cell 2002;1(1):53-62.
91. Keri, Ruth A., Kristen L. Lozada, et al. *Luteinizing hormone induction of ovarian tumors: Oligogenic differences between mouse strains dictates tumor disposition.* Proceedings of the National Academy of Sciences 2000;97(1):383-387.
92. Bai, Wenlong, Beatriz Oliveros-Saunders, et al. *Estrogen stimulation of ovarian surface epithelial cell proliferation.* In Vitro Cellular& Developmental Biology - Animal 2000;36(10):657-666.
93. Silva, E. G., C. Tornos, et al. *Induction of Epithelial Neoplasms in the Ovaries of Guinea Pigs by Estrogenic Stimulation.* Gynecologic Oncology 1998;71(2):240-246.
94. Hamilton, Thomas C., Robert C. Young, et al. *Characterization of a Xenograft Model of Human Ovarian Carcinoma Which Produces Ascites and Intraabdominal Carcinomatosis in Mice.* Cancer Research 1984;44(11):5286-5290.
95. Molpus, Kelly L. , Daniel Koelliker, et al. *Characterization of a xenograft model of human ovarian carcinoma which produces intraperitoneal carcinomatosis and metastases in mice.* International Journal of Cancer 1996;68(5):588-595.
96. Rose, G. S., L. M. Tocco, et al. *Development and characterization of a clinically useful animal model of epithelial ovarian cancer in the Fischer 344 rat.* American Journal of Obstetrics and Gynecology 1996;175(3):593-599.
97. Sallinen, Hanna, Maarit Anttila, et al. *A highly reproducible xenograft model for human ovarian carcinoma and application of MRI and ultrasound in longitudinal follow-up.* Gynecologic Oncology 2006;103(1):315-320.
98. Chen, Weiran, Christopher Thoburn, and Allan D. Hess. *Characterization of the Pathogenic Autoreactive T Cells in Cyclosporine-Induced Syngeneic Graft-Versus-Host Disease.* Journal of Immunology 1998;161(12):7040-7046.
99. Lee, P., D. G. Rosen, et al. *Expression of progesterone receptor is a favorable prognostic marker in ovarian cancer.* Gynecol.Oncol. 2005;96(3):671-677.

100. Cunat, Séverine, Pascale Hoffmann, and Pascal Pujol. *Estrogens and epithelial ovarian cancer.* Gynecologic Oncology 2004;94(1):25-32.
101. Ho, Shuk-Mei. *Estrogen, Progesterone and Epithelial Ovarian Cancer.* Reproductive Biology and Endocrinology 2003;1(73).
102. van Doorn, Helena C., Curt W. Burger, et al. *Oestrogen, progesterone, and androgen receptors in ovarian neoplasia: correlation between immunohistochemical and biochemical receptor analyses.* Journal of Clinical Pathology 2000;53(3):201-205.
103. Lee, Benjamin H., Jonathan Hecht, L., , et al. *WT1, Estrogen Receptor, and Progesterone Receptor as Markers for Breast or Ovarian Primary Sites in Metastatic Adenocarcinoma to Body Fluids.* American Journal of Clinical Pathology 2002;117(5):745-750.
104. Chadha, S., B. R. Rao, et al. *An immunohistochemical evaluation of androgen and progesterone receptors in ovarian tumors.* Human Pathology 1993;24(1):90-95.
105. Ordóñez, Nelson G. *Value of estrogen and progesterone receptor immunostaining in distinguishing between peritoneal mesotheliomas and serous carcinomas.* Human Pathology 2005;36(11):1163-1167.
106. Verri, Elena, Pamela Guglielmini, et al. *HER2/neu Oncoprotein Overexpression in Epithelial Ovarian Cancer: Evaluation of its Prevalence and Prognostic Significance.* Oncology 2005;68(2-3):154-161.
107. Nielsen, J. S., E. Jakobsen, et al. *Prognostic significance of p53, Her-2, and EGFR overexpression in borderline and epithelial ovarian cancer.* International Journal of Gynecological Cancer 2004;14(6):1086-1096.
108. Chauhan, Subhash C., Ajay P. Singh, et al. *Aberrant expression of MUC4 in ovarian carcinoma: diagnostic significance alone and in combination with MUC1 and MUC16 (CA125).* Modern Pathology 2006;19(10):1386-1394.
109. Kildal, Wanja, Björn Risberg, et al. *[beta]-catenin expression, DNA ploidy and clinicopathological features in ovarian cancer: A study in 253 patients.* European Journal of Cancer 2005;41(8):1127-1134.
110. McCluggage, W. G., K. Strand, and A. Abdulkadir. *Immunohistochemical localization of metallothionein in benign and malignant epithelial ovarian tumors.* International Journal of Gynecological Cancer 2002;12(1):62-65.
111. Bayani, Jane, James D. Brenton, et al. *Parallel Analysis of Sporadic Primary Ovarian Carcinomas by Spectral Karyotyping, Comparative Genomic Hybridization, and Expression Microarrays.* Cancer Research 2002;62(12):3466-3476.
112. Surowiak, Paweł, Verena Materna, et al. *Augmented expression of metallothionein and glutathione S-transferase pi as unfavourable prognostic factors in cisplatin-treated ovarian cancer patients.* Virchows Archiv 2005;447(3):626-633.

113. Yamada, l\lanabu, Akihiro Tomida, et al. *Increased expression of thioredoxin/adult T-cell leukemia-derived factor in cisplatin-resistant human cancer cell lines.* Clinical Cancer Research 1996;2(2):427-432.
114. Wei, San-Hua, Fang Lin, et al. *Prognostic significance of stathmin expression in correlation with metastasis and clinicopathological characteristics in human ovarian carcinoma.* Acta Histochemica 2008;110(1):59-65.
115. Balachandran, Raghavan, Manda J. Welsh, and Billy W. Day. *Altered levels and regulation of stathmin in paclitaxel-resistant ovarian cancer cells.* Oncogene 2003;22(55):8924-8930.
116. Alaiya, Ayodele A., Bo FranzÈn, et al. *Phenotypic analysis of ovarian carcinoma: Polypeptide expression in benign, borderline and malignant tumors.* International Journal of Cancer 1997;73(5):678-682.
117. Martoglio, Ann-Marie, Brian D. M. Tom, et al. *Changes in tumorigenesis- and angiogenesis-related gene transcript abundance profiles in ovarian cancer detected by tailored high density cDNA arrays.* Molecular Medicine 2000;6(9):750-765.
118. Ziltener, Herman J., Sarah Maines-Bandiera, et al. *Secretion of bioactive interleukin-1, interleukin-6, and colony- stimulating factors by human ovarian surface epithelium.* Biology of Reproduction 1993;49(3):635-641.
119. Johanna G.W. Asschert, Edo Vellenga, Marcel H. J. Ruiters, Elisabeth G. E. de Vries. *Regulation of spontaneous and TNF/IFN-induced IL-6 expression in two human ovarian-carcinoma cell lines.* International Journal of Cancer 1999;82(2):244-249.
120. Wang, Zhao Yuan, Alessia Gaggero, et al. *Expression of interleukin-18 in human ovarian carcinoma and normal ovarian epithelium: Evidence for defective processing in tumor cells.* International Journal of Cancer 2002;98(6):873-878.
121. Bozkurt, N., K. Yuce, et al. *Correlation of serum and ascitic IL-12 levels with second-look laparotomy results and disease progression in advanced epithelial ovarian cancer patients.* International Journal of Gynecological Cancer 2006;16(1):83-86.
122. Sharrow, Allison C, Brigitte M Ronnett, et al. *Identification and characterization of a spontaneous ovarian carcinoma in Lewis rats.* Journal of Ovarian Research 2010;3(9):9.
123. Spooncer, Elaine, Clare M. Heyworth, et al. *Self-renewal and differentiation of interleukin-3-dependent multipotent stem cells are modulated by stromal cells and serum factors.* Differentiation 1986;31(2):111-118.
124. Reynolds, Brent A., Wolfram Tetzlaff, and Samuel Weiss. *A multipotent EGF-responsive striatal embryonic progenitor cell produces neurons and astrocytes.* Journal of Neuroscience 1992;12(11):4565-4574.

125. Toma, Jean G., Mahnaz Akhavan, et al. *Isolation of multipotent adult stem cells from the dermis of mammalian skin.* Nature Cell Biology 2001;3(9):778-784.
126. Lee, Jeongwu, Svetlana Kotliarova, et al. *Tumor stem cells derived from glioblastomas cultured in bFGF and EGF more closely mirror the phenotype and genotype of primary tumors than do serum-cultured cell lines.* Cancer Cell 2006;9(5):391-403.
127. Colter, David C., Ichiro Sekiya, and Darwin J. Prockop. *Identification of a subpopulation of rapidly self-renewing and multipotential adult stem cells in colonies of human marrow stromal cells.* Proceedings of the National Academy of Sciences 2001;98(14):7841-7845.
128. Burdon, Tom, Austin Smith, and Pierre Savatier. *Signalling, cell cycle and pluripotency in embryonic stem cells.* Trends in Cell Biology 2002;12(9):432-438.
129. Kucia, M., R. Reca, et al. *A population of very small embryonic-like (VSEL) CXCR4+SSEA-1+Oct-4+ stem cells identified in adult bone marrow.* Leukemia 2006;20(5):857-869.
130. Lobo, Neethan A., Yohei Shimono, et al. *The Biology of Cancer Stem Cells.* Annual Review of Cell and Developmental Biology 2007;23(1):675-699.
131. Gil, Justyna, Agnieszka Stembalska, et al. *Cancer stem cells: the theory and perspectives in cancer therapy.* J Appl Genet 2008;49(2):193-199.
132. Tilly, Jonathan L. and Bo R. Rueda. *Stem Cell Contribution to Ovarian Development, Function and Disease.* Endocrinology 2008;149(9):4307-4311.
133. Jones, Richard J. *Cancer stem cells-clinical relevance.* J Mol Med (Berl) 2009;87(11):1105-1110.
134. Obaya, A. J., M. K. Mateyak, and J. M. Sedivy. *Mysterious liaisons: the relationship between c-Myc and the cell cycle.* Oncogene 1999;18(19):2934-2941.
135. Wadugu, Brian and Bernhard K√ºhn. *The role of neuregulin/ErbB2/ErbB4 signaling in the heart with special focus on effects on cardiomyocyte proliferation.* American Journal of Physiology - Heart and Circulatory Physiology 2012;302(11):H2139-H2147.
136. Tam, S. W., A. M. Theodoras, et al. *Differential expression and regulation of Cyclin D1 protein in normal and tumor human cells: association with Cdk4 is required for Cyclin D1 function in G1 progression.* Oncogene 1994;9(9):2663-2674.
137. Resnitzky, Dalia, Manfred Gossen, et al. *Acceleration of the G1/S phase transition by expression of cyclins D1 and E with an inducible system.* Molecular and Cellular Biology 1994;14(3):1669-1679.
138. Meyerson, M. and E. Harlow. *Identification of G1 kinase activity for cdk6, a novel cyclin D partner.* Molecular and Cellular Biology 1994;14(3):2077-2086.

139. Girling, R., J. F. Partridge, et al. *A new component of the transcription factor DRTF1/E2F.* Nature 1993;362(6415):83-87.
140. Wu, C. L., M. Classon, et al. *Expression of dominant-negative mutant DP-1 blocks cell cycle progression in G1.* Molecular and Cellular Biology 1996;16(7):3698-3706.
141. Welch, Peter J. and Jean Y. J. Wang. *A C-terminal protein-binding domain in the retinoblastoma protein regulates nuclear c-Abl tyrosine kinase in the cell cycle.* Cell 1993;75(4):779-790.
142. Whitaker, Laura L., Heyun Su, et al. *Growth Suppression by an E2F-Binding-Defective Retinoblastoma Protein (RB): Contribution from the RB C Pocket.* Molecular and Cellular Biology 1998;18(7):4032-4042.
143. Wade Harper, J., Guy R. Adami, et al. *The p21 Cdk-interacting protein Cip1 is a potent inhibitor of G1 cyclin-dependent kinases.* Cell 1993;75(4):805-816.
144. Casazza, A. M. and C. R. Fairchild. *Paclitaxel (Taxol): Mechanisms of Resistance.* Cancer Treatment and Research 1996;87149-171.
145. Anton, Roman, Hans A. Kestler, and Michael K√ºhl. *β-Catenin signaling contributes to stemness and regulates early differentiation in murine embryonic stem cells.* FEBS Letters 2007;581(27):5247-5254.
146. Okoye, Ujunwa C, Craig C Malbon, and Hsien-yu Wang. *Wnt and Frizzled RNA expression in human mesenchymal and embryonic (H7) stem cells.* Journal of Molecular Signaling 2008;3(16):16.
147. Wang H Fau - Fan, Liangsheng, Xi Fan L Fau - Xia, et al. *Silencing Wnt2B by siRNA interference inhibits metastasis and enhances chemotherapy sensitivity in ovarian cancer.* (1525-1438 (Electronic)).
148. Heinonen Km Fau - Vanegas, Juan Ruiz, Deborah Vanegas Jr Fau - Lew, et al. *Wnt4 enhances murine hematopoietic progenitor cell expansion through a planar cell polarity-like pathway.* (1932-6203 (Electronic)).
149. Louis, Isabelle, Krista M. Heinonen, et al. *The Signaling Protein Wnt4 Enhances Thymopoiesis and Expands Multipotent Hematopoietic Progenitors through β-Catenin-Independent Signaling.* Immunity 2008;29(1):57-67.
150. Elizalde, Carina, Victor M. Campa, et al. *Distinct Roles for Wnt-4 and Wnt-11 During Retinoic Acid-Induced Neuronal Differentiation.* Stem Cells 2011;29(1):141-153.
151. Huang, Chen and Dajiang Qin. *Role of Lef1 in sustaining self-renewal in mouse embryonic stem cells.* Journal of Genetics and Genomics 2010;37(7):441-449.
152. Kanwar, Shailender S., Yingjie Yu, et al. *The Wnt/β-catenin pathway regulates growth and maintenance of colonospheres.* Molecular Cancer 2010;9(212):212.
153. Chhabra, Akanksha, Andrew J. Lechner, et al. *Trophoblasts Regulate the Placental Hematopoietic Niche through PDGF-B Signaling.* Developmental Cell 2012;22(3):651-659.

154. Jiang, Yiwen, Maria Boije, et al. *PDGF-B Can sustain self-renewal and tumorigenicity of experimental glioma-derived cancer-initiating cells by preventing oligodendrocyte differentiation.* Neoplasia 2011;13(6):492-503.
155. Xu, G., J. Shen, et al. *Functional analysis of platelet-derived growth factor receptor-β in neural stem/progenitor cells.* Neuroscience 2013;238(0):195-208.
156. Jansen, Bastiaan J.H., Christian Gilissen, et al. *Functional differences between mesenchymal stem cell populations are reflected by their transcriptome.* Stem Cells and Development 2010;19(4):481-490.
157. Pond, Adam C., Xue Bin, et al. *Fibroblast Growth Factor Receptor Signaling Is Essential for Normal Mammary Gland Development and Stem Cell Function.* Stem Cells 2013;31(1):178-189.
158. Zhang, Jue, Junchen Liu, et al. *FRS2α-Mediated FGF Signals Suppress Premature Differentiation of Cardiac Stem Cells Through Regulating Autophagy Activity.* Circulation Research 2012;110(4):e29-e39.
159. Segklia, Aikaterini, Eve Seuntjens, et al. *Bmp7 regulates the survival, proliferation, and neurogenic properties of neural progenitor cells during corticogenesis in the mouse.* PLoS ONE 2012;7(3):e34088.
160. Zhou, Jiangbing, Julia Wulfkuhle, et al. *Activation of the PTEN/mTOR/STAT3 pathway in breast cancer stem-like cells is required for viability and maintenance.* Proceedings of the National Academy of Sciences 2007;104(41):16158-16163.
161. Vallier, Ludovic, Morgan Alexander, and Roger A. Pedersen. *Activin/Nodal and FGF pathways cooperate to maintain pluripotency of human embryonic stem cells.* Journal of Cell Science 2005;118(19):4495-4509.
162. Qi, Xiaoxia, Teng-Guo Li, et al. *BMP4 supports self-renewal of embryonic stem cells by inhibiting mitogen-activated protein kinase pathways.* Proceedings of the National Academy of Sciences of the United States of America 2004;101(16):6027-6032.
163. Kangsamaksin, Thaned and Rebecca J. Morris. *Bone Morphogenetic Protein 5 Regulates the Number of Keratinocyte Stem Cells from the Skin of Mice.* Journal of Investigative Dermatology 2011;131(3):580-585.
164. Li, Mingming, Xiaobing Li, et al. *Short periods of cyclic mechanical strain enhance triple-supplement directed osteogenesis and bone nodule formation by human embryonic stem cells in vitro.* Tissue Engineering. Part A 2013;2424.
165. Sosa, Maria S., Yeriel Estrada, et al. *Abstract 4262: NR2F1 and SOX9 mediate reprogramming of tumor cells into dormancy: Potential role in dormant bone marrow DTCs*. In: *Proceedings of the 103rd Annual Meeting of the American Association for Cancer Research*. 2012 Mar 31-Apr 4. Chicago, IL: Philadelphia (PA): AACR; Cancer Res 2012;72(8 Suppl): Abstract nr 4262
166. Niwa, Hitoshi, Yayoi Toyooka, et al. *Interaction between Oct3/4 and Cdx2 Determines Trophectoderm Differentiation.* Cell 2005;123(5):917-929.

167. Pacini, Simone, Vittoria Carnicelli, et al. *Constitutive expression of pluripotency-associated genes in mesodermal progenitor cells (MPCs).* PLoS ONE 2010;5(3):e9861.
168. Duester, Gregg. *Families of retinoid dehydrogenases regulating vitamin A function.* European Journal of Biochemistry 2000;267(14):4315-4324.
169. van Raaij, Mark J., Estelle Chouin, et al. *Dimeric Structure of the Coxsackievirus and Adenovirus Receptor D1 Domain at 1.7 √Ö Resolution.* Structure 2000;8(11):1147-1155.
170. Honda, Takao, Hiroshi Saitoh, et al. *The coxsackievirus-adenovirus receptor protein as a cell adhesion molecule in the developing mouse brain.* Molecular Brain Research 2000;77(1):19-28.
171. Seth, Ankur, Parimal Sheth, et al. *Protein Phosphatases 2A and 1 Interact with Occludin and Negatively Regulate the Assembly of Tight Junctions in the CACO-2 Cell Monolayer.* Journal of Biological Chemistry 2007;282(15):11487-11498.
172. Ma, Thomas Y., Michel A. Boivin, et al. *Mechanism of TNF-α modulation of Caco-2 intestinal epithelial tight junction barrier: role of myosin light-chain kinase protein expression.* American Journal of Physiology - Gastrointestinal and Liver Physiology 2005;288(3):G422-G430.
173. Zhao, Weidong, Irfan M Hisamuddin, et al. *Identification of Kruppel-like factor 4 as a potential tumor suppressor gene in colorectal cancer.* Oncogene 2004;23(2):395-402.
174. Wicki, Roland, Cornelia Franz, et al. *Repression of the candidate tumor suppressor gene S100A2 in breast cancer is mediated by site-specific hypermethylation.* Cell Calcium 1997;22(4):243-254.
175. Wang, Chun-Xiang, Madhuri Wadehra, et al. *Epithelial membrane protein 2, a 4-transmembrane protein that suppresses B-cell lymphoma tumorigenicity.* Blood 2001;97(12):3890-3895.
176. Narla, Goutham, Karen E. Heath, et al. *KLF6, a Candidate Tumor Suppressor Gene Mutated in Prostate Cancer.* Science 2001;294(5551):2563-2566.
177. Memon, Ashfaque Ahmed, Boe Sandahl Sorensen, et al. *Down-Regulation of S100C Is Associated with Bladder Cancer Progression and Poor Survival.* Clinical Cancer Research 2005;11(2):606-611.
178. Alaminos, Miguel, Ver√≥nica D√°valos, et al. *EMP3, a Myelin-Related Gene Located in the Critical 19q13.3 Region, Is Epigenetically Silenced and Exhibits Features of a Candidate Tumor Suppressor in Glioma and Neuroblastoma.* Cancer Research 2005;65(7):2565-2571.
179. Alarmo, Emma-Leena, Jenita Pärssinen, et al. *BMP7 influences proliferation, migration, and invasion of breast cancer cells.* Cancer Letters 2009;275(1):35-43.

180. Delic, S., N. Lottmann, et al. *Identification and functional validation of CDH11, PCSK6 and SH3GL3 as novel glioma invasion-associated candidate genes.* Neuropathology and Applied Neurobiology 2012;38(2):201-212.
181. Golubkov, Vladislav S. and Alex Y. Strongin. *Insights into Ectodomain Shedding and Processing of Protein-tyrosine Pseudokinase 7 (PTK7).* Journal of Biological Chemistry 2012;287(50):42009-42018.
182. Giannelli, Gianluigi, Jutta Falk-Marzillier, et al. *Induction of Cell Migration by Matrix Metalloprotease-2 Cleavage of Laminin-5.* Science 1997;277(5323):225-228.
183. Rothhammer, Tanja, Ina Poser, et al. *Bone Morphogenic Proteins Are Overexpressed in Malignant Melanoma and Promote Cell Invasion and Migration.* Cancer Research 2005;65(2):448-456.
184. Weiner, Timothy M, Edison T Liu, et al. *Expression of focal adhesion kinase gene and invasive cancer.* The Lancet 1993;342(8878):1024-1025.
185. Wang, Fengqiang, Scott Reierstad, and David A. Fishman. *Matrilysin over-expression in MCF-7 cells enhances cellular invasiveness and pro-gelatinase activation.* Cancer Letters 2006;236(2):292-301.
186. Baker, Mark S., Pamela Bleakley, et al. *Inhibition of Cancer Cell Urokinase Plasminogen Activator by Its Specific Inhibitor PAI-2 and Subsequent Effects on Extracellular Matrix Degradation.* Cancer Research 1990;50(15):4676-4684.
187. Kruithof, Egbert K.O., ChiênTran-Thang, et al. *Demonstration of a fast-acting inhibitor of plasminogen activators in human plasma.* Blood 1984;64(4):907-913.
188. Sugimoto, Manabu, Toshitaka Oohashi, et al. *cDNA isolation and partial gene structure of the human α4(IV) collagen chain.* FEBS Letters 1993;330(2):122-128.
189. Schuppan, Detlef, Maria C. Cantaluppi, et al. *Undulin, an extracellular matrix glycoprotein associated with collagen fibrils.* Journal of Biological Chemistry 1990;265(15):8823-8832.
190. Yaoita, Hideo, Jean-Michael Foidart, and Stephen I. Katz. *Localization of the collagenous component in skin basement membrane.* Journal of Investigative Dermatology 1978;70(4):191-193.
191. Sakai, Lynn Y., Douglas R. Keene, et al. *Type VII collagen is a major structural component of anchoring fibrils.* The Journal of Cell Biology 1986;103(4):1577-1586.
192. Marinkovich, M. Peter, Ted B. Taylor, et al. *LAD-1, the linear IgA bullous dermatosis autoantigen, is a novel 120-kDa anchoring filament protein synthesized by epidermal cells.* Journal of Investigative Dermatology 1996;106(4):734-738.
193. Steiglitz, Barry M., Douglas R. Keene, and Daniel S. Greenspan. *PCOLCE2 Encodes a Functional Procollagen C-Proteinase Enhancer (PCPE2) That Is a*

Collagen-binding Protein Differing in Distribution of Expression and Post-translational Modification from the Previously Described PCPE1. Journal of Biological Chemistry 2002;277(51):49820-49830.
194. Hieta, Reija, Liisa Kukkola, et al. *The Peptide-Substrate-binding Domain of Human Collagen Prolyl 4-Hydroxylases: Backbone Assignments, Secondary Structure, and Binding of Proline-Rich Peptides.* Journal of Biological Chemistry 2003;278(37):34966-34974.
195. Rousselle, Patricia, Gregory P. Lunstrum, et al. *Kalinin: An Epithelium-Specific Basement Membrane Adhesion Molecule That Is a Component of Anchoring Filaments.* The Journal of Cell Biology 1991;114(3):567-576.
196. George J. Broze, Jr. , Louise A. Warren, et al. *The lipoprotein-associated coagulation inhibitor that inhibits the factor VII-tissue factor complex also inhibits factor Xa: insight into its possible mechanism of action.* Blood 1988;71(2):335-343.
197. Furie, Bruce and Barbara C. Furie. *Thrombus formation in vivo.* The Journal of Clinical Investigation 2005;115(12):3355-3362.
198. Davie, Earl W., Kazuo Fujikawa, and Walter Kisiel. *The coagulation cascade: initiation, maintenance, and regulation.* Biochemistry 1991;30(43):10363-10370.
199. Dean, Michael. *ABC Transporters, Drug Resistance, and Cancer Stem Cells.* Journal of Mammary Gland Biology and Neoplasia 2009;14(1):3-9.
200. Joseph, Immanual, Robert Tressler, et al. *The Telomerase Inhibitor Imetelstat Depletes Cancer Stem Cells in Breast and Pancreatic Cancer Cell Lines.* Cancer Research 2010;70(22):9494-9504.
201. Brennan, Sarah K., Qiuju Wang, et al. *Telomerase Inhibition Targets Clonogenic Multiple Myeloma Cells through Telomere Length-Dependent and Independent Mechanisms.* PLoS ONE 2010;5(9):e12487.
202. Serrano, Diego, Anne-Marie Bleau, et al. *Inhibition of telomerase activity preferentially targets aldehyde dehydrogenase-positive cancer stem-like cells in lung cancer.* Molecular Cancer 2011;10(96):96.
203. Chefetz, Ilana, Jennie C. Holmberg, et al. *Inhibition of Aurora-A kinase induces cell cycle arrest in epithelial ovarian cancer stem cells by affecting NFκB pathway.* Cell Cycle 2011;10(13):2206-2214.
204. Choi, Yoon Pyo, Hyo Sup Shim, et al. *Molecular portraits of intratumoral heterogeneity in human ovarian cancer.* Cancer Letters 2011;307(1):62-71.
205. Chau, W. K., C. K. Ip, et al. *c-Kit mediates chemoresistance and tumor-initiating capacity of ovarian cancer cells through activation of Wnt/beta-catenin-ATP-binding cassette G2 signaling.* Oncogene 2013;32(22):2767-2781.
206. Merchant, Akil A. and William Matsui. *Targeting Hedgehog - a Cancer Stem Cell Pathway.* Clinical Cancer Research 2010;16(12):3130-3140.

207. Alexopoulou, Lena, Agnieszka Czopik Holt, et al. *Recognition of double-stranded RNA and activation of NF-kappaB by Toll-like receptor 3.* Nature 2001;413(6857):732-738.
208. Byrd, Victor M., Dean W. Ballard, et al. *Fibroblast Growth Factor-1 (FGF-1) Enhances IL-2 Production and Nuclear Translocation of NF-κB in FGF Receptor-Bearing Jurkat T Cells.* The Journal of Immunology 1999;162(10):5853-5859.
209. Orlandi, Augusto, Amedeo Ferlosio, et al. *Flt-1 expression influences apoptotic susceptibility of vascular smooth muscle cells through the NF-κB/IAP-1 pathway.* Cardiovascular Research 2010;85(1):214-223.
210. Jeay, Sébastien, Gail E. Sonenshein, et al. *Growth Hormone Prevents Apoptosis through Activation of Nuclear Factor-κB in Interleukin-3-Dependent Ba/F3 Cell Line.* Molecular Endocrinology 2000;14(5):650-661.
211. Spiegelman, Vladimir S., Pete Stavropoulos, et al. *Induction of β-Transducin Repeat-containing Protein by JNK Signaling and Its Role in the Activation of NF-κB.* Journal of Biological Chemistry 2001;276(29):27152-27158.
212. Saccani, Simona, Serafino Pantano, and Gioacchino Natoli. *Modulation of NF-κB Activity by Exchange of Dimers.* Molecular Cell 2003;11(6):1563-1574.
213. Flick, Lisa M., Jason M. Weaver, et al. *Effects of receptor activator of NFκB (RANK) signaling blockade on fracture healing.* Journal of Orthopaedic Research 2003;21(4):676-684.
214. Colotta, Francesco, Fabio Re, et al. *Interleukin-1 Type II Receptor: A Decoy Target for IL-1 That Is Regulated by IL-4.* Science 1993;261(5120):472-475.
215. Freudlsperger, C., Y. Bian, et al. *TGF-beta and NF-kappaB signal pathway cross-talk is mediated through TAK1 and SMAD7 in a subset of head and neck cancers.* Oncogene 2013;32(12):1549-1559.
216. Sun, Tian-Qiang, Bingwei Lu, et al. *PAR-1 is a Dishevelled-associated kinase and a positive regulator of Wnt signalling.* Nature Cell Biology 2001;3(7):628-636.
217. Novak, A. and S. Dedhar. *Signaling through β-catenin and Lef/Tcf.* Cellular and Molecular Life Sciences 1999;56(5-6):523-537.
218. Zorn, Aaron M., Grant D. Barish, et al. *Regulation of Wnt Signaling by Sox Proteins: XSox17α/β and XSox3 Physically Interact with β-catenin.* Molecular Cell 1999;4(4):487-498.
219. Rashid, Sajid, Iwona Pilecka, et al. *Endosomal Adaptor Proteins APPL1 and APPL2 Are Novel Activators of β-Catenin/TCF-mediated Transcription.* Journal of Biological Chemistry 2009;284(27):18115-18128.
220. Seto, Elaine S., Hugo J. Bellen, and Thomas E. Lloyd. *When cell biology meets development: endocytic regulation of signaling pathways.* Genes and Development 2002;16(11):1314-1336.
221. Moloney, Daniel J., Vladislav M. Panin, et al. *Fringe is a glycosyltransferase that modifies Notch.* Nature 2000;406(6794):369-375.

222. Chyung, Jay H., Daniel M. Raper, and Dennis J. Selkoe. *γ-Secretase Exists on the Plasma Membrane as an Intact Complex That Accepts Substrates and Effects Intramembrane Cleavage.* Journal of Biological Chemistry 2005;280(6):4383-4392.
223. Hicks, Carol, Stuart H. Johnston, et al. *Fringe differentially modulates Jagged1 and Delta1 signalling through Notch1 and Notch2.* Nature Cell Biology 2000;2(8):515-520.
224. Zhang, Yong, Xinsheng Gao, et al. *Rheb is a direct target of the tuberous sclerosis tumour suppressor proteins.* Nature Cell Biology 2003;5(6):578-581.
225. Machado-Neto, João Agostinho, Patricia Favaro, et al. *Knockdown of insulin receptor substrate 1 reduces proliferation and downregulates Akt/mTOR and MAPK pathways in K562 cells.* Biochimica et Biophysica Acta (BBA) - Molecular Cell Research 2011;1813(8):1404-1411.
226. Penuel, Elicia and G. Steven Martin. *Transformation by v-Src: Ras-MAPK and PI3K-mTOR Mediate Parallel Pathways.* Molecular Biology of the Cell 1999;10(6):1693-1703.
227. Roux, Philippe P., Bryan A. Ballif, et al. *Tumor-promoting phorbol esters and activated Ras inactivate the tuberous sclerosis tumor suppressor complex via p90 ribosomal S6 kinase.* Proceedings of the National Academy of Sciences of the United States of America 2004;101(37):13489-13494.
228. Sancak, Yasemin, Timothy R. Peterson, et al. *The Rag GTPases Bind Raptor and Mediate Amino Acid Signaling to mTORC1.* Science 2008;320(5882):1496-1501.
229. Lanitis, Evripidis, Denarda Dangaj, et al. *Primary Human Ovarian Epithelial Cancer Cells Broadly Express HER2 at Immunologically-Detectable Levels.* PLoS ONE 2012;7(11):e49829.
230. Jaiswal, Siddhartha, Catriona H. M. Jamieson, et al. *CD47 Is Upregulated on Circulating Hematopoietic Stem Cells and Leukemia Cells to Avoid Phagocytosis.* 2009;138(2):271-285.
231. Chan, Keith Syson, Inigo Espinosa, et al. *Identification, molecular characterization, clinical prognosis, and therapeutic targeting of human bladder tumor-initiating cells.* Proceedings of the National Academy of Sciences 2009;106(33):14016-14021.
232. Willingham, Stephen B., Jens-Peter Volkmer, et al. *The CD47-signal regulatory protein alpha (SIRPa) interaction is a therapeutic target for human solid tumors.* Proceedings of the National Academy of Sciences 2012;109(17):6662-6667.
233. Ohbayashi, Norihiko, Masaki Shibayama, et al. *FGF18 is required for normal cell proliferation and differentiation during osteogenesis and chondrogenesis.* Genes and Development 2002;16(7):870-879.
234. Storey, Dawn J., Robert Rush, et al. *Endometrioid epithelial ovarian cancer.* Cancer 2008;112(10):2211-2220.

235. Fogh, Jørgen and Germain Trempe, *New Human Tumor Cell Lines*, in *Human Tumor Cells In Vitro*, J. Fogh, Editor. 1975, Plenum Press: New York. p. 115-159.
236. Seidman, Jeffrey D., Iren Horkayne-Szakaly, et al. *The histologic type and stage distribution of ovarian carcinomas of surface epithelial origin.* International Journal of Gynecological Pathology 2004;23(1):41-44.
237. Kennedy, Alexander W., Maurie Markman, et al. *Survival Probability in Ovarian Clear Cell Adenocarcinoma.* Gynecologic Oncology 1999;74(1):108-114.
238. Kastan, Michael B., Eileen Schlaffer, et al. *Direct demonstration of elevated aldehyde dehydrogenase in human hematopoietic progenitor cells.* Blood 1990;75(10):1947-1950.
239. Russo, James E. and John Hilton. *Characterization of Cytosolic Aldehyde Dehydrogenase from Cyclophosphamide Resistant L1210 Cells.* Cancer Research 1988;48(11):2963-2968.
240. Schiff, Peter B. and Susan Band Horwitz. *Taxol stabilizes microtubules in mouse fibroblast cells.* Proceedings of the National Academy of Sciences of the United States of America 1980;77(3):1561-1565.
241. Heidemann, Steven R. and Peter T. Gallas. *The effect of taxol on living eggs of Xenopus laevis.* Developmental Biology 1980;80(2):489-494.
242. Ireland, Christine M. and Sally M. Pittman. *Tubulin alterations in taxol-induced apoptosis parallel those observed with other drugs.* Biochemical Pharmacology 1995;49(10):1491-1499.
243. Horacek, P. and J. Drobnik. *Interaction of cis-dichlorodiammineplatinum (II) with DNA.* Biochimica et Biophysica Acta 1971;254(2):341-347.
244. Aletras, Vasilis, Denis Hadjiliadis, and Nick Hadji. *On the Mechanism of Action of the Antitumor Drug cis-Platin (cis-DDP) and its Second Generation Derivatives.* Met Based Drugs 1995;2(3):153-185.
245. Melguizo, Consolación, Jose Prados, et al. *Modulation of MDR1 and MRP3 Gene Expression in Lung Cancer Cells after Paclitaxel and Carboplatin Exposure.* International Journal of Molecular Sciences 2012;13(12):16624-16635.
246. Huang, Peng, Sherri Chubb, et al. *Action of 2',2'-Difluorodeoxycytidine on DNA Synthesis.* Cancer Research 1991;51(22):6110-6117.
247. Bergman, Andries M., Herbert M. Pinedo, and Godefridus J. Peters. *Determinants of resistance to 2',2'-difluorodeoxycytidine (gemcitabine).* Drug Resistance Updates 2002;5(1):19-33.
248. Takezawa, Toshiaki, Manabu Yamazaki, et al. *Morphological and immuno-cytochemical characterization of a hetero-spheroid composed of fibroblasts and hepatocytes.* Journal of Cell Science 1992;101(3):495-501.

249. Lee, Seung- A., Da Yoon No, et al. *Spheroid-based three-dimensional liver-on-a-chip to investigate hepatocyte-hepatic stellate cell interactions and flow effects.* Lab on a Chip 2013.
250. Bazzoni, Gianfranco, Ofelia Maria Martínez-Estrada, et al. *Interaction of Junctional Adhesion Molecule with the Tight Junction Components ZO-1, Cingulin, and Occludin.* Journal of Biological Chemistry 2000;275(27):20520-20526.
251. Aijaz, Saima, Fabio D'Atri, et al. *Binding of GEF-H1 to the Tight Junction-Associated Adaptor Cingulin Results in Inhibition of Rho Signaling and G1/S Phase Transition.* Developmental Cell 2005;8(5):777-786.
252. Chen, Xinming, David C. Johns, et al. *Krüppel-like Factor 4 (Gut-enriched Krüppel-like Factor) Inhibits Cell Proliferation by Blocking G1/S Progression of the Cell Cycle.* Journal of Biological Chemistry 2001;276(32):30423-30428.
253. Yoon, Hong S., Xinming Chen, and Vincent W. Yang. *Krüppel-like Factor 4 Mediates p53-dependent G1/S Cell Cycle Arrest in Response to DNA Damage.* Journal of Biological Chemistry 2003;278(4):2101-2105.
254. Jianwei, Zhu, Bai Enzhong, et al. *Effects of Kruppel-like factor 6 on osteosarcoma cell biological behavior.* Tumor Biology 2013;34(2):1097-1105.
255. Nagy, Nathalie, Carmen Brenner, et al. *S100A2, a Putative Tumor Suppressor Gene, Regulates In Vitro Squamous Cell Carcinoma Migration.* Laboratory Investigation 2001;81(4):599-612.
256. Luo, Jun, Youqing Zhu, et al. *Loss of Reprimo and S100A2 expression in human gastric adenocarcinoma.* Diagnostic Cytopathology 2011;39(10):752-757.
257. Singh, Arun S, Cindy H Chau, et al. *Mechanisms of disease: Polymorphisms of androgen regulatory genes in the development of prostate cancer.* Nature Clinical Practice. Urology 2005;2(2):101-107.
258. Yamakoshi, Yasuo, Taketoshi Kishimoto, et al. *Human Prostate CYP3A5: Identification of a Unique 5'-Untranslated Sequence and Characterization of Purified Recombinant Protein.* Biochemical and Biophysical Research Communications 1999;260(3):676-681.
259. Zhong, Ze-Huai, Wei-Qin Jiang, et al. *Disruption of Telomere Maintenance by Depletion of the MRE11/RAD50/NBS1 Complex in Cells That Use Alternative Lengthening of Telomeres.* Journal of Biological Chemistry 2007;282(40):29314-29322.
260. Jiang, W. Q., Z. H. Zhong, et al. *Identification of candidate alternative lengthening of telomeres genes by methionine restriction and RNA interference.* Oncogene 2007;26(32):4635-4647.
261. Saharia, A. and S. A. Stewart. *FEN1 contributes to telomere stability in ALT-positive tumor cells.* Oncogene 2009;28(8):1162-1167.
262. Zeng, Sicong, Tao Xiang, et al. *Telomere recombination requires the MUS81 endonuclease.* Nature Cell Biology 2009;11(5):616-623.

263. Fan, Qiang, Fan Zhang, et al. *A role for monoubiquitinated FANCD2 at telomeres in ALT cells.* Nucleic Acids Research 2009;37(6):1740-1754.
264. Liu, Suling, Gabriela Dontu, et al. *Hedgehog Signaling and Bmi-1 Regulate Self-renewal of Normal and Malignant Human Mammary Stem Cells.* Cancer Research 2006;66(12):6063-6071.
265. Zhao, Chen, Alan Chen, et al. *Hedgehog signalling is essential for maintenance of cancer stem cells in myeloid leukaemia.* Nature 2009;458(7239):776-779.
266. Hitoshi, Seiji, Tania Alexson, et al. *Notch pathway molecules are essential for the maintenance, but not the generation, of mammalian neural stem cells.* Genes and Development 2002;16(7):846-858.
267. Farnie, Gillian and Robert B. Clarke. *Mammary Stem Cells and Breast Cancer - Role of Notch Signalling.* Stem Cell Reviews 2007;3(2):169-175.
268. Zhou, Jiangbing, Hao Zhang, et al. *NF-κB pathway inhibitors preferentially inhibit breast cancer stem-like cells.* Breast Cancer Research and Treatment 2008;111(3):419-427.
269. Korkaya, Hasan, Suling Liu, and Max S. Wicha. *Regulation of Cancer Stem Cells by Cytokine Networks: Attacking Cancer's Inflammatory Roots.* Clinical Cancer Research 2011;17(19):6125-6129.
270. Reya, Tannishtha, Andrew W. Duncan, et al. *A role for Wnt signalling in self-renewal of haematopoietic stem cells.* Nature 2003;423(6938):409-414.
271. Wang, Yingzi, Andrei V. Krivtsov, et al. *The Wnt/β-Catenin Pathway Is Required for the Development of Leukemia Stem Cells in AML.* Science 2010;327(5973):1650-1653.

Allison C Sharrow

Born February 15, 1982 in Pittsburgh, PA

Education

Doctor of Philosophy; Pathobiology — February 2014

Johns Hopkins University School of Medicine — Baltimore, MD

Dissertation: Identification and Characterization of a Stem Cell-Like Population in Ovarian Cancer

Bachelor of Science; Molecular Biology, Biochemistry Track — April 2004

University of Pittsburgh — Pittsburgh, PA

Magna Cum Laude, Minor: Sociology

Research Experience

Johns Hopkins University School of Medicine — October 2007 – Present

Graduate Researcher — Baltimore, MD

Advisor: Richard J. Jones

- Develop research plan
- Characterize aldehyde dehydrogenase high ovarian cancer cells using cell sorting, flow cytometry, cell culture-based assays and molecular techniques
- Optimize culture and sorting conditions for ovarian cancer stem cells

University of Pittsburgh April 2004 - July 2006

Research Associate Pittsburgh, PA

Advisor: Harry C. Blair

- Examined regulation of osteoblast connectivity
- Isolated human osteoclast precursors to study effects of sex hormones on differentiation
- Supervised undergraduate research associates
- Managed lab supplies

University of Pittsburgh April 2001 - April 2004

Undergraduate Research Associate Pittsburgh, PA

Advisor: James M. Pipas

- Engineered expression vectors and purified overexpressed proteins to determine protein interactions
- Managed lab supplies

University of Pittsburgh September 2000 - April 2001

Undergraduate Research Assistant Pittsburgh, PA

Advisor: Tia-Lynn Ashman

- Managed *Fragaria* greenhouse colony
- Collected and analyzed specimens
- Entered data

Teaching Experience

Towson University August 2010 - May 2011

Adjunct Professor, Biology: The Science of Life Baltimore, MD

- Developed course syllabus
- Prepared and delivered lectures, facilitated class discussions
- Designed and graded assignments and exams
- Supervised laboratory sections

Johns Hopkins Bloomberg School of Public Health August 2008 and 2009

Teaching Assistant, Introduction to Biomedical Sciences Baltimore, MD

- Facilitated active learning exercises
- Prepared and delivered short lectures

University of Pittsburgh Fall Semesters 2001-2003

Teaching Assistant, Freshman Studies Pittsburgh, PA

- Assisted in course planning
- Prepared and delivered lectures
- Facilitated classroom discussions

Honors and Awards

Brackenridge Fellow 2002

University of Pittsburgh

Professional Memberships

American Society of Bone and Mineral Research	2005 - 2006
Western Pennsylvania Division March of Dimes Board of Directors	2004 - 2006
Team Youth Liaison	
Tri-Beta Honors Fraternity	2002 - 2004
Regular Member	
Western Pennsylvania Division March of Dimes Team Youth	2004 - 2006
Volunteer Advisor	
Team Youth Volunteer	1997 – 2004
Chair, Co-Chair and Secretary	

Peer-Reviewed Publications

1. Sharrow AC, Perkins BP, Yu W, Jones RJ. Identification and characterization of aldehyde dehydrogenase high ovarian cancer cells. In preparation.
2. Sharrow AC, Ronnett BM, Thoburn CJ, Barber JP, Giuntoli RL, Armstrong DK, Jones RJ, Hess AD. Identification and characterization of a spontaneous ovarian carcinoma in Lewis rats. J Ovarian Res. 2010 Mar 31; 3:9.
3. Robinson LJ, Tourkova I, Wang Y, Sharrow AC, Landau MS, Yaroslavskiy BB, Sun L, Zaidi M, Blair HC. FSH-receptor isoforms and FSH-dependent gene transcription in human monocytes and osteoclasts. Biochem Biophys Res Commun. 2010 Mar 26; 394(1): 12-17.

4. Sharrow AC, Li Y, Micsenyi A, Griswold RD, Wells A, Monga SS, Blair HC. Modulation of osteoblast gap junction connectivity by serum, TNFalpha, and TRAIL. Exp Cell Res. 2008 Jan 15; 314(2): 297-308.
5. Yaroslavskiy BB, Sharrow AC, Wells A, Robinson LJ, and Blair HC. Necessity of inositol (1,4,5)-trisphosphate receptor 1 and μ-calpain in NO-induced osteoclast motility. J Cell Sci. 2007 Aug 15; 120(16): 2884-2894.
6. Borysenko CW, Garcia-Palacios V, Griswold RD, Li Y, Iyer AK, Yaroslavskiy BB, Sharrow AC, Blair HC. Death receptor-3 mediates apoptosis in human osteoblasts under narrowly regulated conditions. J Cell Physiol. 2006 Dec; 209(3): 1021-8.
7. Sun L, Peng Y, Sharrow AC, Iqbal J, Zhang Z, Papachristou DJ, Zaidi S, Zhu LL, Yaroslavskiy BB, Zhou H, Zallone A, Sairam MR, Kumar TR, Bo W, Braun J, Cardoso-Landa L, Schaffler MB, Moonga BS, Blair HC, Zaidi M. FSH directly regulates bone mass. Cell. 2006 Apr 21; 125(2): 247-60.
8. Yaroslavskiy BB, Zhang Y, Kalla SE, Palacios VG, Sharrow AC, Li Y, Zaidi M, Wu C, Blair HC. NO-dependent osteoclast motility: reliance on cGMP-dependent protein kinase I and VASP. J Cell Sci. 2005 Dec 1; 118(23): 5479-87.

9. Frattini A, Blair HC, Sacco MG, Cerisoli F, Faggioli F, Cato EM, Pangrazio A, Musio A, Rucci F, Sobacchi C, Sharrow AC, Kalla SE, Bruzzone MG, Colombo R, Magli MC, Vezzoni P, Villa A. Rescue of ATPa3-deficient murine malignant osteopetrosis by hematopoietic stem cell transplantation in utero. Proc Natl Acad Sci U S A. 2005 Oct 11; 102(41): 14629-34.

Book Chapters

Sharrow AC, Ghiaur G, Gerber JM, Jones RJ. Cancer Stem Cell Principles. In Translational Cancer Research: Molecular Therapeutics. Wiley. In press.

Presentations and Posters

Fellow Research Day: Poster Presentation — May 14, 2013
Identification and Characterization of Aldehyde Dehydrogenase High Ovarian Cancer Cells — Baltimore, MD

Pathology Young Investigator's Day: Poster Presentation — April 5, 2013
Identification and Characterization of Aldehyde Dehydrogenase High Ovarian Cancer Cells — Baltimore, MD

American Society of Bone and Mineral Research Annual Meeting: Poster Presentation
TRAIL and TNFα Regulate Human Osteocyte-Osteon Structure by Removal of Gap Junctions via Proteasomal Degradation with a Probable β-Catenin Downstream Mechanism — September 24, 2005 — Nashville, TN

March of Dimes National Team Youth Conference: Oral Presentation July 28, 2005

The Gene Pool: Research and the March of Dimes Washington, D.C.

University of Pittsburgh Medical School Pathology Retreat: Oral Presenation

Protein Kinase Activity and Death Receptor Ligands June 25, 2005

Modulate Osteoblast Connectivity Seven Springs, PA

Abstracts

1. Sun L, Zhang Z, Peng Y, Iqbal J, Zaidi S, Papachristou DJ, Zhou H, Sharrow AC, Yaroslavskiy BB, Zhu L, Zallone A, Sairam MR, Kumar TR, Cardoso-Landa L, Schaffler MB, Moonga BS, Blair HC, Zaidi M. FSH Directly Regulates Bone Mass: Implications for Understanding the Pathogenesis of Osteoporosis Due to Hypogonadism. Journal of Bone and Mineral Research. 2005; 20 (Supplement 1): Abstract #1043, pg S12.
2. Zhang Z, Sun L, Peng Y, Iqbal J, Zaidi S, Papachristou DJ, Zhou H, Sharrow AC, Yaroslavskiy BB, Zhu L, Zallone A, Sairam MR, Kumar TR, Cardoso-Landa L, Schaffler MB, Moonga BS, Blair HC, Zaidi M. The Pituitary Hormone, FSH, Directly Enhances Osteoclast Formation and Survival. Journal of Bone and Mineral Research. 2005; 20 (Supplement 1): Abstract #1100, pg S26.
3. Yaroslavskiy BB, Sharrow AC, Papachristou DJ, Virji M, Sun L, Zhang Z, Peng Y, Iqbal J, Zaidi S, Zhou H, Zhu LL, Moonga BS, Zaidi M, Blair HC. FSH as a Direct Regulator of Bone Degradation in the Human. Journal of Bone and Mineral Research. 2005; 20 (Supplement 1): Abstract #F376, pg S92.

4. Robinson LJ, Sharrow AC, Garcia Palacios V, Xue J, Blair HC. Nongenomic Estrogen Signalling Regulates Osteoclast Formation via An Adaptor Protein, BCAR1, that also Modifies Breast Cancer Progression. Journal of Bone and Mineral Research. 2005; 20 (Supplement 1): Abstract #F505, pg S103.
5. Sharrow AC, Li Y, Micsenyi A, Borysenko CW, Lehmann T, Wells A, Kalla SE, Garcia Palacios V, Monga SP, Blair HC. TRAIL and TNFα Regulate Human Osteocyte-Osteon Structure by Removal of Gap Junctions via Proteasomal Degradation with a Probable β-Catenin Downstream Mechanism. Journal of Bone and Mineral Research. 2005; 20 (Supplement 1): Abstract #SA217, pg S140.
6. Yaroslavskiy BB, Kalla SE, Sharrow AC, Blair HC. Guanylyl Cyclase and cGMP-Dependent Protein Kinase I Induce Calcium and Calpain-Dependent Cytoskeletal Rearrangement in Osteoclasts, but Calcium Signals Are not Sufficient to Initiate Motility. Journal of Bone and Mineral Research. 2005; 20 (Supplement 1): Abstract #SA241, pg S143.